



CZECH TECHNICAL UNIVERSITY IN PRAGUE

**Faculty of Civil Engineering
Department of Building Structures**

**Cold Attics
in Humid Cold and Temperate Climate**

DOCTORAL THESIS

Jan Richter

Doctoral study programme: Civil Engineering

Branch of study: Building Engineering

Doctoral thesis tutor: prof. Ing. Jan Tywoniak, CSc.
Ing. Kamil Staněk, Ph.D.

Prague, 1/2020



CZECH TECHNICAL UNIVERSITY IN PRAGUE

Faculty of Civil Engineering

Thákurova 7, 166 29 Praha 6

DECLARATION

Ph.D. student's name: Jan Richter

Title of the doctoral thesis: Cold Attics in Humid Cold and Temperate Climate

I hereby declare that this doctoral thesis is my own work and effort written under the guidance of the tutor prof. Ing. Jan Tywoniak, CSc. and Ing. Kamil Staněk, Ph.D. All sources and other materials used have been quoted in the list of references.

The doctoral thesis was written in connection with research on the project:

In Prague on 22.1.2020

.....
signature

Cold Attics in Humid Cold and Temperate Climate

Jan Richter

DOCTORAL THESIS

Czech Technical University in Prague

Faculty of Civil Engineering

2020



*I would like to dedicate this work to my little dog Mia that passed away a few days ago.
She spent many hour silently guarding me while I typed this work.*



Contents

Abstract in Czech	1
Abstract.....	3
Nomenclature	4
1 Introduction	9
1.1 Background.....	9
1.2 Goals and structure of the thesis.....	12
1.3 Target climate zone	13
1.4 Causes of problems.....	15
1.5 Brief in-situ measurements	18
2 Review of studies	25
2.1 Methods.....	25
2.1.1 Selection of studies and attic designs	25
2.1.2 Selection of comparative parameters	26
2.1.3 Quantification of parameters	29
2.1.4 Quantification of values in moisture-evaluation charts	31
2.1.5 Uncertainties.....	32
2.2 Results.....	34
2.3 Discussion.....	45
2.3.1 General findings	45
2.3.2 Moisture-risk evaluation	48
2.3.3 Grouping of similar designs.....	52
2.3.4 Statistical evaluation.....	54
2.3.5 Comparison of similar attic designs.....	54
2.4 Conclusions	55
3 Development of HAM model	57
3.1 Description of the model	57
3.1.1 Thermal model.....	66
3.1.2 Airflow model	79
3.1.3 Moisture model	86
3.2 Verification	94

3.3	Validation	95
3.3.1	Thermal model validation.....	95
3.3.2	Moisture model validation.....	98
3.3.3	Cavity-airflow model validation	100
3.4	Conclusions	102
4	Conclusions and outlook.....	103
	References.....	105
	Appendices.....	111
	Appendix A – Overview of analysed attic designs.....	111
	Appendix B – Verification of the model – full report.....	122
	Thermal model.....	122
	Thermal + airflow model.....	131
	Moisture model.....	143

Abstract in Czech

Nevytápěný půdní prostor (chladný půdní prostor) je z hlediska jeho tepelně-vlhkostního chování v posledních desetiletích jedním z nejproblematičtějších prostorů ve stavební praxi. Problémy se týkají zpravidla kondenzace, namrzání a růstu plísní na spodní straně střešního pláště. Tyto problémy byly zaznamenány zejména na území Evropy a Severní Ameriky (vlhké chladné a mírné klimatické oblasti). Za účelem vyřešení těchto problémů bylo provedeno mnoho kvalitních studií. Ačkoliv byla na jejich základě odhalena řada důležitých informací, zdá se, že některá zjištění nejsou ve vzájemném souladu a některá z nich se dokonce zdají být v přímém rozporu. Z toho důvodu stále nelze stanovit jeden nebo více designů půdních prostor, které by byly vhodné (zejména vlhkostně bezpečné) pro celou cílovou klimatickou oblast.

Cílem této práce je tedy zjistit, zda takový design lze najít nebo stanovit důvody proč to možné není. Na základě pečlivé rešerše publikovaných studií bylo vybráno 35 designů půdních prostor pro další analýzu. Za účelem najít jejich potenciální společné rysy a logická propojení byly zvoleny a vyčísleny jejich klíčové srovnávací parametry. Následným srovnáním těchto parametrů bylo odhaleno několik nových poznatků, které vedly k několika doporučením pro návrh vlhkostně bezpečného půdního prostoru. Na druhou stranu bylo také zjištěno, že studie ve svých výstupech často sdělují velice málo o skutečné vlhkostní bezpečnosti zkoumaných prostor. Dalším zásadním zjištěním bylo, že přes řadu provedených studií, je stále nedostatek otestovaných designů půdních prostor, zejména těch, které by měly být cílové z hlediska současné a budoucí kvalitní a udržitelné výstavby.

Ve světle zjištěných informací byl vytvořen numerický tepelně-vlhkostní model (HAM model) v softwaru Matlab. Model byl vytvořen především pro vhodný popis různých variant půdních prostor, ale lze ho využít i pro jiné prostory. Model je dynamický, jednodimensionální a implicitní, vytvořen pro výpočty zejména v půlhodinovém nebo hodinovém časovém kroku. Jeho výpočetní jádro je postaveno na klasickém základním balíku rovnic popisujících přenos tepla a hmoty. Model je do značné míry variabilní pro pokrytí širokého rozsahu odlišných půdních prostor. Model byl v rámci práce úspěšně verifikován a validován.

Abstract

An unheated attic space (so called “cold attic”) regarding its moisture performance is in last few decades one of the most problematic spaces in building practice. Problems are associated usually with condensation, frost formation or mould growth on lower surface of roof deck. These problems were recorded mostly in Europe and North America (humid cold and temperate climate zones). In order to solve these problems a number of quality studies were performed. Despite that many important pieces of information have been revealed, it seems that some findings are not always in agreement with one another and in some cases it appears that the studies are in clear contradiction. Therefore it still cannot be stated one or more general cold attic design that would be suitable (especially moisture-safe) for the whole target climate zone.

Aim of this thesis is therefore to find out whether such a design can be found or state reasons why it is not possible. Based on the thorough review of published studies, 35 cold attic designs were selected for further analysis. In order to find their possible common features and logical connections, their key parameters were established and quantified. Based on their consequent comparison, several new pieces of information were found leading to stated suggestions towards moisture-safe cold attic design. On the other hand it was also found, that the studies often provide an outputs that does not say much about real moisture safety of the tested attic designs. Another finding was, that despite the number of studies performed, there is still a lack of tested designs, especially those which would be the most target ones in context of current and future good-quality and sustainable building practice.

In the light of such findings, a numerical hygro-thermal and airflow model (HAM model) was developed in a Matlab software. Model was designed especially for suitable description of various different attic designs, but can be used also for other spaces. Model is dynamic, mainly one dimensional and implicit, meant to work in hourly or half-hourly time steps. Its calculation core is based on traditional set of equations for heat and mass transfer. Model is quite versatile to cover wide range of different attic designs, but can be used also for other applications. Model was successively verified and validated.

Nomenclature

General

Symbol	Quantity	Unit
A	area	m^2
A_A	area of the north inner-attic roof deck / gable wall surface	m^2
A_B	area of the south inner-attic roof deck / gable wall surface	m^2
A_C	area of the east inner-attic roof deck / gable wall surface	m^2
A_D	area of the west inner-attic roof deck / gable wall surface	m^2
A_E	area of the attic floor	m^2
A_F	area of the inner-attic thermal mass constructions (e.g. wooden truss)	m^2
b_{cav}	width of the roof-deck cavity (eave-wise)	m
d	thickness	m
d_{cav}	thickness of the roof-deck cavity (perpendicular to roof surface)	m
g_G	gravitational acceleration = 9.81	m/s^2
m	mass	kg
n_{gas}	amount of gas	mol
p	pressure	Pa
p_0	pressure of standard atmosphere = 101325	Pa
p_{atm}	atmospheric pressure	Pa
R_{gas}	ideal gas constant = 8.314	J/(mol·K)
R_{spec}	mass-specific gas constant (different for each gas)	J/(kg·K)
V_a	volume of air	m^3
x	position, the dimension of which is length	m
φ	slope of the roof deck (from inclined horizontal plane)	°
ρ	density	kg/m^3
ρ_0	dry density	kg/m^3
ρ_a	density of dry air	kg/m^3
ρ_{ae}	exterior air density	kg/m^3
$\rho_{a,cav}$	density of air within a roof-deck cavity	kg/m^3
τ	time	s
$\Delta\tau$	duration of one computational time step	s
ψ_0	open porosity	-

Heat transport

Symbol	Quantity	Unit
C_{heat}	heat capacity of material layer (material node)	J/(m ² ·K)
c_p	specific heat capacity	J/(kg·K)
c_{pa}	specific heat capacity of dry air	J/(kg·K)
F_g	coefficient characterizing the roof orientation to ground	-
F_{sky}	coefficient characterizing the roof orientation to sky	-
h	thermal conductance	W/(m ² ·K)
$h_{\text{ee,wall}}$	thermal conductance between the equivalent outdoor temperature and first computational node of the gable wall	W/(m ² ·K)
$h_{\text{ee,roof}}$	thermal conductance between the equivalent outdoor temperature and first computational node of the roof deck	W/(m ² ·K)
Q	heat flow rate	W
$Q_{\text{c,gain}}$	convective heat gain to the attic space	W
$Q_{\text{r,gain}}$	radiative heat gain to the attic space	W
q	conductive heat flux (density of heat flow)	W/m ²
q_{sol}	solar heat gain (flux) to sloped surface of specified absorptance	W/m ²
$q_{\text{sol,tot}}$	solar heat gain (flux) to sloped surface	W/m ²
q_r	radiative heat flux	W/m ²
$q_{\text{r,to_sky}}$	radiative heat flux from outer surface to apparent sky temperature	W/m ²
R	thermal resistance	m ² ·K/W
T	thermodynamic (absolute) temperature	K
T_a	thermodynamic (absolute) temperature of air	K
α_c	convective heat transfer coefficient	W/(m ² ·K)
$\alpha_{\text{c,buff}}$	convective heat transfer coefficient on the surface of the attic internal thermal buffering constructions	W/(m ² ·K)
$\alpha_{\text{c,e}}$	convective heat transfer coefficient on the external roof surface	W/(m ² ·K)
$\alpha_{\text{c,e,cav}}$	convective heat transfer coefficient on the lower surface of an upper skin of the double-skin roof deck	W/(m ² ·K)
$\alpha_{\text{c,floor}}$	convective heat transfer coefficient on the attic floor	W/(m ² ·K)
$\alpha_{\text{c,i}}$	convective heat transfer coefficient on the lower surface of interior ceiling	W/(m ² ·K)
$\alpha_{\text{c,r}}$	convective heat transfer coefficient on the internal roof-deck surface	W/(m ² ·K)
$\alpha_{\text{c,r,cav}}$	convective heat transfer coefficient on the upper surface of a lower skin of the double-skin roof deck	W/(m ² ·K)
$\alpha_{\text{c,z,zone_air}}$	convective heat transfer coefficient on the inner-attic surface	W/(m ² ·K)
α_r	radiative heat transfer coefficient	W/(m ² ·K)
$\alpha_{\text{r,cav}}$	radiative heat transfer coefficient between the two opposite surfaces in the roof-deck cavity	W/(m ² ·K)
$\alpha_{\text{r,g}}$	radiative heat transfer coefficient between the external roof deck surface and ground (surrounding environment) temperature	W/(m ² ·K)

$\alpha_{r,sky}$	radiative heat transfer coefficient between the external roof deck surface and apparent sky temperature	W/(m ² ·K)
$\alpha_{r,z,mr}$	radiative heat transfer coefficient on the inner-attic surface	W/(m ² ·K)
$\alpha_{s,e}$	equivalent heat transfer coefficient on the external roof surface	W/(m ² ·K)
ε	long-wave thermal emissivity	-
ε_{roof}	long-wave thermal emissivity of the roofing surface	-
$\varepsilon_{s,e,cav}$	long-wave thermal emissivity of the lower surface of the upper skin of the roof deck	-
$\varepsilon_{s,r,cav}$	long-wave thermal emissivity of an upper surface of the lower skin of the roof deck	-
K_{heat}	heat capacity of zonal nodes / total heat capacity	J/K
λ	thermal conductivity	W/(m·K)
λ_a	thermal conductivity of still air	W/(m·K)
θ	temperature in degrees centigrade	°C
$\theta_{1,cav}$	temperature of air in lower part of the roof-deck cavity	°C
$\theta_{2,cav}$	temperature of air in upper part of the roof-deck cavity	°C
θ_{ae}	temperature of outdoor (exterior) air	°C
$\theta_{a,flow}$	temperature of an air that flows through the flow pathway	°C
θ_{ai}	temperature of indoor (interior) air	°C
θ_{ar}	temperature of air in the attic	°C
θ_{cav}	temperature of air within the roof-deck cavity	°C
θ_e	equivalent outdoor temperature	°C
θ_{ecav}	temperature of air in the eave zone (in “length2” roof part)	°C
θ_g	ground temperature	°C
θ_{mr}	mean radiation temperature	°C
θ_{ref}	temperature at which the reference flow coefficient is valid	°C
$\theta_{s,e,cav}$	temperature of the lower surface of the upper skin of the roof deck	°C
θ_{sky}	apparent sky temperature	°C
$\theta_{s,r,cav}$	temperature of the upper surface of the lower skin of the roof deck	°C
ϱ_{sol}	solar absorptance	-
σ	Stefan-Boltzmann constant = 5.67×10^{-8}	W/(m ² ·K ⁴)

Moisture transport

Symbol	Quantity	Unit
b_{sor}	parameter of sorption isotherm function	-
C_{moist}	moisture capacity of material node	kg/m ²
G	water vapour flow rate	kg/s
g	density of water vapour flow rate	kg/(m ² ·s)

k	vapour permeance	m/s
n_{sor}	parameter of sorption isotherm function	-
p_v	partial vapour pressure	Pa
$p_{v,sat}$	saturated partial vapour pressure	Pa
R_a	gas constant of dry air = 287	J/(kg·K)
R_v	gas constant of water vapour = 462	J/(kg·K)
RH	relative humidity	-
s_d	(water vapour diffusion-)equivalent air layer thickness	m
u	water content by mass	kg/kg
$u_{m,sor}$	parameter of sorption isotherm function	kg/kg
W	water content mass by volume	kg/m ³
β	surface convective mass transfer coefficient	m/s
δ_p	water vapour permeability when the driving force is a difference of partial vapour pressure	kg/(m·s·Pa)
δ_{pa}	water vapour permeability of still air when the driving force is a difference of partial vapour pressure	kg/(m·s·Pa)
δ_v	water vapour permeability when the driving force is a difference of vapour concentration	m ² /s
δ_{va}	water vapour permeability of still air when the driving force is a difference of vapour concentration	m ² /s
K_{moist}	moisture capacity of zonal node / total moisture capacity	kg
μ	water vapour resistance factor	-
v	concentration of water vapour in air	kg/m ³
v_{sat}	saturated concentration of water vapour in air	kg/m ³
ω_c	water tank of material node	kg/m ²
ω_k	water tank of zonal node	kg
ξ	specific moisture (adsorption) capacity	kg/kg
ξ_a	specific moisture capacity of air	kg/kg

Airflow

Symbol	Quantity	Unit
a_{wind}	terrain constant	-
D_H	hydraulic diameter	m
C_p	wind pressure coefficient	-
l	flow coefficient	m ³ /(s·Pa ^L)
l_{ref}	reference flow coefficient	m ³ /(s·Pa ^L)
J_d	discharge coefficient for an orifice flow	-
k_{wind}	terrain constant	-
L	flow exponent	-
\dot{m}	mass flow rate	kg/s

\dot{m}_{cav}	mass flow rate through the roof-deck cavity	kg/s
$\dot{m}_{e,cav}$	mass flow rate across the eave opening of the roof-deck cavity	kg/s
$\dot{m}_{p,cav}$	mass flow rate across the peak opening of the roof-deck cavity	kg/s
\dot{m}_{eatt_att}	mass flow rate from ecav space to attic (opening is denoted as eatt)	kg/s
\dot{m}_{eatt_ecav}	mass flow rate from attic to ecav space (opening is denoted as eatt)	kg/s
\dot{m}_e	mass flow rate across an eave opening to ecav space	kg/s
\dot{m}_p	mass flow rate across the peak (ridge) opening to an attic space	kg/s
\dot{m}_{c_att}	mass flow rate across the ceiling (from interior to attic)	kg/s
\dot{m}_{c_int}	mass flow rate across the ceiling (from attic to interior)	kg/s
Nu	Nusselt number	-
ΔP	total pressure difference across an air pathway	Pa
ΔP	total pressure difference across an air pathway	Pa
ΔP_U	pressure difference across an opening forced by wind	Pa
p_m	pressure at the chosen point of medium	Pa
Pr	Prandtl number	-
P_R	reference pressure	Pa
$P_{R,ext}$	exterior reference pressure	Pa
$P_{R,int}$	interior zone reference pressure	Pa
$P_{R,att}$	attic zone reference pressure	Pa
$P_{R,cav}$	roof-deck cavity zone reference pressure	Pa
$P_{R,ecav}$	ecav zone reference pressure	Pa
P_T	pressure gradient factor of the zone	Pa/m
Re	Reynolds number	-
S_U	shelter coefficient	-
U	speed (magnitude of velocity)	m/s
U_{10}	wind speed at a height of 10 meters (reference wind speed)	m/s
U_{cav}	airflow speed within the ventilated roof-deck cavity	m/s
U_o	wind speed acting on an orifice (or equivalent orifice)	m/s
\dot{V}	volumetric flux (density of air flow)	l/(m ² ·s)
W_{cav}	airflow velocity in ventilated roof-deck cavity	m/s
z	height above ground	m
z_o	height of an orifice above ground	m
ϕ	air permeance	l/(s·m ² ·Pa ¹)
$\mu_{dyn,a}$	dynamic viscosity of air	kg/(m·s)
ρ_m	density of fluid medium	kg/m ³
ϖ_{dir}	wind direction at a height of 10 meters	°

1 Introduction

1.1 Background

Cold attic, so called „cold roof“ or „cold loft“, is a space surrounded by pitched roof decks, gable walls and thermally insulated ceiling construction of the highest floor of the building. Although there can be recorded quite high temperature within the cold attic, especially during the summer time, the term „cold“ is associated with heating season, which is usually the most critical part of the year, in terms of attic moisture problems. As there is a minimal heat transport across the insulated ceiling, the temperature within the attic is in cold season close to the temperature of outdoor air [5] (see also section *1.5 Brief in-situ measurements*). Low temperatures of inner-attic surfaces are prerequisites for high surface relative humidity. Therefore the problems of cold attics are mostly associated with condensation, frost formation or mould growth on lower surface of the roof deck, or on its contact with rafters or wall beams (see Fig. 1). In some cases also other inner-attic surfaces can experience similar problems (see Fig. 2). Formed condensate or melted frost can be absorbed into the porous materials of roof deck or can drop or run down onto the attic floor or construction joints. In all cases it often leads to an increase of moisture content of porous materials which can cause changes of their mechanical properties or initiate consequent biodegradable processes [65,66].

However the problems can appear even without any condensation. Sufficiently high relative humidity in combination with suitable temperature (and few other factors) acting for a certain time period can lead to mould growth [65,66]. Although moulds cannot cause any marginal mechanical degradation to the structure, they can prepare a suitable conditions for decay fungi or other biodeteriogens [70,71,72,65]. Presence of moulds within the attic furthermore leads to higher concentration of mould spores within the attic air and consequently also within the interior air, which can cause health problems to the occupants [67,68,69]. Those are the reasons why mould growth is, as well as condensation, usually considered as one of the signs of improper hygro-thermal conditions.

History of moisture problems within cold attics is quite long as one of the first studies (maybe the very first) was presented in 1939 [35]. However a larger increase of such a problems was recorded after the energy crises in 1970s that has led in many countries to a step-increase of the thermal resistance and air-tightness of building envelope constructions (including a ceiling to an unheated attic space) [39, 16, 12]. At the same time also many new or upgraded materials have been presented to the building market. Around 1990 was introduced also the first vapour permeable roof underlay felts (possibly the very first was presented in 1984 on Dach & Wand exhibition [51]). These felts allowed to build the attic unventilated but vapour-permeable to the outdoor environment. However the lack of experience with these new designs and materials in building practice had led to a number of new hygro-thermal problems [39], and cold attics became one of the most moisture-problematic space [16,18,36,40,41,45].

After a several decades a huge step forward was made and a lot of quality studies were performed in order to solve the problems [1-25]. Although the studies tested a lot of different designs and revealed some important pieces of information, few latest reviews pointed out, that there is an apparent disagreement between some of the finding of different studies [21,25].

An example can be mentioned using, for instance, one of the most discussed parameter of an attic design – the ventilation. In Czech Republic (Central Europe) and surrounding areas is the ventilation by outdoor air a traditional and still the best-practice way to keep the attic moisture-safe. Clear evidence can be found, beside others, in an agriculture buildings where the attics often serve as a spaces for dry storage of hay, straw and other supplies. Although such a spaces were often placed above a cattle sheds that provided some moisture load to the attic, stored supplies were still kept sufficiently dry (although the “dryness” of ventilated attic is in any case limited by moisture present within the exterior air itself [5]). Similarly some of the studies claim that the attic should be ventilated [1,2,6]. Other studies however state that there is an optimal ventilation rate and the attic should not be ventilated too much, nor too low [??]. On the other hand some studies found out, that unventilated attics in climate of southern Sweden performs better than ventilated ones [3,5]. Other study say that both designs (ventilated and unvented) performs similarly well in climate of southern Finland [4]. An opposite statement can be found in study performed in southwest coast of Canada, where a mould growth was found and also calculated within an unvented and also ventilated attics [9]. Finally there are studies recommending sealed attic design with mechanical adaptive ventilation [7,12,18,43].

It is obvious that if such a set of statements is obtained without any other context information, it without any doubt looks that the topic is still not satisfactorily understood and solved. It should be emphasised that this was only one property mentioned – the ventilation - from the whole set of other parameters. However when all those parameters and context information would be taken into account, it can be possibly revealed that the studies are in fact not disproving one another, but on the contrary there could be possibly found some logical linkages between them that give more clear picture about the topic.

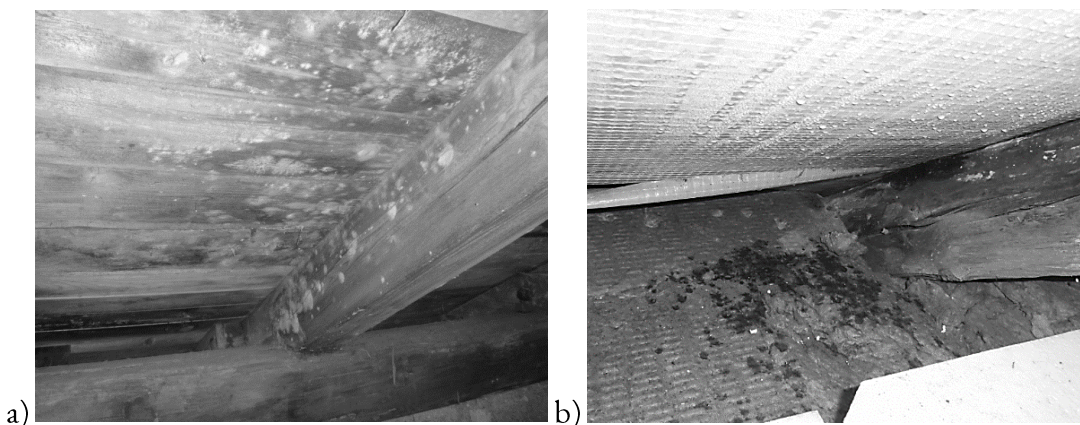


Fig. 1: a) - mould growth on wooden sheathing; b) – condensate droplets on PE underlay foil and wetted mineral wool insulation



Fig. 2: frost accumulation on wooden truss above improperly sealed crack in the ceiling vapour barrier

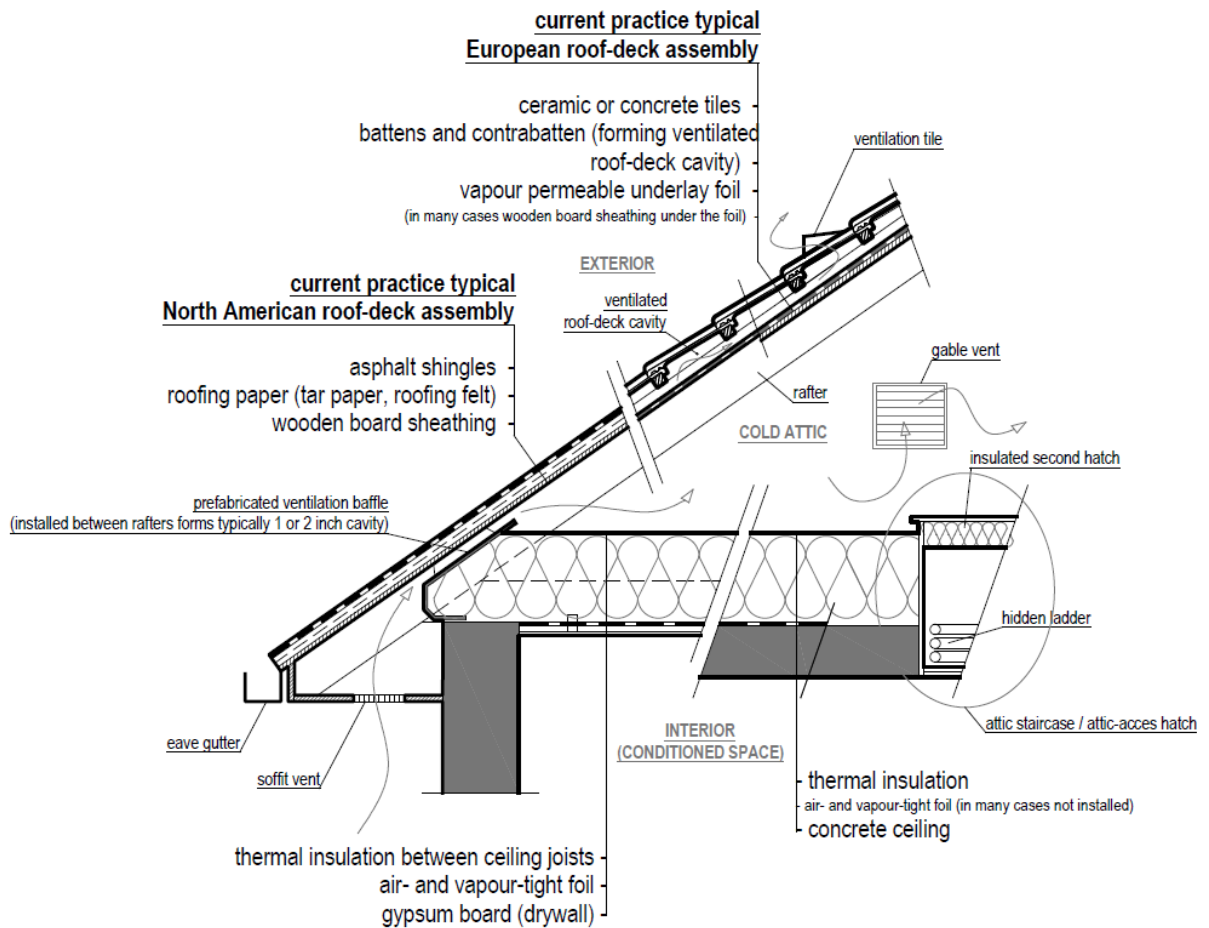


Fig. 3: Glossary scheme of cold attic with depicted typical North-American and European roof-deck assemblies

1.2 Goals and structure of the thesis

- 1) Aim of this thesis is to state if there can be found one or more cold attic design, that is suitable (especially moisture-safe) for the whole or prevailing part of humid cold and temperate climate zone (see section *1.3 Target climate zone*), what are possible exceptions, or state reasons why it is not possible. This work is not focused on future climate as it is based mostly on review of previous studies.
 - To reach the goal a thorough review of credible studies was performed. Key parameters of 35 cold attic designs were quantified and compared (see section *2. Review of studies*). On selected designs their moisture safeness was evaluated (see sections *2.1.4 Quantification of values in moisture-evaluation charts* and *2.3.2 Moisture risk evaluation*) and all designs were sorted into groups according to their similarities (see section *2.3.3 Grouping of similar designs*).
- 2) Second goal of the thesis is to create sufficient HAM model for further numerical analysis and optimisation of cold attics.
 - Model was successively developed, verified and validated (see section *3. Development of HAM model*).

1.3 Target climate zone

Most of the found studies dealing with hygro-thermal performance of cold attics were performed in Cfb and Dfb climate zones (according to updated map of Köppen-Geiger climate classification [73]), while some of the studies were performed also in surrounding areas such as Cfa, Cfc, Dfa and Dfc (see Fig. 4). As the “C” states for “temperate” or “warm temperate” according to [73, 74], respectively and “D” for “cold” or “snow”, while second character “f” for “fully humid”, the whole target area we referred to as “humid cold and temperate climate” (hereafter HCT zone). Looking at figure 4, it can be seen, that besides Europe and North America also other locations are of similar climate conditions, such as part of South America, Africa and Australia, whole New Zealand, part of China and prevailing part of Russia (see Fig. 5). It should be mentioned that Köppen-Geiger climate classification [78,76,77] is based on temperature and precipitation data instead of temperature and relative humidity, which could be more suitable for purposes of this topic. However it is still a useful and illustrative tool for at least rough estimations. Maps depicted in figures 4 and 5 is roughly redrawn from [73], where data from period 1951 - 2000 were used.

Note: Köppen-Geiger classification was firstly introduced by Wladimir Köppen in 1900 [78] as the very first quantitative classification of world climates and was latter updated by Rudolf Geiger in 1954 and 1961 [76,77]. We adopted a map from year 2006 [73], which was the first update since 1961 (see Fig. 4).

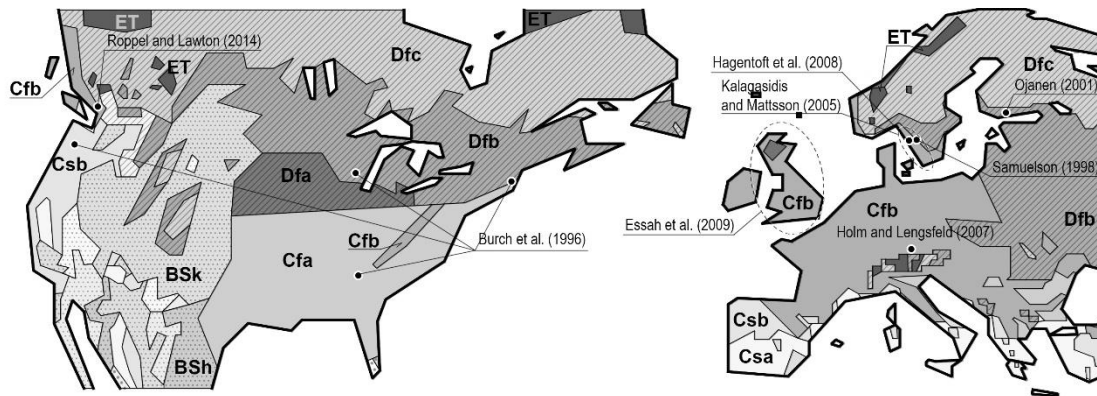


Fig. 4: Map divided into Köppen-Geiger climate zones with depicted locations of studied cold attic designs (roughly redrawn from [73])

Tab. 1: Köppen-Geiger climate classification (according to [73])

Main Climate	Precipitation	Temperature	
warm temperature cl.	dry summer	warm summer	Csb
warm temperature cl.	fully humid	hot summer	Cfa
warm temperature cl.	fully humid	warm summer	Cfb
snow climate	fully humid	hot summer	Dfa
snow climate	fully humid	warm summer	Dfb
snow climate	fully humid	cool summer	Dfc



Fig. 5: World map with roughly depicted areas of HCT climate (roughly redrawn from [73])

1.4 Causes of problems

As mentioned in previous sections, moisture-related problems within cold attics in HCT climate are mostly associated with high moisture levels and mould growth on the lower surface of the roof deck. One of the first-sight explanations of those problems could be that it is mainly caused by lower temperatures within the modern cold attic compared to historical attics that were more supplied with heat transmitting through the less-insulated ceiling. However historical attics were usually well ventilated by leakages in tiled roofing (without any underlayment), by other construction imperfections or by, often well-distributed, intentional vents (see Fig. 7, 8). Therefore the temperature within the historical attics was as well as in modern cold attics close to the temperature of outdoor air (see also section *1.5 Brief in-situ measurements*).

Nevertheless low temperatures of inner-attic surfaces in heating season can lead to high surface relative humidity levels and consequent moisture problems. This risk is closely bonded to the moisture present within the attic air. If the attic is well ventilated and the inner-attic surfaces are close to the temperature of outdoor air, relative humidity levels of such a surfaces are as well close to the relative humidity of outdoor air. However during the cold clear nights the heat from the exterior surface of the roof deck is transmitting out by a longwave thermal radiation to the atmosphere and outer space which can be substituted by an imaginary body having an apparent sky temperature. Since the apparent sky temperature (in case of clear sky) can be much lower than the outdoor air temperature (in order of 10 °C), the roof-deck can be also cooled down below the temperature of outdoor air. This undercooling of the roof deck can affect also its lower surface, which consequently experiences an increase of relative humidity. Then in some cases a ventilation of the attic by outdoor can cause a moisture problems [7, 9], (see also section *2.3 Discussion*). However in most areas of HCT climate the ventilation by outdoor can be stated as not moisture-risky, and on contrary it is often the best-practice recommendation for keeping the attic moisture-safe (as can be found also in next sections). In any way if the inner-attic surface temperature falls below the dew point temperature of an attic air, condensation or frost formation (desublimation or deposition) takes place (see Fig. 1).

Usually the most critical moisture source for cold attic in HCT climate is the interior air that, in cold season, contain more moisture compared to outdoor air (in Czech Republic, it is about twice the amount), (see also section *1.5 Brief in-situ measurements*). Interior moisture can be transported into the attic by an airflow (convection) through leakages in the ceiling construction and by diffusion. As the airflow is the dominant mechanism for moisture transport, regarding ordinary constructions and pressure differences, ceiling air-tightness is the most recommended measure in terms of attic moisture-safeness, while its vapour-tightness follows with lower priority [5,11,6,8,3,28,22,37]. Main pathways for the air to come up to the attic space are leakages around an attic staircases, around electric conduits, ceiling fixtures and around any other constructions that penetrates the ceiling [1,6,32,37].

Another potential source of moisture can be a built-in moisture that should be avoided or removed directly after erection of the building [11, 18].

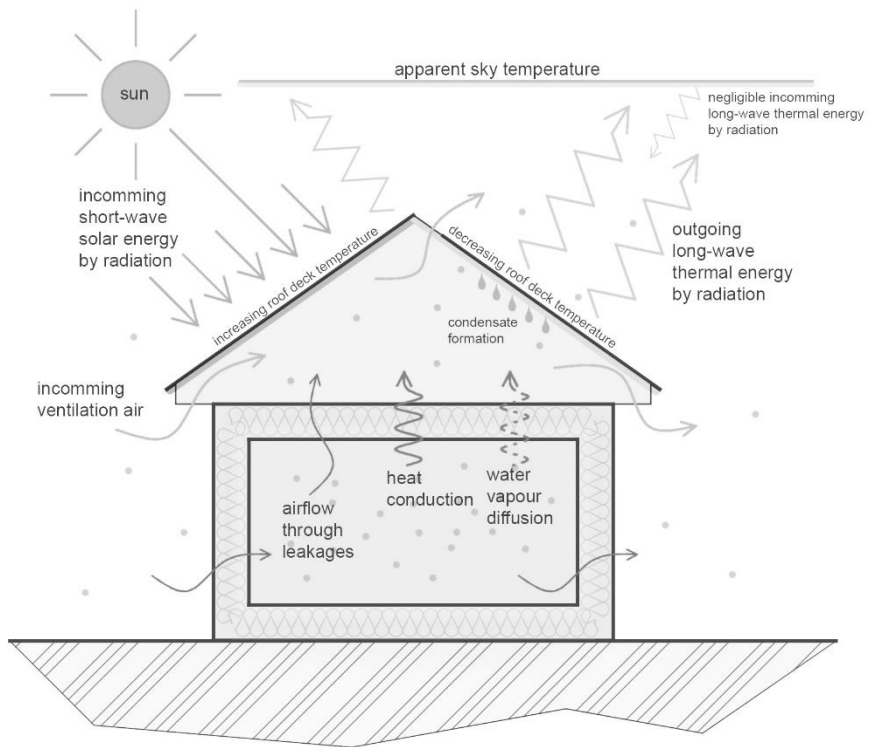


Fig. 6. Scheme of the moisture transport processes within the cold attic



Fig. 7. Examples of historical attic spaces in Czech Republic

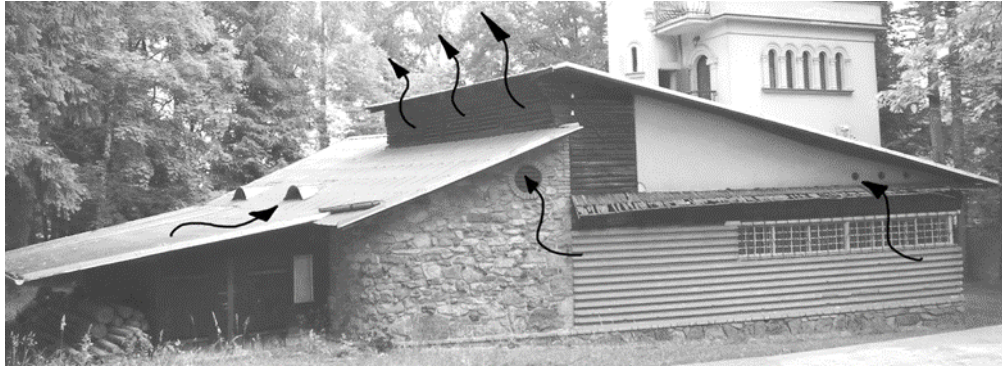


Fig. 8. Historical dwelling with steel-plate roofing and intentional openings (woods of Křivoklátsko – west from Prague)

1.5 Brief in-situ measurements

To gain more insight into the usual hygro-thermal conditions within the attics in Czech Republic, a set of 3 basic measurements in different attic designs were performed - historical attic, well-performing cold attic, bad-performing cold attic. All attics were located near Prague.

In figures 9-11 can be seen a geometry and photo of one historical and two modern cold attics. In figures 12-14 are compared courses of measured temperatures, vapour concentrations and relative humidity within the attics in period of chosen 3 weeks of winter time. In table 2 are summarized averages of measured values.

Historical cold attic is situated under the upper part of mansard roof. Upper part of the roof has a slope of 35° . As there are 4 sloped roof segments their orientation is towards the cardinal points. Roof deck is formed by a ceramic tiled roofing on a laths without any underlayment. The ceiling construction below the attic is formed by the wooden beams with a gravel between them. On top of the historical ceiling is performed 50 mm concrete layer.

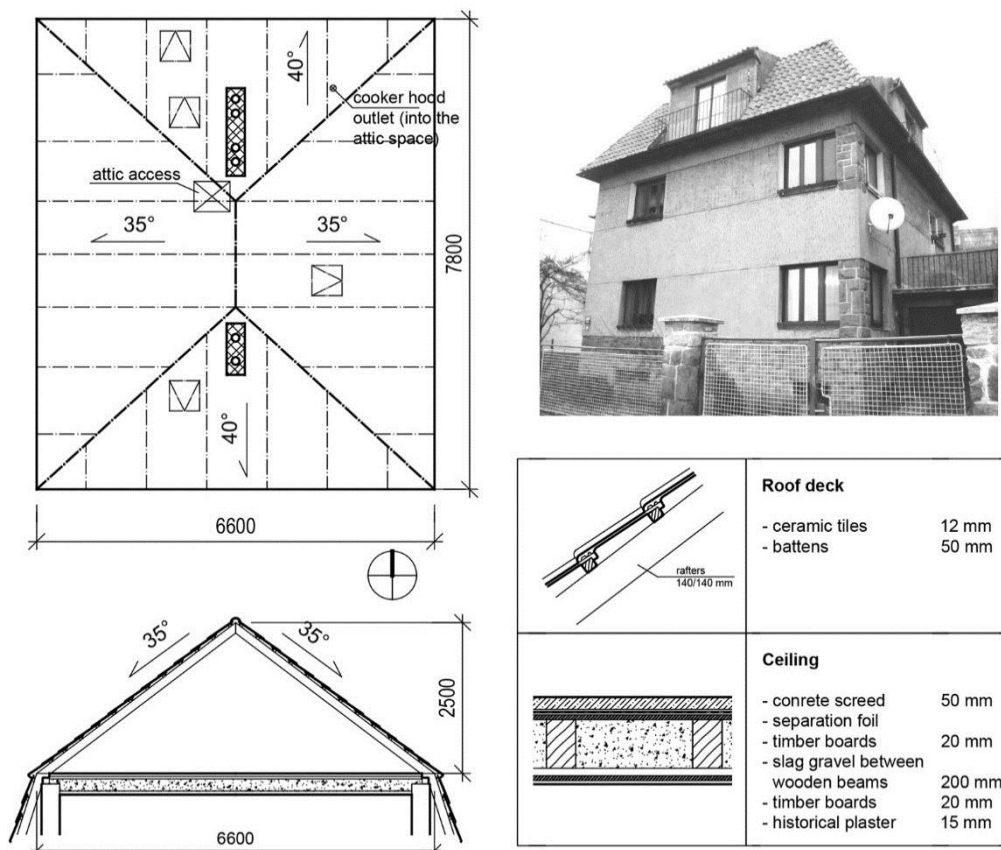


Fig. 9: Geometry and construction assemblies of historical attic

Modern cold attic with gable roof depicted in figure 10 is slightly ventilated by intended leakages in an unsealed overlaps of the vapour-permeable underlay felt. Roofing is made out of concrete tiles on laths and contra-laths that formed ventilated roof-deck cavity. Roof slope is 40 ° and roof decks are oriented to south and north. Ceiling construction is formed by wooden beams with a mineral wool insulation in between them, vapour tight foil from interior side covered by the gypsum boards. There was observed during the construction process that the workmanship in terms of the airtight quality of the air-barrier layer is very good. On the top of the ceiling there is an OSB board forming the attic floor.

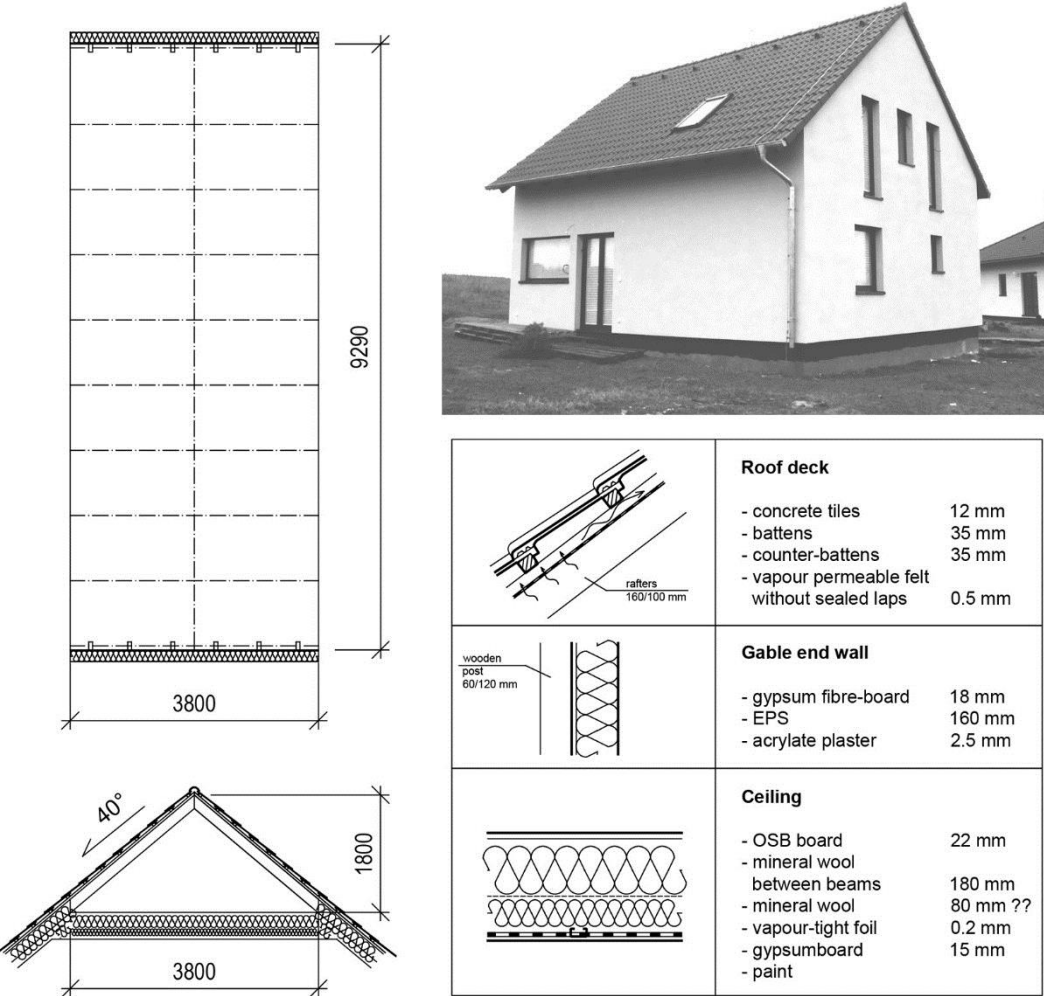


Fig. 10: Geometry and construction assemblies of the modern cold attic with vapour permeable underlay felt

Geometry and constructions of cold attic in figure 11 is quite similar to the previous one (see Fig. 10). However instead of vapour-permeable underlay felt, there is a vapour-tight foil installed in the roof deck assembly. In a not-sealed overlaps of the foil there are, under normal use, placed plastic bottles that keep the overlaps open in order to provide attic ventilation. This measure was performed by owners when they found a condensation on the underlay foil. Attic ventilation that was performed keeps the attic without condensation. However for purposes of measurement the ventilation gaps in the foil were provisionally taped (sealed) to get worst case scenario (although there were still some limited ventilation).

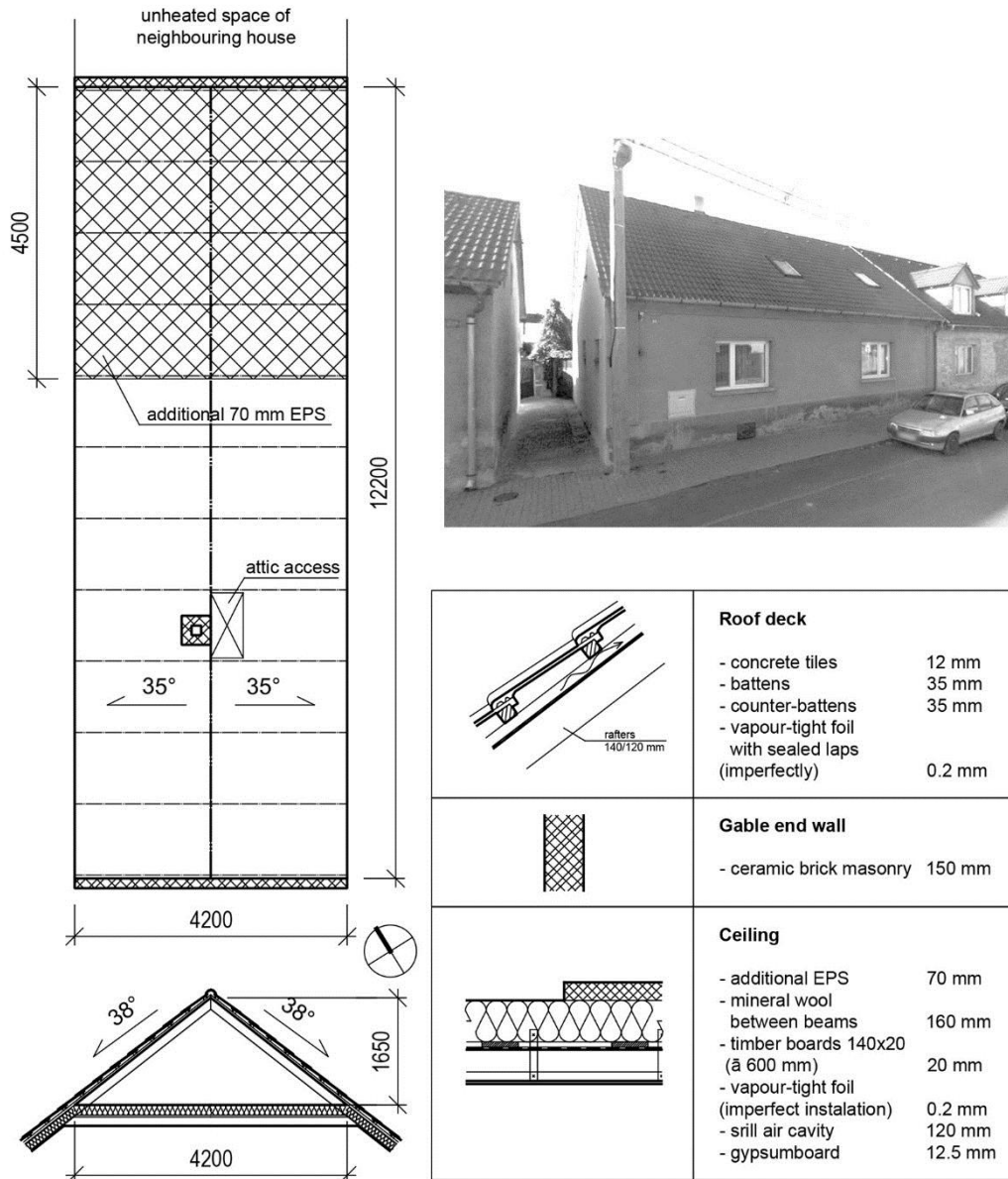


Fig. 11: Geometry and construction assemblies of the modern cold attic with vapour-tight underlay foil

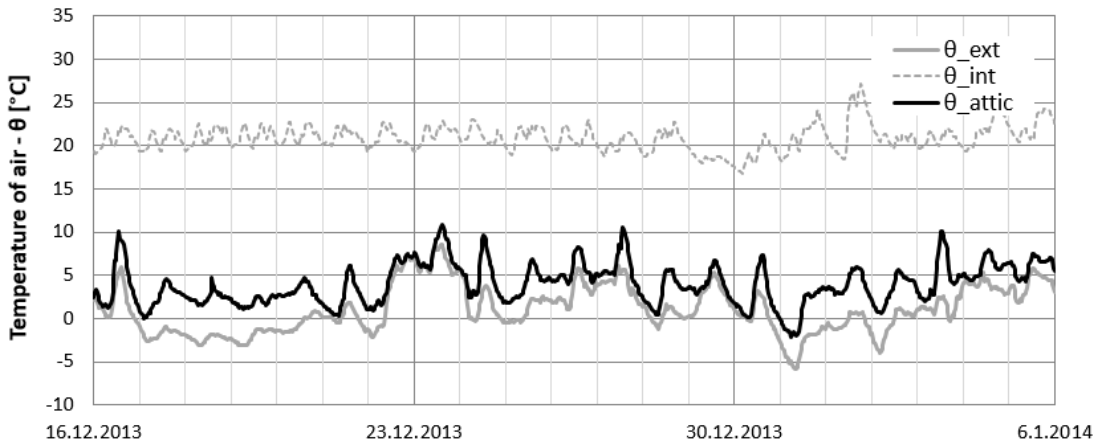
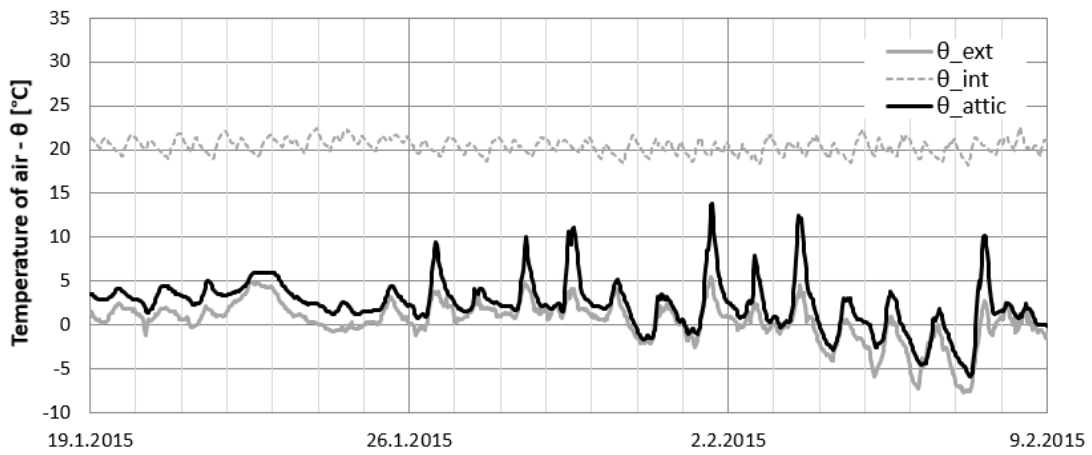
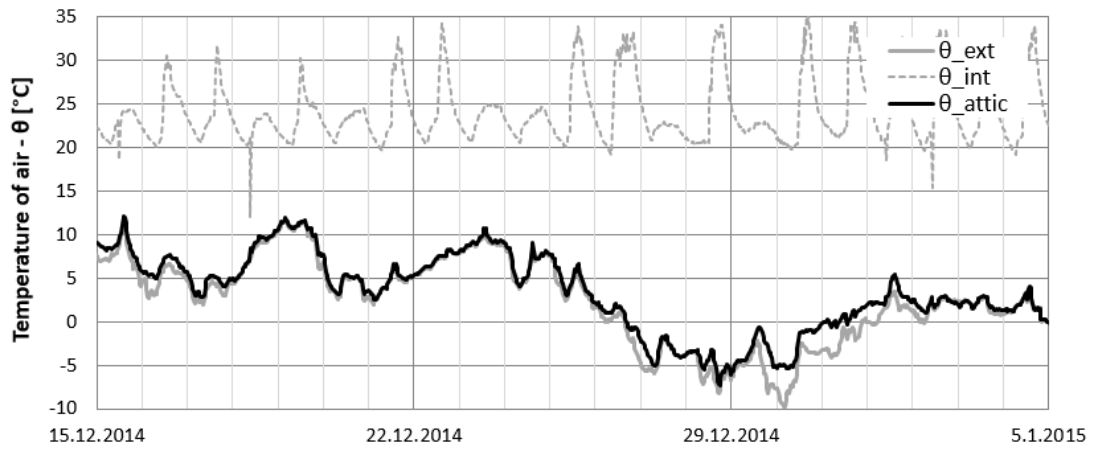


Fig. 12: Temperature courses related to three attic designs – top: historical attic, middle: modern attic with vapour-permeable underlay felt, bottom: modern cold attic with vapour-tight underlay foil.

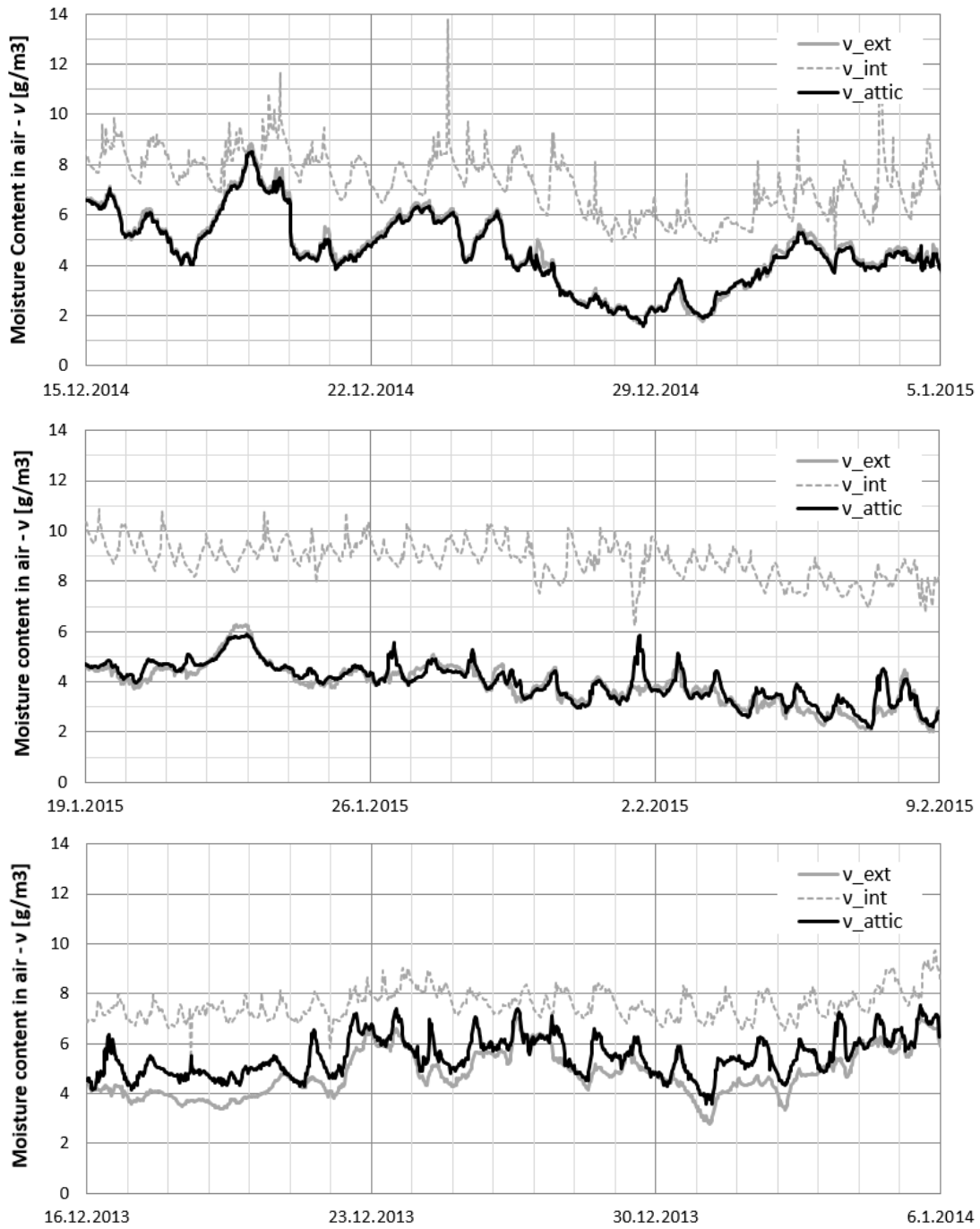


Fig. 13: Water vapour concentration courses related to three attic designs – top: historical attic, middle: modern attic with vapour-permeable underlay felt, bottom: modern cold attic with vapour-tight underlay foil.

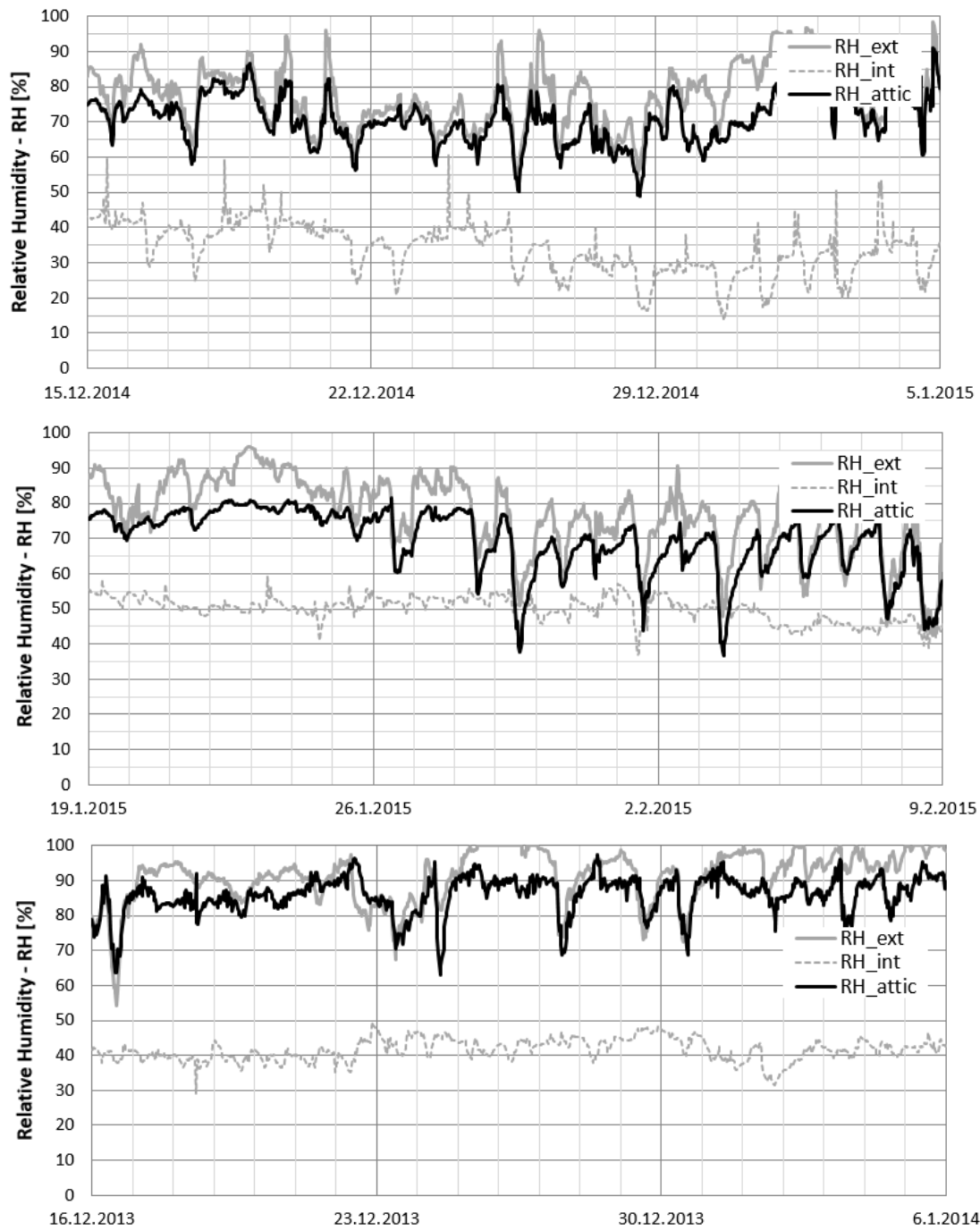


Fig. 14: Relative humidity courses related to three attic designs – top: historical attic, middle: modern attic with vapour-permeable underlay felt, bottom: modern cold attic with vapour-tight underlay foil.

Tab. 2: Comparison of average values of temperature and vapour concentration from brief measurements on three different attic designs

	average temperature [°C]				average vapour concentration [g/m ³]			
	θ_{int}	θ_{ext}	θ_{att}	$(\theta_{att} - \theta_{ext})$	v_{int}	v_{ext}	v_{att}	$(v_{att} - v_{ext})$
historical attic	24.1	2.5	3.4	0.9	7.3	4.6	4.5	-0.1
modern cold attic with vapour permeable underlay felt	20.4	0.5	2.4	1.9	8.8	3.9	4.0	0.1
modern cold attic with vapour-tight underlay foil	20.9	1.1	4.0	2.9	7.6	4.8	5.5	2.8

As can be seen in figures 12-14 and table 2, the hygro-thermal conditions in historical attic space are kept very close to the outdoor environment. It is due to the high ventilation rate of the attic. Measured average temperature of attic air within the analysed 3 weeks is 0.9 °C higher than the temperature of outdoor air. Average measured vapour concentration is practically the same as in outdoor air (although there are quite massive air leakages from interior - through the attic staircase and exhausted air from the kitchen hood that end in the attic).

The average temperature in modern, slightly ventilated cold attic with vapour-open roof underlay is about 2 °C higher compared to outdoor air. Since the ceiling construction below the attic is well insulated and has good quality of air-tightness, the reason for the temperature can be twofold – small ventilation rate and high number of sunny days. As can be seen in a relevant figure, the course of outdoor air temperature implies that there were a number of sunny days and thus both reasons for high average temperature in attic are relevant. Small ventilation rate is confirmed also by vapour concentration courses, where can be seen that although the average values of the attic and outdoor air concentrations are the same, the attic concentration course has lower extremes which means that inner constructions (mainly wooden) had a time to work with a moisture (adsorbing and releasing). This effect can be also caused by the vapour-permeability of the underlay foil which needs some time to let pass the vapour through. Vapour concentration courses also confirm good quality of air- and vapour-tightness of the ceiling as the concentration within the attic is not affected by the higher concentration in interior.

In last case – modern cold attic with poor quality of ceiling air-tightness, low ventilation of the attic and vapour-tight underlay foil – can be seen higher temperature and concentration rise affected most likely by the airflow from interior to the attic space. Average temperature is 3 °C higher than an outdoor air (also a lot of sunny days during measurement were present) while the average measured vapour concentration was 2.8 g/m³ higher compared to outdoor air. Since the average attic air temperature was 4 °C while the saturated vapour concentration at that temperature is 5.0 g/m³, the average measured concentration 5.5 g/m³ means that there was possibly often a conditions for underlay surface condensation. That is confirmed also by figure 1b which was taken in this attic space.

Based on presented data can be illustratively seen how the different attic designs affects their hygro-thermal conditions in climate of Prague (Czech Republic).

2 Review of studies

In order to gain a deeper insight into the problematic, the set of attic designs tested in the most credible studies were compared. Processes of selection of the studies and attic designs that were tested within them are described in following section.

2.1 Methods

2.1.1 Selection of studies and attic designs

A set of 25 quality studies dealing with hygro-thermal performance of cold attics were found [1-25]. Studies were published mostly in period 1996 – 2019 (except one from 1941), which corresponds to historical development of new materials and assemblies, that was mentioned in an Introduction section. From the studies were further excluded those that do not contain enough information for further analysis. Also in cases where more than one study of the same authors presented similar results, just one representative study was selected, while others were removed from the list. Two more studies were later also excluded due to specific reasons – one of them was found not to be located within a HCT climate [24] and second was found to be in essential contradiction with all others and thus was labeled as an outlying study (similarly to outlying values in statistical sample set) [21]. After the selection process, only 9 studies remained [1-9].

In next step a particular attic designs were selected from the studies for further analysis. Not all the designs presented within all selected studies were taken, but only the representative ones to cover the whole range of different attic designs within each particular study. If very similar designs with similar behaviour were presented related to one study, just one representative was picked. Finally a set of 28 designs was selected for further comparison process (see table 3). Another 7 designs (supplementary designs) are presented within the table as well. Those designs are not for different reasons included in the main comparison, but are present within the table as they possibly contain some supplementary pieces of information to possibly confirm some of the logical patterns that will be found in the main comparison or seal some gaps in the overall picture of the problematic. Reasons for not including those design are as follows:

- Designs 1-3 were excluded because of very short period of measurement in moreover constant conditions (several days of measurement instead of at least 3 months as the shortest period according to all other selected designs)
- designs 22-24 were excluded from the main design set because of using mechanical adaptive ventilation of the attic and thus were not comparable with others)
- design 35 was excluded because it is not actually an attic space, but just standalone roof (without any dwelling below it) of a mailbox exposed to the outside conditions.

Numbering of the designs within table 3 are ascending according to the year of studies publication dates.

2.1.2 Selection of comparative parameters

For an appropriate comparison of the selected attic designs it was needed to choose an appropriate key parameters. Hygro-thermal performance of an attic space depends, in general, on the two surrounding environments (interior and exterior) and on properties of an envelope constructions. Therefore it is quite straight forward the state that the key parameters have to be an air and vapour permeance and thermal resistance of an attic envelope constructions (thermal and moisture capacities of those constructions are considered to not affect the overall hygro-thermal conditions remarkably and thus are not included to the key parameters). Choosing a particular physical quantities representing such a properties is however not that straight forward. Reasons for their selection follows.

Ceiling air permeance

As mentioned in section “1.4 Causes of problems”, the most important parameter affecting moisture performance of cold attic is an air-tightness of ceiling construction. This property is most usually expressed as air permeance - ϕ [$1/(s \cdot m^2 \cdot Pa^L)$]. Since the most frequented reference pressure differences for air permeance are 50 and 75 Pa, in this study is used reference value at 50 Pa pressure difference $\phi_{50,ceil}$ [$1/(s \cdot m^2 \cdot Pa^L)$] to be one of the key parameters listed in table 3.

Although the ϕ_{50} has an illustrative reference value that can be compared with other constructions, it is not much informative in terms of real airflow rate across the ceiling under real building operation or during the experiment or simulation. Reason is that the airflow through the ceiling is affected, beside others, also by the air-tightness of an interior and attic space (of their envelope constructions). If the envelope constructions of one or both of them (excluding the ceiling) would be perfectly air-tight, no flow across the ceiling takes place, even when leaky (if not considered parallel two-direction flow across the ceiling). Also if there would be a lower pressure kept on the interior side of the ceiling (generated for instance by interior exhausted ventilation system), there will also be no flow from interior into the attic space, even when the ceiling would be leaky. Many other cases can be stated to confirm that the real airflow across the ceiling is quite regardless of its reference air permeance value. Therefore for the purposes of further analysis is needed to quantify the real density of volumetric airflow (volumetric flux) under the real pressure difference across the ceiling $\dot{V}_{real,ceil}$ [$1/(s \cdot m^2)$], that covers air-tightness and pressure differences of all envelope and ceiling constructions in itself. However this parameter is still not sufficient enough for purposes of designs comparison in table 3. That is because the attic moisture safeness is not just related to the realistic amount of interior air (and so the moisture) entering the attic space, but also related to the attic volume. Obviously there will be higher moisture risk within a smaller attic than within a larger one having the same ceiling area and same air (and so moisture) input. Therefore the second, but possibly the most important parameter chosen for comparison of attic designs in table 3 is the attic air change rate related to the real interior-attic air flow ($n_{real,ceil}$ [ach]). It should be emphasized that this quantity is evaluated regarding the attic volume instead of interior volume.

Ceiling vapour permeance

Ceiling vapour permeance is much less important regarding attic moisture safeness compared to the air permeance (see section 1.4 *Causes of problems*). In any case the diffusion is a mechanism of possible moisture transport to the attic and thus it should not be underestimated. The more the ceiling construction is air-tight, the relatively much important role the vapour permeability can play. Ceiling vapour permeance represented by equivalent air layer thickness ($s_{d,ceil}$ [m]) is therefore the third key parameter for designs comparison.

Ceiling thermal resistance

Thermal resistance of the ceiling construction affects temperature within the attic space, which is directly linked to relative humidity and so with attic moisture safeness. However the ceiling thermal resistances (in cold attics) are much higher (at least around 3.3 m²K/W according to the selected studies) compared to the ordinary roof-deck construction (ca. 0.3 m²K/W), and thus the temperature within the attic is in cold season only about 1-2 °C higher than outdoor air temperature, even without attic ventilation (neglecting sky radiation effect). Therefore this parameters seem to not be as important, however there is no doubt that it should be included in the presented parameters as one of the general characteristic and due to its illustrativeness. Thermal transmittance (U_{ceil} [W/(m²K)]) was used instead of thermal resistance value in table 3.

Roof-deck vapour permeance

There are many discussions about vent or not to vent the attic in distinct climates. Both options seem to work satisfactorily, but in the same time both options recoded moisture problems. If the attic is designed as unventilated (so called sealed) it is preferable to use a vapour-permeable underlay felt under ventilated roof-deck cavity. However some studies tested an unventilated attic designs using a vapour-tight PE underlay foils. Since there could be a difference in moisture safeness according to this difference, an equivalent air layer thickness of the roof-deck ($s_{d,r.deck}$ [m]) is stated as another key parameter in table 3. In case of double-skin roof decks with ventilated cavities, s_d -value of just the lower skin is considered.

Thickness of ventilated roof-deck cavity

However this parameter can seem to not be much important, it is at first an illustrative information to imagine the roof deck construction when looking at table 3. Second reason is that such a ventilated cavity inhibits longwave sky radiation and so the solar radiation acting on the top surface of the roof deck. Therefore it affects the inner attic surface temperature and thus this information can be useful for further considerations about differences in moisture consequences.

Attic ventilation air change rate and ventilation ratio

As mentioned above, there are many discussions about whether the attic should be ventilated in distinct locations and how much. Therefore the attic real air change rate caused by ventilation by outdoor air ($n_{\text{real,ext}}$ [ach]) is another key parameter in table 3. Second parameter according to the attic ventilation (that is evaluated in brackets) is what we call a ventilation ratio. Regarding attic ventilation, there is a well-known ventilation rule (so called 1:300 rule or more modern 1:150 rule). This rule was stated based on study from 1939 [35] and up to present it seems still satisfactorily useful. It says that area of all attic vents should be ca. 1:300 of the attic floor area. We accordingly state for most of selected attic design their ratios of an attic ventilation opening area and attic floor area and called it “ventilation ratio”.

Moisture-related consequences

The most interesting information regarding a particular attic designs is obviously its suitability for HCT climate (i.e. its moisture safeness in such conditions). However most of the studies do not provide such an information. Nevertheless they provide an information about the moisture performance that is described in last column of table 3. Although the different studies adopted different parameters and approaches how to provide such an information, it can give some clue in further considerations about moisture safeness.

More information about quantification of values that were not completely provided within the studies and assumptions made in such a calculations can be found in following section.

2.1.3 Quantification of parameters

In table 3 are listed values of key parameters of different attic designs. These parameters were chosen for further comparison and their selection process is described in previous section. Nevertheless almost none of the studies provided all the parameters sharply or in the specific way that is intended to work with. Therefore some of the values had to be calculated based on other pieces of information available.

According to table 3, values typed in black normals are exact values that were stated in particular studies (i.e. values cited from the studies). Values typed in black italics are values that were calculated directly according to the pieces of information presented within particular studies. For example, if a figure of an attic floor plan with dimensions was provided, we calculated attic floor area based on such a figure. Such a value is then written in black italics. The black italics were used also when the values were calculated using commonly known properties of building materials. For example, if a material layers of a ceiling assembly were provided without other information, an equivalent air layer thickness was calculated using commonly known material properties. Since such a values are not precise, they are all accompanied with “circa” (ca.).

Values typed in grey italics are still based on information presented within the original studies, but more calculations and assumptions were made for their evaluation. Most common assumptions related to such a calculations are listed in following text.

Ceiling air permeance

$n_{\text{real,ceil}}$ - this value is an attic air change rate corresponding to interior-attic airflow under real conditions (more information can be found in previous section). If only an information about ceiling air-tightness was provided in the particular study, this value is calculated considering an interior overpressure 4 Pa (in adequate cases). Such a pressure difference value is in realistic range for buildings and therefore also a value used for determination of an equivalent leakage area (ELA) [57,58]. For the calculation a power law is adopted (see eq.(6)) with flow exponent $L=0.67$, which is a common value for many building assemblies [for instance 58, 69]. Values calculated in such a way are accompanied with upper index (*). For cases with well-sealed attics or interior spaces, the calculation is made using 2 Pa interior overpressure. Those values are signed with (**).

If the study provides $n_{\text{real,ceil}}$ or $\dot{V}_{\text{real,ceil}}$, but not a reference n_{50} or $\phi_{50,\text{ceil}}$ value, those reference values were calculated based on the same assumptions about the real pressure difference across the ceiling (if not provided more accurate information). Such reference values are signed with (*) and (**).

All airflow calculations are performed using power law with flow exponent $L = 0.67$ when the flow takes place across an assembly and $L=1.0$ when the flow takes place across a single material without any joints.

Ceiling vapour permeance

If the ceiling contains an air-barrier (e.g. PE foil), it is assumed that this foil has s_d -value 10 m. Since this layer is in most cases the dominant in terms of vapour resistance, the rest of the layers are mostly neglected. In relevant cases the values are slightly adjusted with respect to other layers. s_d -value of wood or wooden based sheathing without a specification of its thickness is assumed to be 2.5 m. This value is in relevant cases adjusted based on information present in the particular study. For all other calculations are assumed commonly known material properties.

Ceiling thermal transmittance

Value was calculated considering convective heat transfer coefficients evenly on both surfaces equal to $\alpha_c = 7.7 \text{ W}/(\text{m}^2\cdot\text{K})$. When the thermal conductivity value of thermal insulation was not specified, value 0.04 was used. For other materials was used common material properties.

Roof-deck vapour permeance

Single-skin roof decks with asphalt shingles as a roofing is uniformly considered s_d -value equal to 200 m. In cases of double-skin roof decks with ventilated cavity just vapour resistance of the lower deck was considered. Mostly the underlay s_d -value was specified. In cases where just an information that PE foil was used as an underlay, s_d -value = 10 m was considered.

Thickness of ventilated roof-deck cavity

When the cavity was formed by the battens and contra-battens, the cavity thickness was considered as ca. 50 mm. No other cases were finally present.

Attic ventilation air change rate and ventilation ratio

This parameter was mostly, in some form, present within most of the studies. However the value present in table 3 was calculated very differently using many different assumptions. Those particular assumptions are described in the footnotes of table 3 (according to the index labels). In relevant cases, the value was stated as an average within the heating season (as the critical part of the year).

Moisture-related consequences

It was tried to provide short but complete information of the possible worst conditions and their duration. As each study provided different quantity as the result of hygro-thermal conditions within the attic space, the stated moisture consequences have different forms, units etc.

2.1.4 Quantification of values in moisture-evaluation charts

In order to get a deeper insight in attic designs moisture safeness, two charts for rough graphical estimations were created (see Fig. 15 and 16). Charts are very similar, using weekly and monthly averaged data of temperature, relative humidity and wood moisture content. Therefore the designs whose moisture performance was characterized just by mould index or amount of condensate were not displayed within the charts. However also some of the designs characterized by relative humidity or roof sheathing moisture content did not provide all the data needed, most often the temperature data. In this section are therefore described an assumptions for quantification of such a values. Assumptions are mostly very simple to keep the quantification process as easy and clear as possible. More information about the moisture safeness assessment based on mentioned charts are presented in section 2.3.2 *Moisture-risk evaluation*.

Temperature quantification

First set of assumptions is related to temperature values that were not described in original studies. In those cases a temperature from a climate chart according to [79] was used. The average temperature within a cold attic during heating season is commonly around 1 and 2 °C higher than within an outdoor environment in ventilated and unventilated attic respectively. These values are therefore added to the monthly averaged temperature value taken from climate charts. Moreover regarding a weekly averaged values there could be obviously a higher temperature recorded within an attic compared to monthly average. For weekly values we therefore added extra 3 °C as an estimated maximal difference between the two temperatures. Adding instead of subtracting the value is on a safe side as the conditions for mould growth are more suitable the higher the temperature (in reasonable limits). The same 3 °C were added to monthly averaged temperatures that were provided in original study (in order to get weekly averaged values).

In cases when the temperature values were provided as a courses within a chart, their weekly and monthly averages were best estimated from the chart.

Relative humidity quantification

Relative humidity values were usually provided in charts regarding hourly or weekly averages or in table providing usually monthly averages. To get a weekly values from monthly ones, we add “just” 3 %RH because of two reasons. First is related to the weekly temperature – it is not much likely to record maximal weekly average of relative humidity within the same week where maximal averaged value of temperature was recorded. Second reason is that in high relative humidity levels where we want to be more precise than in lower levels there is a higher and higher sorption capacity of wooden truss (and also of most of other materials), that inhibits the rise of relative humidity value.

Wood moisture content quantification

Some studies provided a data of moisture content by mass of wood-based roof sheathing. In such a cases the values were again best estimated from chart courses, if available. When just a monthly averages were provided the values were firstly converted to equilibrium relative humidity according to sorption isotherm of spruce wood described in [50]. Than a 3 % of relative humidity were added to obtained value as well as in case of editing non-converted values of relative humidity described previously.

Relation between the relative humidity and wood moisture content depicted on an opposite axes in charts 15 and 16 is based on the same sorption isotherm description.

2.1.5 Uncertainties

There are many uncertainties of different types within the results of this study. To be realistically sceptical about the results, the main uncertainties are mentioned in following text.

At first, the uncertainties are bonded with the original studies themselves – e.g. uncertainty of experimental design, of measurement and data processing or uncertainties of numerical models and their simplifications. Other uncertainties are bonded with boundary conditions as the measurement would have been performed during an unusual weather conditions or in case of numerical modelling there is an uncertainty of properly selected weather dataset.

Uncertainties are bonded also with an original authors' interpretations of the findings as well as with our understanding to them. Finally there are uncertainties of our calculations and possibly the largest uncertainties of our assumed values.

Despite all, if the sample set (dataset) will be sufficiently large, there should be possible to find some logical patterns and common features between similar attic designs, which is the goal of this study.

2.2 Results

Tab. 3. Summary of selected cold attic set-ups

Design no.	Study	Study type	Attic location	Kuppen-Geiger climate class. according to [73]	Interior conditions	Attic design parameters							Moisture-related consequences
						$n_{50, \text{ceiling}}$ [ach] ($\phi_{50, \text{ceiling}}$ [l/s/m ² /50Pa ^{0.5}])	$n_{\text{real}, \text{ceiling}}$ [ach] ($\dot{V}_{\text{real}, \text{ceiling}}$ [l/s/m ²])	$S_{d, \text{ceiling}}$ [m]	U_{ceiling} [W/m ² /K]	$S_{d, \text{r. deck}}$ [m]	Ventilated roof-deck cavity thickness [mm]	$n_{\text{real}, \text{ext}}$ [ach]; (ventilation rule)	
28	Essah et al. (2009) [8]	C	United Kingdom	Cfb 	20-25 °C 40-70 %RH (according to high occupancy in mentioned standard) $n_{50} = 5$ ach (1 year sim.)	0	0	ca. 0.5 ^{ee}	ca. 0.15	0.02	ca. 50	estimated ca 0.1 no intentional openings (roof leakage flow rate is several orders of magnitude lower than intentional ventilation)	2 kg/year of condensate on the attic underlay (ca. 26 g/m ² /year)
10	Samuelson (1998) [3]	E	Bores, Sweden	Cfb 	ca. 17 - 24 °C 31-55 %RH (1 year meas.)	0	0	ca. 10	0.077	ca. 2.5	ca. 50	ca. 0.2 ^{2a} non-ventilated	max monthly avg. RH = 90 % (december)
11	Samuelson (1998) [3]	E	Bores, Sweden	Cfb 	ca. 17 - 24 °C 31-55 %RH (1 year meas.)	0	0	ca. 10	0.077	ca. 2.5	ca. 50	ca. 32 ³³ natural eave ventilation (ca. 1:84)	max monthly avg. RH = 93 % (december)

18	Kalagasidis and Mattsson (2005) [5]	C	South-west coastal area of Sweden	Cfb  wind exposure – city	22 °C 40 - 70 %RH (1 year sim.) exhaust-supply ventilation (exhaust 120 m ³ /h – supply 90 %)	0	0	ca. 11	ca. 0.077	ca. 2.6	ca. 50	mean 0.1 (unventilated design)	Mould index = 0.001 ^{*,#d} (four year simulation)
27	Essah et al. (2009) [8]	C	United Kingdom	Cfb  wind exposure – city	20-25 °C 40-70 %RH (according to high occupancy in mentioned standard) n ₅₀ = 5 ach (1 year sim.)	0	0	ca. 0.5 ^{*,e}	ca. 0.15	moisture dependent 0.6–4.6	ca. 50	estimated ca 0.1 no intentional openings (roof leakage flow rate is several orders of magnitude lower than intentional ventilation)	66 kg/year of condensate on the attic underlay (ca. 870 g/m ² /year)
9	Samuelson (1998) [3]	E	Bores, Sweden	Cfb  wind exposure – city	ca. 17 - 24°C 31-55 %RH (1 year meas.)	0	0	ca. 10	0.077	ca. 10	ca. 50	mechanical 2 ach	max monthly avg. RH = 96 % (december)
21	Hagentoft et al. (2008) [7]	C	Gothenburg region, Sweden	Cfb  wind exposure – city	30–60 %RH; - balanced ventilation (1 year sim.)	0	0	ca. 10	ca. 0.10	ca. 12	ca. 50	ca. 22 ^{*,#} (130 ach at 50 Pa p. dif.)	Mould index = 1.35 [#] (total of 11 weeks in 90-100 %RH and 0-5 °C; 5 weeks in 80-90 %RH and 5-15 °C; 3 weeks in 70-80 %RH and above 15 °C)

26	Essah et al. (2009) [8]	C	United Kingdom	Cfb 	20-25 °C 40-70 %RH (according to high occupancy in mentioned standard) n ₅₀ = 5 ach (1 year sim.)	0	0	ca. 0.5 ^{ee}	ca. 0.15	40	ca. 50	estimated ca 0.1 no intentional openings (roof leakage flow rate is several orders of magnitude lower than intentional ventilation)	83 kg/year of condensate on the attic underlay (ca. 1100 g/m ² /year)
25	Essah et al. (2009) [8]	C	United Kingdom	Cfb 	20-25 °C 40-70 %RH (according to high occupancy in mentioned standard) n ₅₀ = 5 ach (1 year sim.)	0	0	ca. 0.5 ^{ee}	ca. 0.15	40	ca. 50	ca. 4.6 ^{rk} (ca. 1:170) (28 ach at 50 Pa p.dif.) (20 mm openings along the eaves)	0 kg/year of condensate on the attic underlay
8	Burch et al. (1996) [2]	C	Madison (WI), USA	Dfb 	20 - 24 °C ca. 20 - 60 % (1 year sim.)	0	0	ca. 2.6	ca. 0.24	ca. 200	N	ca. 9 ^{hb} (1:300)	highest weekly MC of north roof sheathing (within 1 year sim.) = 14 %
14	Ojanen (2001) [4]	E	Espoo, Finland	Dfb 	22 °C ca. 35 %RH (6 month meas.) 20Pa nterior overpress.	ca. 0.01 th (ca.0.002 th)	ca. 0.001 ^{**} (ca. 0.0002 ^{**})	ca. 10	ca. 0.15	ca. 0.02	ca. 50	ca. 0.1 ^{ti} (no intentional vents)	max weekly MC = 18 % (6 months meas.)

32	Essah et al. (2009) [8]	C	United Kingdom	Cfb 	20-25 °C 40-70 %RH (according to high occupancy in mentioned standard) n ₅₀ = 2 ach (1 year sim.)	0.9 [†] (0.24 [†])	0.18 [*] (0.05 [*])	ca. 10	ca. 0.15	40	ca. 50	ca. 3.3 ^{rk} (ca. 1:340) (ca. 20 ach at 50 Pa p.dif.) (10 mm openings along the eaves)	43 kg/year of condensate on the attic underlay (ca. 560 g/m ² /year)
33	Essah et al. (2009) [8]	C	United Kingdom	Cfb 	20-25 °C 30-60 %RH (according to normal occupancy in mentioned standard) n ₅₀ = 2 ach (1 year sim.)	0.9 [†] (0.24 [†])	0.18 [*] (0.05 [*])	ca. 10	ca. 0.15	40	ca. 50	ca. 3.3 ^{rk} (ca. 1:340) (ca. 20 ach at 50 Pa p.dif.) (10 mm openings along the eaves)	4 kg/year of condensate on the attic underlay (ca. 53 g/m ² /year)
20	Hagentoft et al. (2008) [7]	C	Gothenburg region, Sweden	Cfb 	30-60 %RH; - balanced ventilation (1 year sim.)	0.3 (0.09)	0.22 (0.06) (annual average)	ca. 10	ca. 0.10	ca. 12	ca. 50	ca. 22 ^{***} (130 ach at 50 Pa p. dif.)	Mould index = 3.24 [†] (total of 12 weeks in 90-100 %RH and 0-5 °C; 6 weeks in 80-90 %RH and 5-15 °C; 3 weeks in 70-80 %RH and above 15 °C)
17	Kalagasidis and Mattsson (2005) [5]	C	South-west coastal area of Sweden	Cfb  wind exposure – city	22 °C 40 - 70 %RH (1 year sim.) exhaust-supply ventilation (exhaust 120 m ³ /h – supply 90 %)	ca. 1.4 ^(*) (ca.0.44 ^(*))	ca. 0.25 ^(*) (ca. 0.08) (heating season avg.)	ca. 11	ca. 0.077	ca. 2.6	ca. 50	mean 0.1 (unventilated design)	Mould index = 4.9 ^{*,#d} (four year simulation)

15	Kalagasidis and Mattsson (2005) [5]	C	South-west coastal area of Sweden	Cfb  wind exposure – city	22 °C 40 - 70 %RH (1 year sim.) exhaust-supply ventilation (exhaust 120 m ³ /h – supply 90 %)	ca. 1.4 ^(*) ca. 0.44 ^(*)	ca. 0.25 ^(*) (ca. 0.08) (heating season avg.)	ca. 11	ca. 0.077	ca. 2.6	ca. 50	mean 2.2 (natural eave ventilation)	total of 15 weeks in 90-100 %RH and 0-10 °C; 4 weeks in 80-90 %RH and 0-10 °C; 1.8 weeks in 80-90 %RH and 10-20 °C Mould index = 0.25 ^{*,#d} (four year simulation)
16	Kalagasidis and Mattsson (2005) [5]	C	South-west coastal area of Sweden	Cfb  wind exposure – open area	22 °C 40 - 70 %RH (1 year sim.) exhaust-supply ventilation (exhaust 120 m ³ /h – supply 90 %)	ca. 1.4 ^(*) ca. 0.44 ^(*)	ca. 0.25 ^(*) (ca. 0.08) (heating season avg.)	ca. 11	ca. 0.077	ca. 2.6	ca. 50	mean 13.9 (natural eave ventilation)	total of 11 weeks in 90-100 %RH and 0-10 °C; 7 weeks in 80-90 %RH and 0-10 °C; 4 weeks in 80-90 %RH and 10-20 °C Mould index = 0.33 ^{*,#d} (four year simulation)
29	Essah et al. (2009) [8]	C	United Kingdom	Cfb 	20-25 °C 40-70 %RH (according to high occupancy in mentioned standard) n ₅₀ = 5 ach (1 year sim.)	2.2 ⁻¹ (0.6 ⁻¹)	0.27 ^{**} (0.07 ^{**})	ca. 0.5 ^{se}	ca. 0.15	0.02	ca. 50	estimated ca 0.1 no intentional openings (roof leakage flow rate is several orders of magnitude lower than intentional ventilation)	17 kg/year of condensate on the attic underlay (ca. 220 g/m ² /year)

31	Essah et al. (2009) [8]	C	United Kingdom	Cfb 	20-25 °C 40-70 %RH (according to high occupancy in mentioned standard) n ₅₀ = 5 ach (1 year sim.)	2.2 ^{±1} (0.6 ^{±1})	0.36 [*] (0.1 [*])	ca. 0.5 ^{±e}	ca. 0.15	0.02	ca. 50	ca. 4.6 ^{±k} (ca. 1:170) (28 ach at 50 Pa p.dif.) (20 mm openings along the eaves)	175 kg/year of condensate on the roof underlay (ca. 2300 g/m ² /year)
30	Essah et al. (2009) [8]	C	United Kingdom	Cfb 	20-25 °C 40-70 %RH (according to high occupancy in mentioned standard) n ₅₀ = 5 ach (1 year sim.)	2.2 ^{±1} (0.6 ^{±1})	0.36 [*] (0.1 [*])	ca. 0.5 ^{±e}	ca. 0.15	40	ca. 50	ca. 4.6 ^{±k} (ca. 1:170) (28 ach at 50 Pa p.dif.) (20 mm openings along the eaves)	207 kg/year of condensate on the attic underlay (ca. 2700 g/m ² /year)
34	Roppel and Lawton (2014) [9]	I	Vancouver (BC), Canada	Cfb 	24.1 °C; 30.7 %RH (winter 2011/2012 averages)	ca. 2.1 ^(*) (ca.0.6 ^(*))	ca. 0.38 (ca. 0.11)	ca. 10.5	ca. 0.12	ca. 200	N	ca. 1 - 8 (depending on measurement method) avg. 4.5 (1:232) baffle vents	Mould index = ca. 4 [±] (observed and also calculated), worst weekly combination of temperature and moisture content of east sheathing was ca. 13 °C; 25 %MC
6	Burch et al. (1996) [2]	C	Madison (WI), USA	Dfb 	20 - 24 °C ca. 20 - 60 % (1 year sim.)	ca. 4.0 ^{±g} (ca. 0.3 ^{±g})	ca. 0.46 ^{**} (ca.0.04 ^{**})	ca. 2.6	ca. 0.24	ca. 200	N	ca. 1 ^{±b} by leakages	highest weekly MC of north roof sheathing (within 1 year sim.) = 28 %

13	Ojanen (2001) [4]	E	Espoo, Finland	Dfb 	22 °C ca. 35 %RH (1 year meas.) (simulated moisture gain – water vessel within attic)	simulated ca. 2.6 ^(*) (ca 0.54 ^(*)) real. ca.0.01 ^{#h} (ca. 0.002 ^{#h})	simulated 0.48 (0.1) real. ca.0.001 ^{**} (ca. 0.0002 ^{**})	ca. 10	ca. 0.15	ca. 0.02	ca. 50	ca 0.1 ^{#i} (no intentional vents)	max weekly MC = 21 % (1 year meas.)
12	Ojanen (2001) [4]	E	Espoo, Finland	Dfb 	22 °C ca. 35 %RH (1 year meas.) (simulated moisture gain – water vessel within attic)	simulated ca. 2.6 ^(*) (ca.0.54 ^(*)) real. ca.0.01 ^{#h} (ca. 0.002 ^{#h})	simulated 0.48 (0.1) real. ca.0.002 [*] (ca. 0.0004 [*])	ca. 10	ca. 0.15	ca. 10	ca. 50	ca. 10 ^{#a} natural eaves (+ridge)	max weekly MC = 21 % (1 year meas.)
4	Burch et al. (1996) [2]	C	Madison (WI), Portland (OR), Atlanta (GA); USA	Dfb  Csb  Cfa 	20 - 24 °C ca. 20 – 60 % (1 year sim.)	ca. 4.0 ^{#g} (ca. 0.3 ^{#g})	ca. 0.74 [*] (ca.0.06 [*])	ca. 2.6	ca. 0.24	ca. 200	N	ca. 9 ^{#b} (1:300)	highest weekly MC of north roof sheathing (within 1 year sim.) = 16 %
5	Burch et al. (1996) [2]	C	Boston (MA); USA	Dfb 	20 - 24 °C ca. 20 – 60 % (1 year sim.)	ca. 4.0 ^{#g} (ca. 0.3 ^{#g})	ca. 0.74 [*] (ca.0.06 [*])	ca. 2.6	ca. 0.24	ca. 200	N	ca. 9 ^{#b} (1:300)	highest weekly MC of north roof sheathing (within 1 year sim.) = 18 %

7	Burch et al. (1996) [2]	C	Madison (WI), USA	Dfb 	20 - 24 °C ca. 45 - 60 % (1 year sim.)	ca. 4.0 ^g (ca. 0.3 ^g)	ca. 0.74 [*] (ca.0.06 [°])	ca. 2.6	ca. 0.24	ca. 200	N	ca. 9 ^h (1:300)	highest weekly MC of north roof sheathing (within 1 year sim.) = 25 %
19	Holm and Lengsfeld (2007) [6]	E	Holzkirchen, Germany	Cfb 	20 - 22 °C 50 - 60 %RH (3 months meas.)	ca. 6.8 ^g (ca.0.85 ^g)	1.25 (0.16)	ca. 10	estimated ca. 0.13	0.22	ca. 50 (non-continuous cavity)	ca. 18 ^h (ca. 1:154) 3 mm eave openings and 20 mm ridge opening	in 11 certain time points (from Jan. to March) a total of 138 g of condensate was wiped from an area of 0.06 m ² of the underlay foil (i.e. 2300 g/m ²) maximum of a single wiping was ca. 30 g/0.06m ² (i.e. 500 g/m ²), measured moisture contents of wooden rafters – in weekly averages ca. 23 %MC in 4 °C; 22 %MC in 5 °C; 19 %MC in 8 °C;
3	Rowley et al. (1941) [1]	E - lab.	Conditioned chamber	-21 °C (condi. chamber)	constant. 21 °C 40 %RH (5 days meas.)	ca. 0.45 (ca. 0.17) (19 mm plaster)	ca. 0.05 ^{**} (ca. 0.019 ^{**})	ca. 0.3	ca. 0.52	ca. 200	N	ca. 0.3 ^h by leakages (no vents)	ca. 52 g/m ² /24h of condensate on underlay sheathing
2	Rowley et al. (1941) [1]	E - lab.	Conditioned chamber	-21 °C (condi. chamber)	constant. 21 °C 40 %RH (6 days meas.)	ca. 0.45 (ca. 0.17) (19 mm plaster)	ca. 0.08 [*] (ca. 0.03 [*])	ca. 0.3	ca. 0.52	ca. 200	N	ca. 4 ^h (ca. 1:98)	ca. 12 g/m ² /24h of condensate on underlay sheathing
1	Rowley et al. (1941) [1]	E - lab.	Conditioned chamber	-21 °C (condi. chamber)	constant. 21 °C 40 %RH (ca. 2 day meas.)	ca. 2.0 (ca. 0.76) (19 mm plaster, leaky attic stair well)	ca. 0.37 [*] (ca. 0.14 [*])	ca. 0.2	ca. 0.52	ca. 200	N	ca. 3 ^h (ca. 1:98)	avg. ca. 75 g/m ² /24 h of condensate on underlay sheathing

24	Hagentoft et al. (2008) [7]	C	Gothenburg region, Sweden	Cfb 	30–60 %RH; - balanced ventilation (1 year sim.)	0	0	ca. 10	ca. 0.10	ca. 12	ca. 50	ca. 0.6 ^{#f} + 1 ach when adaptive ventilation is running (unintentional 17 ach at 50 Pa p. dif.)	Mould index = 0.00 [#] (total of 0 weeks in 90-100 %RH and 0-5 °C; 0 weeks in 80-90 %RH and 5-15 °C; 0 weeks in 70-80 %RH and above 15 °C)
22	Hagentoft et al. (2008) [7]	C	Gothenburg region, Sweden	Cfb 	30–60 %RH; - balanced ventilation (1 year sim.)	0.3 (0.09)	ca. 0.1 ^{#c} (ca.0.03 ^{#c}) (annual average)	ca. 10	ca. 0.10	ca. 12	ca. 50	ca. 0.1 ^{#f} + 1 ach when adaptive ventilation is running (unintentional 11 ach at 50 Pa p. dif.)	Mould index = 1.03 [#] (total of 8 weeks in 90-100 %RH and 0-5 °C; 2 weeks in 80-90 %RH and 5-15 °C; 0 weeks in 70-80 %RH and above 15 °C)
23	Hagentoft et al. (2008) [7]	C	Gothenburg region, Sweden	Cfb 	30–60 %RH; - balanced ventilation (1 year sim.)	0.3 (0.09)	ca. 0.1 ^{#c} (ca.0.03 ^{#c}) (annual average)	ca. 10	ca. 0.10	ca. 12	ca. 50	ca. 0.1 ^{#f} + 5 ach when adaptive ventilation is running (unintentional 11 ach at 50 Pa p. dif.)	Mould index = 0.02 [#] (total of 1 weeks in 90-100 %RH and 0-5 °C; 0 weeks in 80-90 %RH and 5-15 °C; 0 weeks in 70-80 %RH and above 15 °C)
35	Roppel and Lawton (2014) [9]	I	Vancouver (BC), Canada	Cfb 	exterior conditions ca. 3-10 °C; 80-95 %RH	no ceiling (roof deck exposed to outdoor cond.)	no ceiling (roof deck exposed to outdoor cond.)	no ceiling (roof deck exposed to outdoor cond.)	no ceiling (roof deck exposed to outdoor cond.)	ca. 200	N	fully ventilated (roof deck exposed to outdoor cond.)	Mould index = ca. 4 [#] (observed and also calculated), worst weekly combination of temperature and moisture content of east sheathing was ca. 9 °C; 24 %MC

Study type:

- C – computational study
- E – experimental study
- E-lab – experimental study under laboratory conditions
- I – in-situ measurement

Parameters:

- $n_{50, \text{ceiling}}$ - reference interior-attic air change rate at 50 Pa pressure difference (related to attic volume) [ach]
- $n_{\text{real}, \text{ceiling}}$ - real interior-attic air change rate under real conditions (experimental, real or numerically simulated), (related to attic volume) [ach], (see sections 2.1.2 and 2.1.3)
- $n_{\text{real}, \text{ext}}$ - real attic air change rate by ventilation with outdoor air [ach]
- $\phi_{50, \text{ceiling}}$ - reference air permeance across the ceiling construction at 50 Pa pressure difference [$\text{l/s/m}^2/50\text{Pa}^4$]
- $\dot{V}_{\text{real}, \text{ceiling}}$ - real volumetric flux across the ceiling construction under real conditions (experimental, real or numerically simulated) [l/s/m^2], (see sections 2.1.2 and 2.1.3)
- $S_{d, \text{ceiling}}$ - equivalent air layer thickness of the ceiling construction [m]
- $S_{d, r, \text{deck}}$ - equivalent air layer thickness of the roof-deck construction [m]
- U_{ceiling} - thermal transmittance of the ceiling construction [$\text{W/m}^2/\text{K}$]
- vent. ratio - well known rule for attic ventilation, commonly known as 1:300 or 1:150 rule firstly stated in [35]. It is a ratio of total area of all attic ventilation openings to an area of attic floor

Other:

- MC – moisture content [%]
- simulated – simulated by water vessels within the attic with controlled moisture evaporation rate
- real. – realistic value

Notes:

- # - according to VTT mould growth model (1999) [63]
- * - values calculated for 4 Pa interior overpressure using power law with exponent 0.67 (more information in section 2.1.3 Quantification of parameters)
- ** - values calculated for 2 Pa interior overpressure using power law with exponent 0.67 (more information in section 2.1.3 Quantification of parameters)
- *** - air change is calculated for wind speed range 2.5 m/s and wind pressure coefficients 0.25 and -0.5 on the opposite sides respectively (thus total pressure difference across opposite attic vents is 2.8 Pa). Pressure difference across inlet openings is assumed to be half of the value (1.4 Pa). In case of orifice flow, discharge coefficient considered 0.6, flow exponent 0.5 and air density 1.21 kg/m^3 (than the airflow [m^3/s] is ca. 0.9 times opening area [m^2])
- (*) - values calculated from $n_{\text{real}, \text{ceiling}}$ or $\dot{V}_{\text{real}, \text{ceiling}}$ considering that “real” pressure difference is 4 Pa (interior overpressure) and using power law with exponent 0.67 (more information in 2.1.3 Quantification of parameters)
- (**) - values calculated from $n_{\text{real}, \text{ceiling}}$ or $\dot{V}_{\text{real}, \text{ceiling}}$ considering that “real” pressure difference is 2 Pa (interior overpressure) and using power law with exponent 0.67 (more information in 2.1.3 Quantification of parameters)
- ^a - estimated according to specified ventilation regime and values of other studies, taken into account particular experimental design of the study
- ^b - evaluated for wind speed 2.5 m/s according to the chart provided in the study
- ^c - annual average of ceiling leakage is in the study quantified just for sealed attics – for well-sealed attics we consider ca. 0.5 of the values for sealed attic
- ^d - calculated by authors of this paper using data provided by prof. Sasic-Kalagasidis, (VTT mould growth model (1999) [63] was used for calculation)
- ^e - no information about vapour barrier found within the study
- ^f - calculated using power law with flow exponent 0.67 and pressure difference 1.4 Pa (ca. corresponding to surrounding wind speed 2.5 m/s), (see note ***)
- ^g - calculated based on equations and coefficients provided in the study
- ^h - based on assembly specification and found air permeance values of air-barriers without any joints [61]
- ⁱ - calculated based on provided air-permeability data of the underlay, multiplied the value three times and use power law with flow exponent 0.67 and pressure difference 1.4 Pa
- ^j - evaluated based on chart provided within the study
- ^k - calculated based on stated air change rate at 50 Pa pressure difference and using orifice flow equation for 1.4 Pa pressure difference (see note ***)
- ^l - calculated based on set of equations provided within the original study (building air change rate = 5 or 2 ach; parameter b = 0.25)

Table 3 contains 35 rows that represent 28 main and 7 supplementary cold attic designs with evaluated key parameters (see section 2.1.3 *Quantification of parameters*). A lot of values were not sharply stated within the studies and thus we evaluate them as responsibly as we were able to. Values and text typed black normal are sharply stated in the particular. Values and text typed in black italics are calculated based on direct data provided in the original studies. Values and text typed in grey italics are calculated based on other assumptions that are described in sections 2.1.2 *Selection of comparative parameters* and 2.1.3 *Quantification of parameters*. Other assumptions are assigned to each particular value as an upper index label while their explanation can be found in note list below table 3.

Attic designs are numbered ascending according to the year of the study publication and sorted from top to bottom according to the airflow from interior to the attic space, represented by attic air change rate ($n_{\text{real,ceiling}}$). Values are sorted from the lowest to the largest. If multiple designs have the same air change rate, they are sorted according to the vapour permeance of particular roof decks from the most to the least permeable. If also the roof deck permeances are the same, cases of the same roof deck permeability design are sorted according to the amount of ventilation air change rate from the lowest to the largest.

7 supplementary designs are located below the 28 main ones and are distinguished by grey-backgrounded cells.

From the main 28 designs are 7 performed by experimental measurement, 1 by in-situ measurement and 20 by numerical computation.

Designs were performed in 6 countries – USA, Canada, Sweden, Finland, United Kingdom and Germany.

6 designs are located in North America and 22 in Europe while 9 (32 % of all designs) are located in Sweden. Another 9 designs are located in UK and 10 belongs to the rest of the countries. Most of the main designs are located in Cfb climate zone (20 designs), while 7 designs are located in Dfb and 1 in Cfa zones. However the designs are often located very closely to the border of two climate zones and thus these numbers cannot be taken rigidly, and even less when taking into running climate changes.

10 attic designs are non-ventilated while the rest 18 are considered to be ventilated.

Selected studies were published in years 1941 to 2014. Range of real interior-attic air change rate ($n_{\text{real,ceiling}}$) within the main designs is 0 – 1.25 ach with average value 0.27 ach (related to attic volume). Ceiling equivalent air layer thickness ($s_{d,\text{ceiling}}$) is in range of 0.5 – 11 m with average value 6.5 m. Ceiling thermal transmittance is in range of 0.077 to 0.24 W/(m²K) with average value 0.14 W/(m²K) (within the main designs). In the other parameters there are huge differences according to whether the attic should be sealed and vapour-permeable or ventilated, therefore an average values are not relevant to present. Range of equivalent air layer thickness of the roof deck ($s_{d,\text{r.deck}}$) is 0.02 – 200 m, while the lower value represents an underlay felt of double-skin roof deck with ventilated cavity and higher value roof deck made of construction boards with roofing paper and asphalt shingles. The range of exterior-attic air change rate ($n_{\text{real,ext}}$) is in range of 0.1 – 32 ach under realistic conditions. For non-ventilated attics it was mostly around 0.1-0.2 ach while for ventilated attics mostly around 5-18 ach.

2.3 Discussion

2.3.1 General findings

Although table 3 shows well-arranged values of key parameters and the attic designs are sorted in special order to keep the table as much as possible understandable and useful, it can be still quite difficult to orient within it in order to compare different attic designs. As the table takes up several pages, it makes it even more user-unfriendly. However if one wants to work with precise pieces of information, it can be found an appropriate.

By first observation there can be found some relative differences in moisture-related consequences between similar designs related to single study. For instance non-ventilated design 10 that is practically without any moisture input from interior and with medium vapour permeable roof deck has highest monthly averaged relative humidity 90 %RH. The same, but ventilated design 11 records 93 %RH. This difference may seem to be quite low but in those such a high levels of relative humidity the line between moisture-safe and moisture-risky design can be very thin. Anyway the unventilated design seems to be advantageous when there is no moisture input from interior.

In case of more vapour permeable ceiling and less permeable roof deck an opposite moisture consequence can be found – sealed attic design 26 records 83 kg of condensate within a year while ventilated design 25 performs without any condensation.

Similar result can be found by comparing designs 3 and 2, where a huge decrease of condensate amount is recorded within ventilated attic design.

If the air leakage from interior across the ceiling is present, ventilation of the attic can be advantageous as well, as can be seen by comparing designs 17 and 15. A huge drop of mould index is recorded, caused by attic ventilation.

However by simulating two times higher air leakage from interior under Finish (Dfb) conditions, it was found that sealed attic with highly vapour permeable underlay felt has similar moisture performance as ventilated design. It can be found by looking at designs 13 and 12.

All in all based on those relative comparisons it can be stated, that with minimal moisture input from interior, it is advantageous to let the attic to be unventilated but vapour permeable. When the ceiling has low vapour resistance or there is an air leakage present across it, it is advantageous to ventilate the attic (when the outdoor air does not have parameters suitable for mould growth). Moreover it seems that the colder the climate, the more advantageous could the ventilation be. However such a statements still contain large uncertainty since they are stated based just on very few samples. However both statements can be found already presented in some of the most credible studies [5, 18, 24].

Regarding attic ventilation in cold climates, it can be furthermore advantageous as there can be a long periods of snow cover in such an areas. Snow laid on the roof can remarkably increase its thermal resistance and in case of non-ventilate attic the temperature within it can rise up, preparing more suitable conditions for mould growth, when the amount of moisture is sufficient. Higher temperature within the attic can also lead to formation of ice dams [28]. Problem with increased temperature due to snow cover is higher in an attics with single-skin roof deck without ventilation cavity. Although ventilation of the attic in snow or even polar areas can drift some amount of snow into the attic via ventilation openings, but as revealed in [24] it should not cause any moisture problems.

Another relative comparisons between the attic designs can be found related to a change of interior moisture conditions. Comparing ventilated designs 33 and 32, there is a difference of relative humidity ranges of interior spaces beneath them within one year period from 30-60 %RH to 40-70 %RH with equal temperature 20-25 °C. Based on this difference of relative humidity, a tenfold increase of condensate amount on the attic underlay foil was recorded. Affirmatively ventilated designs 4 and 7 located both in Madison (WI), USA, that differ by their interior relative humidity from 20-60 %RH to 45-60 %RH at 20-24 °C, cause an increase of highest weekly averaged moisture content of wooden underlay sheathing from 16 %, which can be still considered as moisture-safe to risky 25 %. It should be mentioned that all four mentioned designs have some air-leakage from interior to the attic. Anyway it can be seen, that even quite small changes of interior relative humidity can cause a difference between moisture-safe and moisture-risky attic design.

Other relative comparison can be made between designs 4 and 5, where just a locality of the simulated attic makes the difference between the two. In design 4 are contained three different locations and also climate zones (Csb, Dfb and Cfa) as the design behaved very similarly at all three places (regarding weekly averages), (see the original study [2]). However the same attic design located in Boston (MA), (design 5) recorded higher moisture content of wooden sheathing underlay (18 % instead of 16 % recorded in design 4). It is questionable whether discussing this difference is relevant, but as the values lay on a border of critical wood moisture content (corresponding to ca. 79 – 83 %RH according to [50]), the difference can be decisive.

One more consideration according to designs 4 and 5 can be made. Although the design 5, located in Boston, belongs to Dfb climate zone as well as one of the attics contained in design 4, it recorded higher sheathing moisture content (as previously mentioned). This difference can be caused by the Boston's maritime location, which could be more humid compared to inland area. This consideration is based on findings from few other studies performed in maritime areas of HCT climate, where the ventilation by outdoor air leads to moisture problems within an attics [7, 9] (as already mentioned in an introduction). Compared to design 4 containing three locations, Madison (WI) and Atlanta (GA) and Portland (OR), it can be stated, that Madison and Atlanta (GA) are inland cities where a different climate can be expected, but Portland (OR) is located quite close to the coast as well as Boston. However Portland lays in Csb climate zone which does not anymore belong to fully humid climates (and so to the stated HCT climate). Therefore, although this location can be more humid compared to the rest of Csb climate, it is not more humid for the HCT climates.

Ventilated design 21, located in Gothenburg region in Sweden records mould index 1.35 during one year simulation, which means a mould growth (as mould index 1 refers to start of the mould spores germination and therefore is suggested by the authors of the study to be the limit of mould index dividing moisture safe and risky designs) [7]. The second study from Canada revealed by in-situ observation and also by modelling a mould growth in ventilated attics located in Lower Mainland in Vancouver (south-west coast of Canada). Visible moulds on roof sheathing and calculated mould index ca.4 were recorded (see design 34). It was also found, that in this area the exterior air itself provides a suitable conditions for mould growth on wooden roof sheathing. Measurement was performed on a standalone roof exposed to the outdoor environment (see design 35).

Based on all previous findings it can be stated that maritime areas of HCT climate are often more humid and ventilation of the attic in such an areas can lead to moisture problems. Potentially suitable design for such a climates can be an unventilated attic with vapour-permeable underlay felt and sufficiently low moisture input from interior space. This can be, with some uncertainty, derived also by looking at design 18 (in table 3) that were performed in one of the potentially problematic areas (South-west coastal area of Sweden), while resulting in mould index 0 (without mould-growth risk). It should be however mentioned that this mould index value was not provided by the original study, but calculated by authors of this paper, using data provided by prof. Sasic-Kalagasidis. Another approach towards finding suitable attic design for humid maritime areas is to combine previously mentioned design with an adaptive mechanical ventilation, as suggested by authors of Swedish studies [7,12,43].

2.3.2 Moisture-risk evaluation

Although in table 3 can be found some important pieces of information, there would be much more to say, if there will be an information about moisture-safeness of each particular attic design. Table 3 does not contain a column of such an information, because only a few studies provided it. Studies often presented measured or computed data of different moisture-related quantities, such as relative humidity, moisture content of wooden sheathing, amount of condensate or mould index, however those mostly does not say much about the overall moisture safeness of the particular attic design – on one hand, studies reporting an amount of condensate on the roof sheathing within a year do not state what amount of condensate causes a moisture risk (or any other supplementary information). It can be also pointed out that even if there is no condensation on the inner-attic surfaces within a year and thus the amount of condensate is zero, it does not exclude a mould growth. Therefore even the design with co condensation present cannot most likely be stated as moisture-safe (without providing more information). On the other hand, there are studies reporting mould index according to VTT mould growth model [63,64]. However even when the mould index is sufficiently low for any mould growth (commonly < 1), there is still a possibility of condensation or frost accumulation on the inner-attic surfaces, especially in periods when temperature is below freezing point (at which a lot of mould growth models consider no growth). In that case melted frost can consecutively run down onto and into the construction joints or assemblies and cause local moisture problems (without causing a mould growth within an attic space). Nevertheless this second case we consider quite low probable and we still consider the mould index as the most relevant quantity for moisture safeness assessments. Many other considerations can be made regarding proper approach of moisture safeness assessment within an attic space, but such a topic would have taken whole another thesis.

Anyway in order to give just a bit deeper insight into the moisture-safeness of particular attic designs, there was additionally tried to evaluate moisture safeness of some of the attic designs using very simplified approach. There were generated two charts using an information and equations from original VTT mould growth model [63] and within them there were plotted an averaged data of the worst combination of temperature and relative humidity or temperature and wood moisture content (of wooden-based roof sheathing materials), (depending on study) of most of the attic designs. One chart was generated using worst weekly averaged data (see Fig. 15) and the second using worst monthly averaged data (see Fig.16). Left axis represents relative humidity while right axes corresponding equilibrium wood moisture content. Relation between the two quantities is determined by sorption isotherm of spruce wood presented in [58]. In some cases not all the data was provided by the original studies. In those cases we quantified the values using a set of assumptions that are described in section (2.1.4 *Quantification of values in moisture-evaluation charts*).

In both charts (Fig. 15, 16) can be seen multiple lines. The bold one represents well known critical relative humidity for mould growth as suggested by authors of VTT model. This line connects a set of conditions (combination of temperature and relative humidity) that are at least needed for the mould growth if applied for an infinite time period. The area at the top right represents a set of conditions more suitable for mould growth the more top and right are placed. Dashed lines represent a set of points (combination of conditions) at whose the mould index 1 (starting mould germination) is reached in the labelled particular time period. It can be clearly seen

that the more top and right the conditions are the shorter is the time period for reaching a mould growth. Moreover in each chart is one horizontal line while the area above the line was suggested to be an area of high condensation risk. As the worst weekly averages are obviously worse than worst monthly averages, this line is placed at relative humidity 94 % in the first chart (Fig. 15) and at 92 % at the second one (Fig. 16).

In both charts are presented values from 16 main designs (from total of 28) and 1 supplementary design (of total 7). In the first chart is just illustratively depicted also first 3 designs that resulted in frost accumulation. Attic designs that reports mould index or amount of condensate was not possible to include in the charts.

In the chart with weekly averages are shown mostly all weeks that belongs to the area of mould growth conditions and area of high condensation risk. Moreover there are some more weeks that was found to be close to the border. Designs that have no weekly averaged conditions located in the risk area are represented mostly just by one worst week point.

It can be seen, that there is no week point inside the “1 week area” which would have by any doubts confirm such a design to be moisture risky. The worst design regarding mould growth risk seems to be design 34 that has 3 week points in the middle of the “1 month area” (which is possibly around “3 weeks area”). But at least it does not confirm the design to be moisture risky as those 3 weeks would have gone right after each other to form a continuous 3 week period. Otherwise there can be no mould grow. Unfortunately the same can be stated according to the design 17, where a large set of week points can be found in the risk area. However it can be quite clearly stated that designs 4, 5, 8, 12, 14, and 18 are mould growth- and condensation-safe.

Although the chart with weekly averages can be useful for some estimations, chart in figure 16, presenting monthly averages, revealed some more information. As can be seen, it confirmed that the designs 34, 17 and 35 are mould growth-risky (which can be also seen in table 3 where an evaluated mould indices can be found). Chart also suggests that designs 6, 9, 11 and 15 are condensation-risky and designs 6, 7, 10, 16 moisture-safe.

By using this quite simple approach we were able to label most of the attic design as moisture-safe or risky:

- Attic designs that have the mould index already stated within their original study, were evaluated accordingly ($MI < 1$ – moisture safe, $MI \geq 1$ – moisture-risky)
- Moisture safeness of studies that provided just an information about an amount of condensate within a year or a certain time period, was stated based on another set of assumptions that are not presented in this study. Anyway based on those assumptions the dividing value of moisture-safe or risky was suggested to be $70 \text{ g/m}^2/\text{year}$ of condensate.

Finally all attic designs were stated as moisture-safe or moisture risky that was the first step towards more detailed analysis.

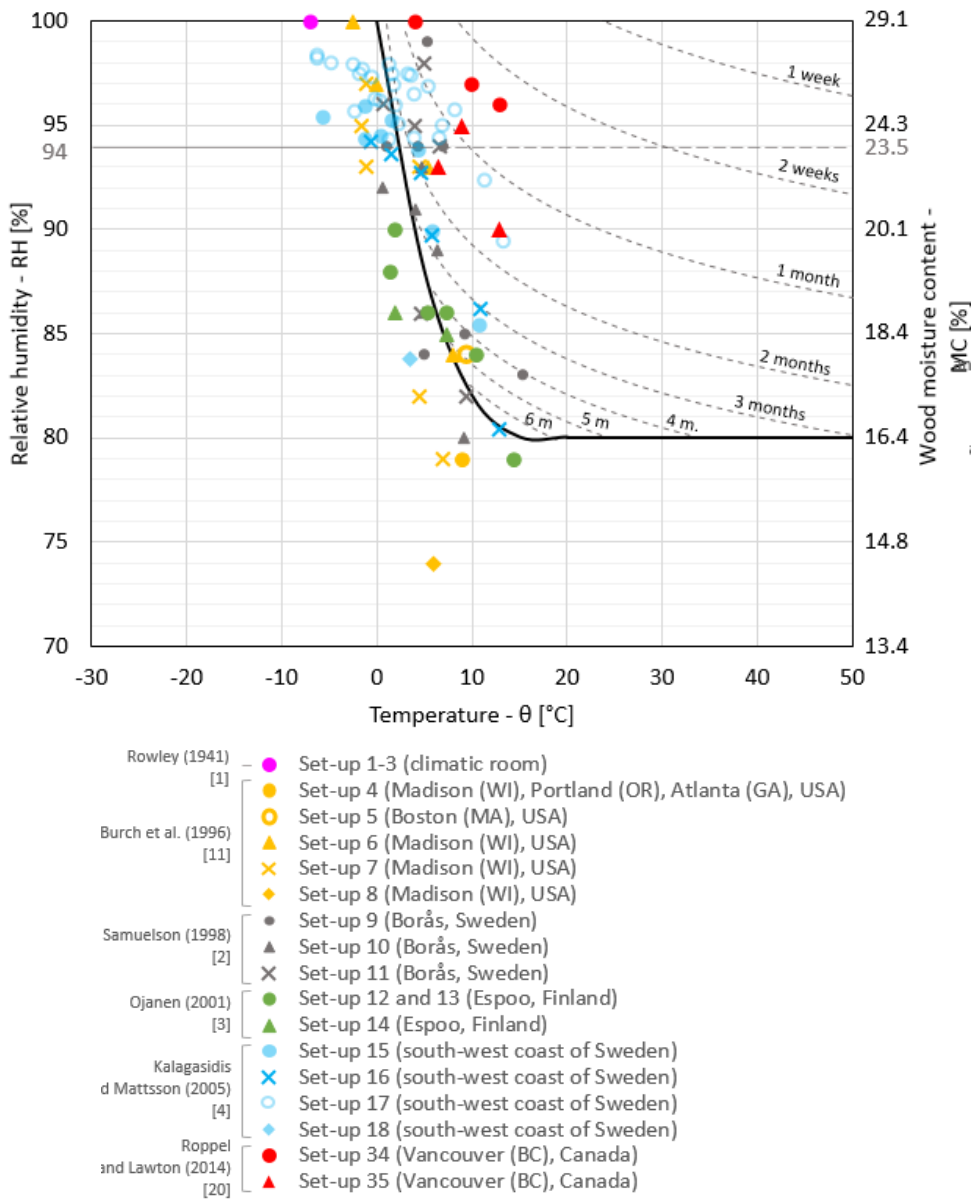


Fig. 15: Moisture risk evaluation chart – worst weekly averages

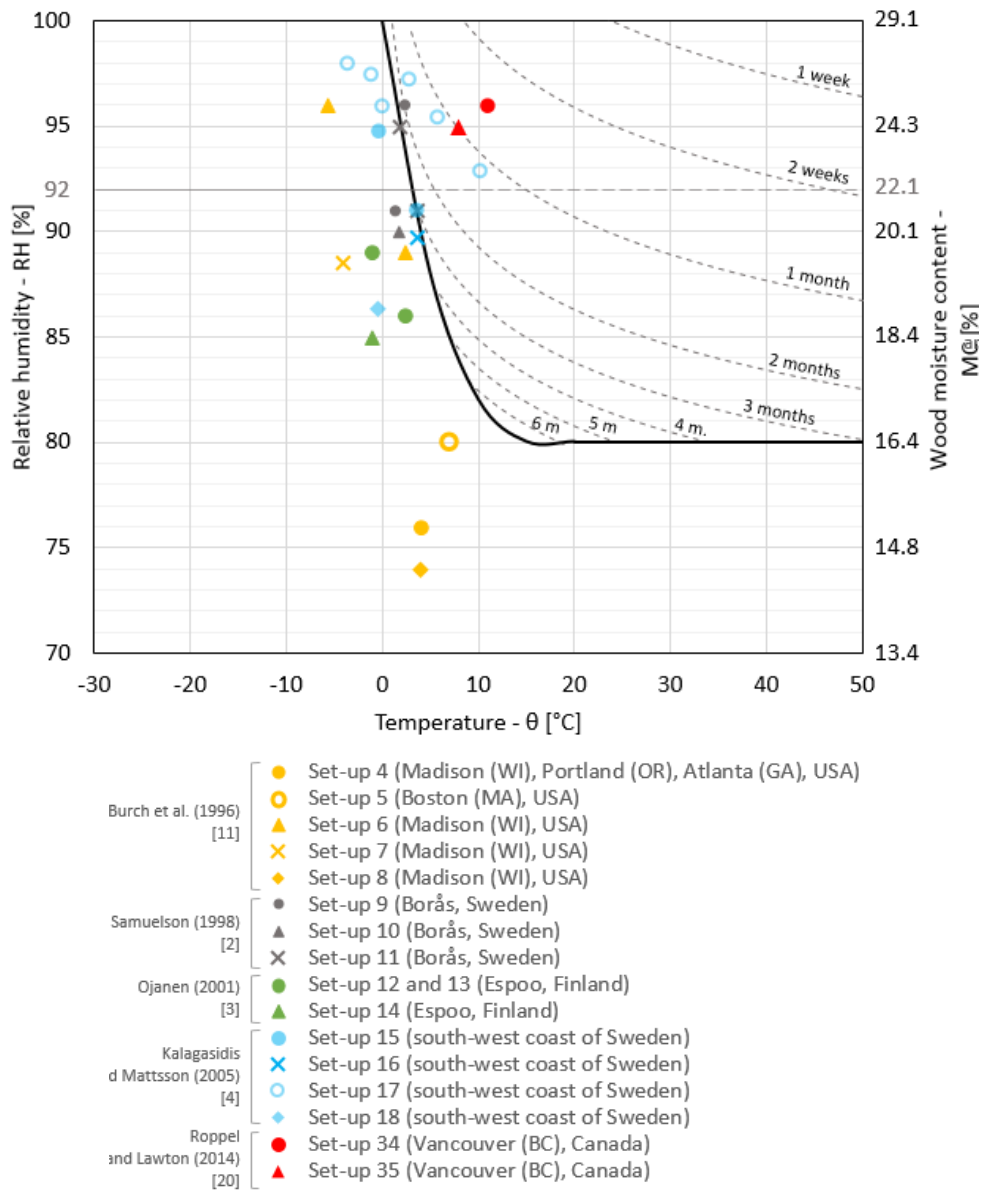


Fig. 16: Moisture risk evaluation chart – worst monthly averages

2.3.3 Grouping of similar designs

Although table 3 presents well-arranged list of designs according to their key parameters, it is still not quite easy to find all similar designs to be compared as there are not stated any borders of parameter values that could be considered as “similar”.

To group similar designs it was needed to state ranges of values of selected parameters. Here we present the selection process of those ranges. To not have too much individual groups, just 3 parameters that we found to be the most relevant were selected - $n_{real,ceil}$, $s_{d,r,deck}$, $n_{real,ext}$. Finally the set of overall 36 possible attic designs was established (see table 2). In following text can be found a brief information about selection of the ranges of each parameter.

Ceiling air permeance ranges

Based on ranges stated in studies [7,18,37] and on passive house requirements for an air-tightness [52] together with pieces of information from in-situ measurements [33], ranges of reference air change rates of the attic air due to the ceiling leakages at 50 Pa pressure difference were stated. Evaluation process is not described within this study. Based on reference ranges at 50 Pa pressure difference and by using power law with flow exponent 0.67, an air change rate ranges for 4 Pa pressure difference were evaluated. Those were considered as the ranges of attic air change rates due to infiltration of interior air under usual building operation. It should be emphasized that those ranges are not ranges of ceiling air-tightness (as this standalone parameter says nothing about real air leakages during building operation), but ranges of real leakage to the attic including all parameters that affect it. Chosen ranges are as follows:

extremely low leakage -	$n_{real,ceil} = 0.00 - 0.04$ ach
low leakage -	$n_{real,ceil} = 0.04 - 0.10$ ach
medium leakage -	$n_{real,ceil} = 0.10 - 0.18$ ach
high leakage -	$n_{real,ceil} > 0.18$ ach

Roof-deck vapour permeance ranges

According to already quite distinguished values of roof-decks s_d -values, ranges were chosen as follows:

permeable -	$s_{d,r,deck} = 0.02 - 0.3$ m
medium permeable -	$s_{d,r,deck} = 2.5 - 2.6$ m
vapour-tight -	$s_{d,r,deck} \geq 10$ m

Attic ventilation ranges

According to the values of different designs and best assumptions the ranges were stated as follows:

- unventilated (sealed) - $n_{\text{real,ext}} = 0.0 - 0.3 \text{ ach}$
- slightly ventilated - $n_{\text{real,ext}} = 0.6 - 3.3 \text{ ach}$
- ventilated - $n_{\text{real,ext}} \geq 4 \text{ ach}$

Tab. 4: Table of full range of possible attic design groups with filled the analysed 28 attic designs

<i>ceiling</i>	<i>roof deck</i>	<i>ventilation regime</i>	<i>Attic design no. and</i>
extremely low leakage	permeable	unventilated	28(0), 14(0)
		slightly ventilated	
		ventilated	
	medium permeable	unventilated	10(0), 18(0), 27(3)
		slightly ventilated	
		ventilated	11(2)
	vapour-tight	unventilated	26,
		slightly ventilated	9(2)
		ventilated	25(0), 8(0), 21(1)
low leakage	permeable	unventilated	
		slightly ventilated	
		ventilated	
	medium permeable	unventilated	
		slightly ventilated	
		ventilated	
	vapour-tight	unventilated	
		slightly ventilated	
		ventilated	
medium leakage	permeable	unventilated	
		slightly ventilated	
		ventilated	
	medium permeable	unventilated	
		slightly ventilated	
		ventilated	
	vapour-tight	unventilated	
		slightly ventilated	33(0.5), 32(3)
		ventilated	
heavy leakage	permeable	unventilated	29(1.5), 13(0)
		slightly ventilated	
		ventilated	31, 19(3)
	medium permeable	unventilated	17(3)
		slightly ventilated	15(1)
		ventilated	16(0)
	vapour-tight	unventilated	
		slightly ventilated	6(1)
		ventilated	34(3), 30(3), 4(0), 5(0), 7(0), 12(0), 20(3)

2.3.4 Statistical evaluation

Table 4 shows 4 main attic design groups according to the interior-attic air leakage under real building operation. As the “extremely low leakage” across the ceiling is in building practice usually almost impossible to achieve, it is assumed that building practice should target at the second “low leakage” or, at least the third “medium leakage” group. However it can be seen that almost none of selected attic designs has parameters to fulfil the criteria of such a ranges.

Mostly a numerically simulated designs (and one experimental design) were performed with no (or negligible) interior-attic leakage – the first group. The rest of tested designs were found to be on the other side with “heavy leakage” across the ceiling construction, leaving the two middle groups almost empty.

In terms of statistical evaluation of the overall 36 groups of attic designs (see Tab.4), it can be seen that only a few groups contain more than one sample and just 3 groups contain more than two samples. Under those circumstances it could be quite difficult, to state any solid conclusions or to find any linkages between the designs. All in all it can be seen that although a lot of previous studies were performed there is still place for further investigations, especially in a range of “low” and “medium” leakage groups (according to the table 4).

2.3.5 Comparison of similar attic designs

As all designs are now evaluated according to the moisture-risk and sorted into groups, there can be stated some moisture-related comparison. Looking at table 4 it can be seen that unventilated design with vapour permeable roof deck and extremely low interior-attic leakage can be moisture-safe since both of the two samples are without any moisture risk.

2.4 Conclusions

Based on study review it was investigated whether there could be found one or more cold attic design suitable for whole or prevailing part of the HCT (humid cold and temperate) climate.

Main findings were:

- Since the potentially highest moisture source for cold attics in HCT climate is usually the interior air, the first key measure for designing a moisture-safe attic is to make the ceiling construction as air-tight as possible, while its vapour tightness is also preferable but considerably less important.
- It was also revealed that seemingly quite a small change in interior moisture conditions can cause a huge difference in an attic hygro-thermal performance. Therefore a reasonable limits of interior humidity should be kept.
- It was found that maritime (coastal) areas of HCT climate are often more humid compared to inland parts of the climate zone. Exterior air in those coastal areas can cause moisture problems if the attic is ventilated (e.g. Gothenburg (Sweden), Vancouver (Canada). Therefore in those areas can be advantageous to use an unventilated attic with vapour permeable roof deck (e.g. double-skin roof deck with vapour permeable underlay felt as the lower skin) and indeed air- and vapour-tight ceiling construction.
- Generally if the ceiling construction is not sufficiently tight, the attic ventilation is usually advantageous (except the mentioned maritime areas). However if the ceiling is reasonably tight it seems that both designs (ventilated and unventilated but with vapour permeable roof-decks) perform similarly well (regarding moisture safeness). However it seems that the more northern the attic is located (particularly Dfb and Dfc climates) the more advantageous can be the use of ventilated design. It was proven that even in polar regions, the snow that drifts into the attic via ventilation openings does not cause any significant moisture problems. Accordingly in case of non-ventilated attics in areas with long-term snow coverage, the snow laying on the roof deck can lead to an increase of temperature within the attic, which together with possibly sufficient amount of moisture can lead to mould growth problems.
- It is most likely that the studies dealing with hygro-thermal performance of cold attics and related problems were performed mostly in areas where the problems were recorded. If so, it can be stated that in an inland areas of Central and Western Europe as well as in most of the inland part of North America there were possibly not much of such a problems and so the ventilation of cold attic (as mostly the best practice traditional measure) keeps in these areas the attic moisture-safe (as well as it is for centuries in Czech Republic).

- In North America there is potentially higher moisture risk within an attics (compared to Europe) because of the traditional single-skin roof deck assembly. The inner-attic surfaces of such a roof deck are more prone to undercooling by sky radiation during cold clear nights. The wooden-based roof sheathing has moreover some thermal capacity (compared to an underlay felt as the lower skin of the common European roof-deck) which can help to maintain lower temperature for a certain time period and thus can increase moisture risks. Another potential disadvantage of traditional North American roof deck is its vapour tightness that can also affect the overall moisture behaviour of an attic space.
- On the other hand the typical European double-skin roof deck contains usually ventilated cavity between the two skins that inhibits extremes of temperature acting on the upper roofing. Moreover the lower skin can be vapour permeable (made out of underlay felt) allowing some moisture transport between the attic and ventilated cavity.
- It was revealed that although many studies were performed, a very few of tested attic designs is in a range of what can be considered as the target attic design of current and future best-practice. This finding on the other hand implies what the future studies can be focussed on.

3 Development of HAM model

3.1 Description of the model

For further hygro-thermal analyses of cold attics was developed a dynamic, mostly one-dimensional and implicit HAM (heat air and moisture) model, built-up in software Matlab R2018b [46]. Model is fitted especially for attics but can be used also for other spaces. It is also quite versatile as there can be specified particular geometry, orientation, number of roof decks and their slopes etc. Special attention was paid to the description of ventilated roof-deck cavities and to cavities located within a pitched part of the ceiling above the heated space, that create ventilation channels connecting exterior and cold attic (see Fig. 17).

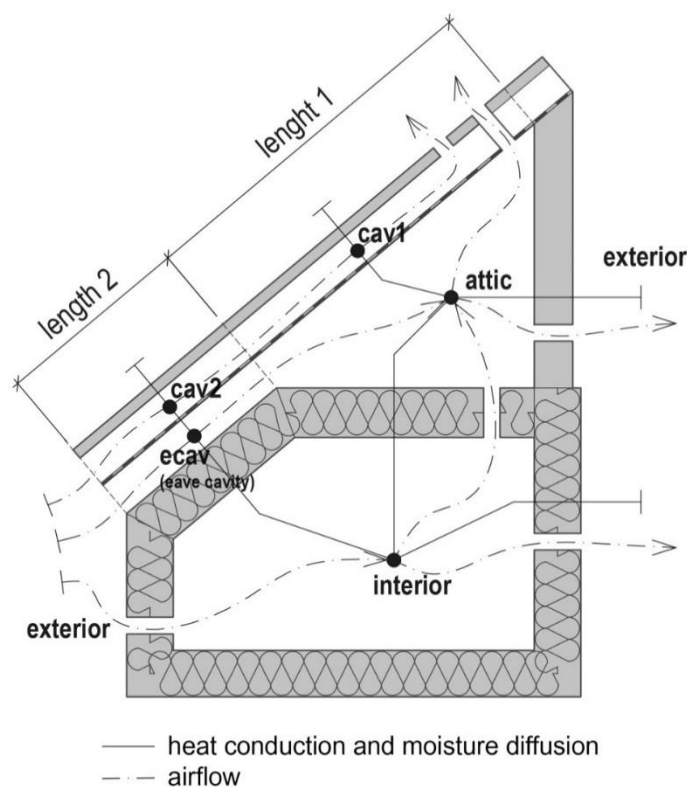


Fig. 17: Simple geometrical scheme of the model

Basic geometrical scheme of the model is depicted in figure 17. There can be seen 5 nodes representing an individual zones. Nodes also represent temperature and absolute humidity of the ideally (perfectly) mixed air within the particular zone (so no stratification or local differences of such a quantities are considered within the zone space). Although in the figure can be seen 5 zones depicted, the number of zones can vary as there are maximum of 4 attic envelope segments (except the ceiling construction) available to be set as roof-decks or gable walls. Thus in case of four roof-decks a set of 14 zones are present within the model.

Regarding the airflow model (see the dashed line), roof-deck cavities (each containing two zone nodes) are connected to the exterior by eave and ridge vents but are separated from all other

zones, creating an individual airflow paths. On the other hand the attic node is linked to the rest of zones making a net of 2 - 6 of them. Each interior wall (four walls) and each gable wall can contain an opening to an exterior environment (however only one opening area can be determined to each construction, representing an intentional vent or unintentional construction leakage). Airflow opening within the ceiling construction can be specified in the same way.

The zones referred as “ecav” (eave cavity) represent the airflow ducts from exterior to the attic space. If the attic is situated above an occupied loft, with inclined ceiling parts, such a cavities can be quite long (ca. 2-4 m). Therefore the air within the cavity can be affected by the surrounding environments (exterior and interior) before it enters the attic space. That is the reason why the “ecav” spaces (ducts) were created within the model. As well as the roof-deck cavities, it is considered, that the width of an “ecav” cavities is equal to the length of the eave. The length of “ecav” space is characterized by “length 2” (see Fig.17) which is one of the geometrical inputs within the model, while “length 1” is the length of the roof-deck in contact with the attic space. By adjusting those two lengths a various attic designs can be modeled.

Except the airflow part of the model, it can be seen, that all zone nodes are interconnected by thermal-conductances and water-vapour permeances between them (see the solid lines in the scheme).

In the figure can be seen a square-shaped interconnection of four nodes (two roof-deck cavity nodes, attic and ecav node). This is the only part of the model that is not calculated in an implicit scheme. The airflow between lower nodes (cav_2 and ecav) and upper nodes (cav_1 and attic) is calculated explicitly as that is a connection of two implicit matrices (one connecting the interior – attic – cav_1 – exterior and second connecting interior – ecav – cav_2 – exterior) . It is also the only part of the model having 2D character.

In figure 18 can be seen more detailed geometrical scheme of the model with depicted some of the options that are predefined within the model. For instance there can be easily chosen whether the roof deck is with or without the ventilation cavity and if the underlay is formed just by one thin foil (or felt) layer or there are some other layer (e.g. a sheathing layer). Also the gable wall can be quickly set to be made of one or two layers and the top layer of the ceiling construction can be easily set to be formed just by loosely laid thermal insulation or there is an extra layer on top of it (e.g. the flooring).

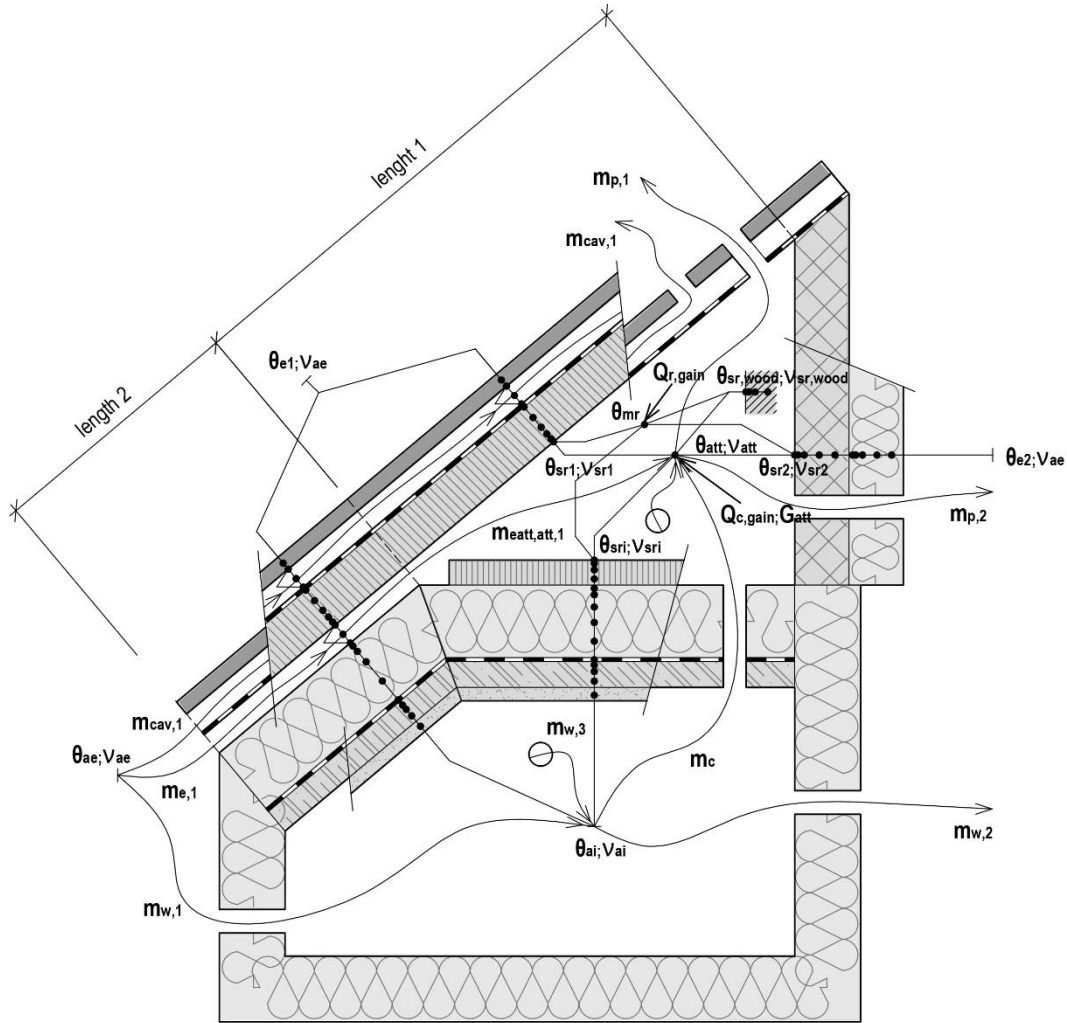


Fig. 18 Detailed geometrical scheme of the model

In figure can be also seen a computational nodes within the material layers. In most of the layers the number of nodes can be adjusted and is automatically logarithmically distributed from the more to the less important surface (mostly the attic- or ventilation cavity-facing surfaces). Foil layers are set to contain no more than one node.

Each air zone includes in fact two nodes. One representing the air temperature and the second the mean radiation temperature (areas-weighted average of surface temperatures of all surrounding constructions). This two-nodal approach instead of using just one node has two crucial benefits. First is that the surface temperatures are more precise as the model respects a radiation heat exchange between the surfaces. This could be very important in terms of studying surface condensation or mould growth. Second benefit is that the model outputs the air temperature than can be easily compared to a measurement, instead of some combined air and radiant temperature that results from one-nodal approach. Also obtained surface temperatures can be easily compared with measurements.

In figure 19 can be further seen a logical scheme of the model. The scheme is divided traditionally into three main parts: Inputs, Calculation core and Outputs.

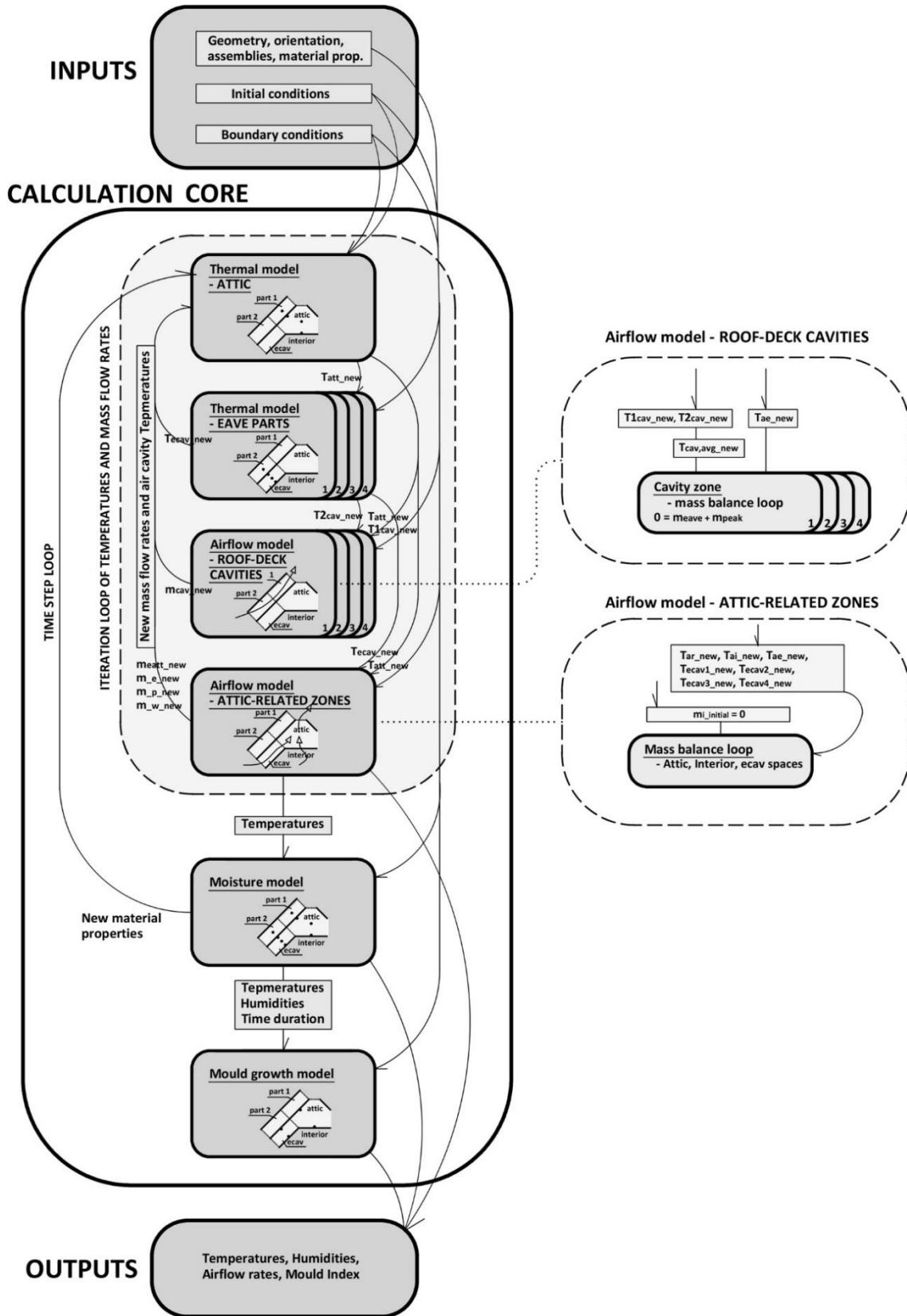


Fig. 19: Logical scheme of the model

Inputs

At first it is needed to provide to the model a set of computational parameters. It is mainly the geometry and orientation of the attic space, landscape roughness and presence of close wind obstacles (see also section 3.1.2 *Airflow model*). It should also be stated constructions assemblies (type and thicknesses of material layers) and number of nodes within them. For this purpose there is basic material database provided in the model (see Tab.5). It is therefore only needed to select a material from the database that contains all the parameters needed for the calculation. It is also possible to check or change the parameters. Finally there should be provided a boundary conditions of exterior and interior environments, preferably in hourly or half-hourly time step. Particularly the parameters needed are: temperature, relative humidity, wind speed and direction at 10 metres, solar gain (for specific slope and orientation of each attic envelope segment) and preferably also an apparent sky radiation (it can be also calculated within the model but with quite high possible inaccuracy). Eventually also heat and moisture gains or losses can be inputted.

In terms of geometry, the user can work with maximum of 4 attic envelope constructions (except the ceiling) that could be set as roof decks or gable walls. Although each envelope segment can have different area, slope and orientation, all roof decks and also all gable walls are made out of one assembly. There is quite high variability of the virtual attic geometry (see figure ??), but regarding the wind pressure coefficients acting on the different attic and house surfaces, there is only one set of functions of such a coefficients that corresponds to the detached rectangular, two story house with gable roof. Therefore there can be quite high uncertainty of the attic ventilation when considering different attic geometry. However the coefficients can be adjusted by the user, when the specific geometry is known.

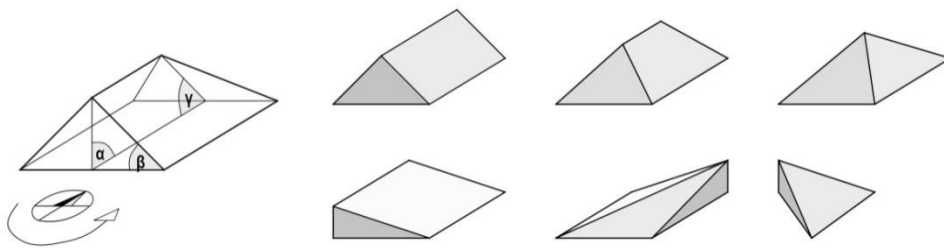


Fig. 20: Cases of possible attic geometries that can be defined within the model

Tab. 5: Material database of the model

	ρ_0 [kg/m ³]	λ [W/(m·K)]	c_p [J/(kg·K)]	μ [-]	ξ [kg/kg]	ϑ_{sol} [-]	ε [-]
spruce	470	0.170	2510	-1*	-1*	0.85	0.90
OSB_board	470	0.170	2510	-2*	-1*	0.85	0.90
wood_fibreboard_low_dens_1	50	0.040	2100	1.5	-1*	0.85	0.90
wood_fibreboard_low_dens_2	160	0.040	2100	3	-1*	0.85	0.90
wood_fibreboard_med_dens	270	0.048	2100	5	-1*	0.85	0.90
wood_fibreboard_high_dens	650	0.100	2100	17	-1*	0.85	0.90
red_brick	1800	0.800	800	8	0.002	0.75	0.90
unburned_brick	1800	1.300	800	8	0.050	0.80	0.90
plaster	1600	0.900	840	9	0.010	0.60	0.90
concrete	2200	1.300	1020	20	0.018	0.80	0.90
reinforced_concrete	2500	1.600	1020	29	0.018	0.80	0.90
gypsumboard	710	0.310	850	8	0.008	0.70	0.90
gypsum_fibreboard	1150	0.320	1100	13	0.020	0.60	0.90
EPS	30	0.038	1270	55	0.014	0.65	0.90
mineral_wool	25	0.039	840	2	0.008	0.50	0.90
foil_diffusively_open	260	0.300	1000	40	0.001	0.80	0.90
foil_PVC	1400	0.160	960	16700	0.000	0.30	0.90
tiles_concrete_dark_grey	2200	1.300	1020	20	0.018	0.85	0.90

* - values that tells the model to use a more detailed calculation of such a parameters, values (-1) refers to use a functions of moisture-dependent mu-value and moisture capacity of wood , and (-2) moisture-dependent mu-value of an OSB board

- ρ_0 - dry density
- λ - thermal conductivity
- c_p - heat capacity
- μ - water vapour resistance factor
- ξ - specific moisture capacity
- ϑ_{sol} - surface solar absorptance
- ε - surface thermal emittance

Calculation core

Model is consisting of combined thermal and airflow model, moisture model and additional mould growth model adopted from [63,64].

The physical core is based on traditional set of equations for such a purposes: thermal model is based on Fourier's law (law of heat conduction) (eq.1) and Stefan–Boltzmann law (eq.2), moisture model is based on Fick's law (law of diffusion) (eq.3), and airflow models on Bernoulli's equation (eq.4), ideal gas law (eq.5) and power law for an airflow rate across an opening or construction assembly calculations (eq.6). In all computational nodes also a mass and energy balances are valid (eq.7).

No latent heat effects are considered within the model as well as no liquid water transport. Amount of condensate and formed frost is buffered within the particular computational node and can further accumulate or be dried according to the surrounding conditions. It also affects the absolute humidity values of the layers the nodes represent.

The principles of the airflow models development were adopted from [31,34,56].

Empirical mould growth model was adopted from [63,64].

- Fourier's law (law of heat conduction):

$$q = -\lambda \cdot \text{grad}\theta = -\lambda \frac{d\theta}{dx} \quad (1)$$

- Stefan–Boltzmann law

$$q_r = \varepsilon\sigma T^4 \quad (2)$$

- Fick's first law (law of diffusion):

$$g = -\delta_p \frac{dp_v}{dx} = -\delta_v \frac{dv}{dx} \quad (3)$$

- Bernoulli's equation for an incompressible flow:

$$\frac{1}{2} \rho_m U^2 + \rho_m gz + p_m = \text{const.} \quad (4)$$

- ideal gas law:

$$pV = n_{\text{gas}} R_{\text{gas}} T = m R_{\text{spec}} T \quad (5)$$

- power law for an airflow

$$\dot{m} = \rho_a I \cdot \Delta P^L \quad (6)$$

- mass/energy balance:

$$\text{Income} = \text{Outcome} + \text{Accumulation} \quad (7)$$

- *Thermal and airflow model*

As can be seen in figure 19, in the first part of the calculation core there is a combined thermal and airflow model as temperature and mass flow rate are mutually affected by each other. Therefore there is an iteration loop of such a quantities. As can be seen, the loop contains four parts that are consecutively executed - Thermal model – ATTIC, Thermal model – EAVE PARTS, Airflow model ROOF-DECK CAVITIES, Airflow model – ATTIC.

At the first part “Thermal model – ATTIC” are calculated temperatures of all nodes present within an attic envelope constructions, and the attic node itself. This is done implicitly by solving a system of equations. No mass flow across any vent is considered in the first time step.

The same is performed within the next part of the model “Thermal model – EAVE PARTS”. There are possibly four eave parts (means parts of “length 2” or parts of sloped ceiling). Temperatures of each part are calculated within its particular system of equations.

In next step the calculated temperatures of upper and lower part of ventilated roof-deck cavity, together with exterior temperature, are provided to an airflow model of the cavities (Airflow model ROOF-DECK CAVITIES), which provides the mass flow rate in each cavity. Except the thermal stack, there are indeed taken into account the wind pressures acting on ventilation openings (see also section 3.1.2 *Airflow model*).

Similarly the temperatures within an attic space and eave spaces, together with exterior and interior boundaries are put to the attic airflow model (Airflow model – ATTIC), where the mass flow rates across all the openings related to the attic and interior space are calculated. Although there are a power law equations used, a linear system solver is used for such a purpose (more information can be found in section 3.1.2 *Airflow model*).

All calculated mass flow rates are used in new iteration loop as an inputs to the “Thermal model – ATTIC” and “Thermal model – EAVE PARTS”. Not more than 15 iteration cycles are needed to obtain sufficiently accurate result.

- *Moisture model*

As the moisture model does not work with any liquid water transport or latent heat, it does not affect the thermal model nor an airflow model. However it needs a temperatures in all nodes and mass flow rates across all openings and constructions as an inputs to calculate a saturation values of absolute humidity and amount of moisture transported by an airflow. Model is divided in two parts, similar to the thermal model (as the eave parts are calculated using one system of equations and the attic second). Similarly to the thermal model the part are “Moisture model – ATTIC” and “Moisture model – EAVE PARTS” (there can be from one to four eave parts).

- *Mould growth model*

Mould growth model was adopted from [63,64]. Model requires temperature and relative humidity courses of the space in which the analyzed surface is present. To use the model sufficiently, the surface should be made out of spruce or pine wood. Results of the model is a quantity called mould index ($M [-]$), which is a measure of mould growth activity on the surface or ratio of surface coverage. It is in range 0-6, where values < 1 means no growth, 1 means starting spore germination and 6 means that ca. 100 % of the surface is visually covered by the mould.

Outputs

Outputs are temperature, absolute humidity and relative humidity courses in time. There are also obtained courses of condensate (frost) amount within a virtual liquid and solid moisture storage tanks that are bonded to each computational node, and finally a mould index courses on inner attic surfaces.

By using such an output quantities many valuable analyses can be performed towards an attic moisture-safeness assessments or its hygro-thermal optimisation.

3.1.1 Thermal model

Preliminary calculations:

- **Thermal conductances and capacities within material layers**

Based on stated materials layers, their thicknesses and number of nodes within each of them, a heat capacities of computational layers and thermal conductances between the computational nodes are calculated. Heat capacity of each material layer (of each computational node representing such a layer) is calculated according to equation (8), and thermal conductance between two nodes within the same material is calculated according to equation (9). Often the thermal conductivity between two nodes is not uniform (as there can be more than one material layer having different properties between the two nodes). Since the total thermal resistance of the set of layers is calculated by adding the individual thermal resistance values and thermal conductance is an inverse value to the resistance, an equation (10) is used in those cases.

It should be also mentioned, that as the model is one-dimensional the heat capacity of each material layer is expressed per square meter.

$$C_{\text{heat}} = d \cdot \rho_0 \cdot c_p \quad (8)$$

$$h = \lambda / d \quad (9)$$

$$h = \frac{1}{R} = \sum_{k=1}^n \frac{1}{R_k} = \frac{1}{R_1 + R_2 + \dots + R_n} = \frac{1}{\frac{d_1}{\lambda_1} + \frac{d_2}{\lambda_2} + \dots + \frac{d_n}{\lambda_n}} \quad (10)$$

- **Thermal capacities of an air zones**

The air zones with specified volume have to be calculated using heat flow rates instead of heat fluxes that are related to squared meter. Therefore also the heat capacity of the zone has different units and is calculated using volume instead of thickness:

$$\kappa_{\text{heat}} = V_a \cdot \rho_a \cdot c_{pa} \quad (11)$$

- **Equivalent temperature acting on the outer surface of the roof deck**

For each of four roof segments is calculated its equivalent temperature acting on its exterior surface. This temperature is a combination of outdoor air temperature, solar gain with respect to roofing solar absorptance and thermal exchange due to the longwave radiation between roof to sky and roof to ground with respect to orientation and slope of the roof.

$$\theta_{e(i)} = \frac{\alpha_{c,e} \cdot \theta_{ae(i)} + F_{\text{sky}} \cdot \alpha_{r,\text{sky}(i)} \cdot \theta_{\text{sky}(i)} + F_g \cdot \alpha_{r,g(i)} \cdot \theta_{g(i)} + q_{\text{sol}(i)}}{\alpha_{c,e} + F_{\text{sky}} \cdot \alpha_{r,\text{sky}(i)} + F_g \cdot \alpha_{r,g(i)}} \quad (12)$$

Note: indexes in brackets states for loops: (i) for time step loop and (y) for iteration loop

Sky temperature is calculated from measured outgoing heat flux using following equation (however many other equations can be used depending on the data available – in those cases, the sky temperature has to be put into the model as already calculated input):

$$\theta_{\text{sky}(i)} = \left(\frac{q_{\text{r,to_sky}(i)}}{\sigma} \right)^{\frac{1}{4}} - 273.15 \quad (13)$$

Temperature of ground and other surfaces surrounding the attic is assumed to be very close to the temperature of outdoor air, and thus:

$$\theta_{\text{g}(i)} = \theta_{\text{ae}(i)} \quad (14)$$

Convective heat transfer coefficient on external side of the roof is highly affected by the wind speed by the surface, but in this model it was simplified using constant value.

$$\alpha_{\text{c,e}} = 20 \text{ W}/(\text{m}^2\text{K}) \quad (15)$$

Solar gains to roofing surfaces are calculated using roofing shortwave solar absorptance as follows:

$$q_{\text{sol}(i)} = q_{\text{sol,tot}(i)} \cdot \mathcal{G}_{\text{sol}} \quad (16)$$

Radiation heat transfer coefficients on the external side of the roof are calculated as follows (considering that external surface of the roofing is equal to the sky and ground temperature respectively – keeping in mind that it is a radical simplification):

$$\alpha_{\text{r,g}(i)} = 4 \cdot \varepsilon_{\text{roof}} \cdot \sigma \cdot (\theta_{\text{g}(i)} + 273.15)^3 \quad (17)$$

$$\alpha_{\text{r,sky}(i)} = 4 \cdot \varepsilon_{\text{roof}} \cdot \sigma \cdot (\theta_{\text{sky}(i)} + 273.15)^3 \quad (18)$$

Coefficients characterizing the roof orientation towards sky and towards the ground comes from stated roof geometry and thus are calculated according to roof slope.

$$F_{\text{g}} = 0.5(1 - \cos \varphi) \quad (19)$$

$$F_{\text{sky}} = 0.5(1 + \cos \varphi) \quad (20)$$

- **Equivalent heat transfer coefficient on the outer surface of the roof deck**

Except equivalent temperature acting on the outer surface of the roof deck θ_e , also an equivalent heat transfer coefficient of the external roof surface, that combines convective and radiative parts of heat transfer, is calculated:

$$\alpha_{\text{s,e}(i)} = \alpha_{\text{r,sky}(i)} \cdot F_{\text{sky}} + \alpha_{\text{r,g}(i)} \cdot F_{\text{g}} + \alpha_{\text{c,e}(i)} \quad (21)$$

Thermal model – ATTIC

- **Convective heat transfer coefficients within roof-deck cavities**

Convective heat transfer coefficients of surfaces in ventilated cavities are calculated using following equation:

$$\alpha_{c,r,cav(i)} = \frac{\text{Nu}_{(i)} \cdot \lambda_a}{D_H} \quad (\text{eq.5.24 in [60]}) \quad (22)$$

Following relation between Nusselt and Reynolds number was chosen according to references [60,48].

$$\text{Re}_{(i)} \leq 2300; \quad \text{Nu}_{(i)} = 8 \quad (\text{in [70]}) \quad (23)$$

$$\text{Re}_{(i)} > 2300; \quad \text{Nu}_{(i)} = 0.023\text{Re}_{(i)}^{(0.8)} \cdot \text{Pr}^{(0.4)} \quad (\text{pg.424 in [60]}) \quad (24)$$

Previous equation is valid only if $0.7 < \text{Pr} < 16$. Prandtl number for dry air in atmospheric pressure and temperature between -20 and 100 °C varies approximately in range of 0.72 and 0.70 and therefore constant value $\text{Pr} = 0.71$ was chosen and thus the previous equation is valid.

Thermal conductivity of dry still air is in atmospheric pressure and temperature between -20 and 100 °C approximately in range of 0.022 and 0.032 W/(m·K) [49]. Therefore a most commonly used value $\lambda_a = 0.024$ W/(m·K) were employed.

Hydraulic diameter of ventilated cavity is calculated using relation for parallel plates flow:

$$D_H = 2 \cdot d_{cav} \quad (25)$$

Reynolds number is defined as follows:

$$\text{Re}_{(i)} = \frac{\rho_a U_{cav(i)} L}{\mu_{dyn,a}} \quad (26)$$

For density of fluid (air) as well as for its dynamic viscosity were chosen constant values $\rho_a = 1.23$ kg/m³ and $\mu_{dyn,a} = 17.8 \times 10^{-6}$ kg/(m·s). Quantity L states for characteristic linear dimension which is in case of ducts or parallel plates flow equal to hydraulic diameter D_H , thus:

$$\text{Re}_{(i)} = \frac{\rho_a U_{cav(i)} D_H}{\mu_{dyn,a}} \quad (27)$$

The airflow velocity within the cavity ($W_{cav(i)}$) is calculated from mass flow rate (see eq. 28). The mass flow rate is in first iteration step considered to be zero, in next steps it is an output from the previous step of an airflow model. Value of mass flow rate is bonded with a sign that characterizes the flow direction. Similarly the calculated velocity includes the same sign. However for many purposes it is needed to express just the magnitude (scalar absolute value) of the flow velocity vector (the flow speed). In this model it is referred as $U_{cav(i)}$. Such a quantity is useful for instance for validation with measurement (see also section 3.3 *Validation*), expressing an average flow speed within the cavity and also for an evaluation of the Reynolds number (see eq. 27).

$$W_{cav(i)} = \dot{m}_{cav(i,z)} / (\rho_{a,cav(i)} \cdot b_{cav} \cdot d_{cav}) \quad (28)$$

b_{cav} and d_{cav} are an input values, while b_{cav} is the width of the cavity within 1 meter of eave length, thus for instance if there are 50 mm-width rafters, one per each meter of eave length, b_{cav} is 0.95 m.

Air density is calculated according to eq. 29.

$$\rho_{a,cav(i)} = \frac{1.293 \cdot 273.15}{\theta_{cav(i,z-1)} + 273.15} \quad (29)$$

$$U_{cav(i)} = \text{abs}(W_{cav(i)}) \quad (30)$$

Value of convective heat transfer coefficient of an opposite surface of the ventilated cavity $\alpha_{c,e,cav(i)}$ is set to be the same as $\alpha_{c,r,cav(i)}$.

- **Radiative heat transfer coefficient within roof-deck cavities**

Considering a geometry simplification to parallel plates, the radiative heat transfer coefficient between the two surfaces is calculated as follows:

$$\alpha_{r,cav(i)} = \frac{4 \cdot \sigma \cdot \left(\frac{(\theta_{s,e,cav(i)} + 273.15) + (\theta_{s,r,cav(i)} + 273.15)}{2} \right)^3}{\frac{1}{\varepsilon_{s,e,cav}} + \frac{1}{\varepsilon_{s,r,cav}} - 1} \quad (31)$$

- Convective heat transfer coefficients on the inner-attic surfaces

Convective heat transfer coefficients of the inner-attic surfaces were set as constant values.

$$\alpha_{c,r} = 3.2 \text{ W}/(\text{m}^2\text{K})$$

$$\alpha_{c,\text{floor}} = 0.7 \text{ W}/(\text{m}^2\text{K})$$

$$\alpha_{c,\text{buff}} = 3.2 \text{ W}/(\text{m}^2\text{K})$$

- Radiative heat transfer coefficients on the inner-attic surfaces

Radiative heat exchange between all inner-attic surfaces is simplified with the use of mean radiation temperature (see also paragraph “*Mean radiation temperature node*” in following text). The radiative heat transfer between the surface and all other surfaces is substituted by an exchange between the surface and just one (mean radiation) temperature. The relation is similar as in case of parallel plates (see eq.31).

- Convective heat transfer coefficients on the lower (interior) surface of the ceiling

$$\alpha_{c,i} = 5 \text{ W}/(\text{m}^2\text{K})$$

- Outermost thermal conductance

In the model there is no exterior surface node considered. Therefore the outermost computational node of the roof deck or gable wall is placed in the middle of the outermost layer (roofing or the outer gable wall layer). For an evaluation of the thermal conductance between the equivalent outdoor temperature and the first computational node an equation for adding conductances is used as follows:

$$h_{ee,\text{roof}(i)} = \frac{h_{se(i)} \cdot h_{\text{ext_roof}}}{h_{se(i)} + h_{\text{ext_roof}}} \quad (32)$$

$$h_{ee,\text{gwall}(i)} = \frac{h_{se(i)} \cdot h_{\text{ext_gwall}}}{h_{se(i)} + h_{\text{ext_gwall}}} \quad (33)$$

- **Nodal equations**

For every node an energy balance is valid (see eq. 7), thus all incoming energy can only be stored or released. In terms of thermal energy a following general relation can be expressed for each time step (i):

$$\sum_{k=1}^n \mathcal{Q}_{in(i),k} = \sum_{j=1}^m \mathcal{Q}_{out(i),j} + \frac{\kappa_{heat} \cdot (\theta_{(i)} - \theta_{(i-1)})}{\Delta \tau} \quad (34)$$

- Material nodes

A typical situation is a material node within construction where only two heat-transfer branches are connected to this node. Moreover one-dimensional transport can be related to one squared meter of construction. Than a simplified version of eq. 34 can be expressed using heat fluxes instead of heat flow rates:

$$q_{in(i)} = q_{out(i)} + \frac{C_{heat} \cdot (\theta_{(i)} - \theta_{(i-1)})}{\Delta \tau} \quad (35)$$

If the thermal conductivities between the calculated node and neighbouring nodes are the same, by substituting equation (34) with Fourier's law (1) and with known distances between the nodes, for node "z" we can get:

$$\frac{-\lambda}{d_{z-1,z}} (\theta_{z(i)} - \theta_{z-1(i)}) = \frac{-\lambda}{d_{z,z+1}} (\theta_{z+1(i)} - \theta_{z(i)}) + \frac{C_{heat,z} \cdot (\theta_{(i)} - \theta_{(i-1)})}{\Delta \tau} \quad (36)$$

By substitution with equation (9) or (10) it can be written:

$$h_{z-1,z} (\theta_{z-1(i)} - \theta_{z(i)}) = h_{z,z+1} (\theta_{z(i)} - \theta_{z+1(i)}) + \frac{C_{heat,z} \cdot (\theta_{z(i)} - \theta_{z(i-1)})}{\Delta \tau} \quad (37)$$

- Zonal nodes (air nodes)

Zonal nodes are representing an average temperature of air within the zone. Heat exchange takes place between the air and surrounding surfaces by convection and also by mixing with ventilation air. In the attic zone also direct heat gain to the air node can be attributed (e.g. chimney wall, lights, heating device). It should be emphasised that just convective part of the possible heat source $\mathcal{Q}_{c,gain}$ has to be attributed to the zone air node. General equation (34) can be than modified to form:

$$\sum_{k=1}^n \mathcal{Q}_{in,surface(i),k} + \sum_{l=1}^o \mathcal{Q}_{in,airflow(i),l} + \mathcal{Q}_{c,gain(i)} = \sum_{j=1}^m \mathcal{Q}_{out,surface(i),j} + \sum_{p=1}^q \mathcal{Q}_{out,airflow(i),p} + \frac{\kappa_{heat} \cdot (\theta_{(i)} - \theta_{(i-1)})}{\Delta \tau} \quad (38)$$

In the case of zonal nodes representing an air volume, the calculation has to be performed using the total heat flow rates instead of heat fluxes (as in case of material nodes calculation). Thus the final equation used in the model (for a general node “z”) is in following form (considering that all surrounding temperatures including the incoming air has higher temperature compared to the air within the zone):

$$\sum_{k=1}^n \alpha_{c,k} \cdot A_k (\theta_{s,k(i)} - \theta_{z(i)}) + \sum_{l=1}^o \dot{m}_{l,(i)} \cdot c_{pa} (\theta_{a,l(i)} - \theta_{z(i)}) + Q_{c,gain(i)} =$$

$$= \frac{\kappa_{heat} \cdot (\theta_{z(i)} - \theta_{z(i-1)})}{\Delta \tau} \quad (39)$$

○ Interface nodes

Nodes that are lying in the interface of two material layers representing a plane instead of volume (as material or zonal nodes), have no heat capacity and therefore the general equation (34) can be expressed in simplified form using heat fluxes:

$$q_{in(i)} = q_{out(i)} \quad (40)$$

Similarly to equation (37) the previous relation can be expand to form:

$$h_{z-1,z} (\theta_{z-1(i)} - \theta_{z(i)}) = h_{z,z+1} (\theta_{z(i)} - \theta_{z+1(i)}) \quad (41)$$

○ Surface nodes

Surface nodes are in contact with the air zones and as well as interface nodes have no heat capacity. However except the conduction heat exchange with the material node that the surface belongs to, the surface nodes have two more heat transport branches – convective and radiative. Convective heat exchange takes places between the surface node and the zonal node (air node). Radiative heat exchange takes place between the surface node and the mean radiation temperature node of the zone (see next section “*Mean radiation temperature nodes*”). Such a radiation heat transport branch, that is connected to only one other temperature, is a massive simplification compared to the real situation, where the radiation heat exchange takes place between all the surfaces that are exposed to the node, depending on individual surface temperature, area and geometry of the space. Moreover there is a different radiation exchange taking place on every single point of the surface that is represented by the node. Equation (34) can be for surface nodes simplified to form:

$$q_{in(i)} = q_{c,out(i)} + q_{r,out(i)} \quad (42)$$

Final form used for the calculation (using general node “z”) is as follows:

$$h_{z-1,z} (\theta_{z-1(i)} - \theta_{z(i)}) = \alpha_{c,z,zone_air} (\theta_{z(i)} - \theta_{zone_air(i)}) + \alpha_{r,z,mr} (\theta_{z(i)} - \theta_{mr(i)}) \quad (43)$$

○ Mean radiation temperature nodes

Mean radiation temperature is in every zone represented by one imaginary node that averages all inner surface temperature values with respect to the surface areas. This node represents no volume and thus has no heat capacity. However as it uses a surface areas for its computation, the energy balance equation has to uses heat flow rates instead of heat fluxes. Equation (34) can be therefore, for such a nodes, expressed as:

$$\sum_{k=1}^n Q_{r,in(i),k} + Q_{r,gain(i)} = \sum_{j=1}^m Q_{r,out(i),j} \quad (44)$$

Note: It should be emphasised, that there is quite large simplification as in the model the mean radiation temperature is only one averaging all the surface temperatures and this one temperature communicates (energy-wise) with all the surfaces. However the more realistic approach would be to have one imaginary mean radiation temperature for each surface to communicate with – each of the radiation temperatures would have been calculated as an area weighted mean of all inner-attic surfaces but indeed except the one particular surface that it radiates with.

Equation (44) can be than written as:

$$\sum_{k=1}^n \alpha_{r,k} \cdot A_k (\theta_{s,k(i)} - \theta_{mr(i)}) + Q_{r,gain(i)} = 0 \quad (45)$$

- **Expression of unknowns**

From the set of nodal equations presented in previous part is built up a system of equations having the same number of unknowns. Using an implicit scheme, there has to be created a left-side matrix of the non-temperature parts of the terms bonded with particular unknown temperatures. To keep all the equations correct, there has to be also a multiplicative vector of an unknown temperatures present on the left side. On the right side there is a vector of the terms with known values. To easily create such a matrix and vectors the following expression of the nodal equations were performed (in all cases using general node “z”).

- Material nodes

$$\theta_{z-1(i)} \left(-h_{z-1,z} \right) + \theta_{z(i)} \left(h_{z-1,z} + \frac{C_{\text{heat},z}}{\Delta \tau} + h_{z,z+1} \right) + \theta_{z+1(i)} \left(-h_{z,z+1} \right) = \theta_{z(i-1)} \cdot \frac{C_{\text{heat},z}}{\Delta \tau} \quad (46)$$

- Zonal nodes

$$\begin{aligned} \sum_{k=1}^n \theta_{s,k(i)} \left(-\alpha_{c,k} \cdot A_k \right) + \theta_{z(i)} \left(\sum_{k=1}^n \left(\alpha_{c,k} \cdot A_k \right) + \sum_{l=1}^o \left(\dot{m}_{l,(i)} \cdot c_{\text{pa}} \right) + \frac{K_{\text{heat}}}{\Delta \tau} \right) + \\ + \sum_{l=1}^o \theta_{a,l(i)} \left(-\dot{m}_{l,(i)} \cdot c_{\text{pa}} \right) = \theta_{z(i-1)} \cdot \frac{K_{\text{heat}}}{\Delta \tau} + Q_{c,\text{gain}(i)} \end{aligned} \quad (47)$$

- Interface nodes

$$\theta_{z-1(i)} \left(-h_{z-1,z} \right) + \theta_{z(i)} \left(h_{z-1,z} + h_{z,z+1} \right) + \theta_{z+1(i)} \left(-h_{z,z+1} \right) = 0 \quad (48)$$

- Surface nodes

$$\begin{aligned} \theta_{z-1(i)} \left(-h_{z-1,z} \right) + \theta_{z(i)} \left(h_{z-1,z} + \alpha_{c,z,\text{zone_air}} + \alpha_{r,z,\text{mr}} \right) + \\ + \theta_{\text{zone_air}(i)} \left(-\alpha_{c,z,\text{zone_air}} \right) + \theta_{\text{mr}(i)} \left(-\alpha_{r,z,\text{mr}} \right) = 0 \end{aligned} \quad (49)$$

- Mean radiation temperature nodes

$$\sum_{k=1}^n \theta_{s,k(i)} \left(-\alpha_{r,k} \cdot A_k \right) + \theta_{\text{mr}(i)} \left(\sum_{k=1}^n \left(\alpha_{r,k} \cdot A_k \right) \right) = Q_{r,\text{gain}(i)} \quad (50)$$

- **Creating the system of equations using matrices**

As previously mentioned, to let the Matlab solve the system of equations there have to be determined a left-side matrix of the parts of the terms bonded with an unknown temperatures, vector of an unknown temperatures and right-side vector of known values. Left-side matrix is composed of a nodal equations of all five construction assemblies surrounding the attic space, and the inner thermal-buffering constructions. As the user can vary the number of construction layers and number of nodes within layers, building-up the matrix is quite complex. For that reason, there are at fist formed an independent matrices of the particular constructions and consequently put together with an addition of an attic air and mean radiation temperature nodes.

For each roof deck segment with cavity a preliminary matrix is formed as follows (let it be denoted as matrix A_{left}):

$$\begin{pmatrix} h_{ee(i)} + \frac{C_1}{\Delta\tau} + h_{1,2} & -h_{1,2} & 0 & 0 & 0 & 0 & 0 & 0 \\ -h_{1,2} & h_{1,2} + \alpha_{ce,cav(i)} + \alpha_{r,cav(i)} & -\alpha_{ce,cav(i)} & -\alpha_{r,cav(i)} & 0 & 0 & 0 & 0 \\ 0 & -\alpha_{ce,cav(i)} & \alpha_{ce,cav(i)} + \frac{\kappa_{cav}}{\Delta\tau} + \alpha_{cr,cav(i)} & -\alpha_{cr,cav(i)} & 0 & 0 & 0 & 0 \\ 0 & -\alpha_{r,cav(i)} & -\alpha_{cr,cav(i)} & \alpha_{cr,cav(i)} + \alpha_{r,cav(i)} + h_{4,5} & -h_{4,5} & 0 & 0 & 0 \\ 0 & 0 & 0 & -h_{4,5} & h_{4,5} + \frac{C_5}{\Delta\tau} + h_{5,6} & -h_{5,6} & 0 & 0 \\ \vdots & \vdots \\ 0 & 0 & 0 & 0 & 0 & 0 & h_{n-1,n} + \frac{C_n}{\Delta\tau} + h_{n,n+1} & -h_{n,n+1} \\ 0 & 0 & 0 & 0 & 0 & 0 & -h_{n,n+1} & h_{n,n+1} + \alpha_{cr} + \alpha_{\pi(i)} \end{pmatrix}$$

It can be seen, that first row (first equation) relates to node in the centre of the roofing, that is connected to the outdoor equivalent temperature by conductance $h_{ee(i)}$. Second row is related to the upper surface of the ventilated cavity – there can be seen both, convective and radiative heat transport coefficients, $\alpha_{cr,cav(i)}$ and $\alpha_{r,cav(i)}$ respectively. Last row is related to the inner-attic surface of the roof deck, again with the radiative and convective heat transport coefficients. It should be emphasised that there are two more unknown temperatures that have to be present within the matrix – attic air temperature and attic mean radiation temperature. Those are not forgotten, but will be added later in the final form of the overall attic-related left-side matrix (described in following text). Down below can be seen a provisional form of the system of equations for one roof deck construction using matrices.

$$A_{left} \cdot \begin{pmatrix} \theta_{1(i)} \\ \theta_{se,cav(i)} \\ \theta_{cav(i)} \\ \theta_{sr,cav(i)} \\ \theta_{5(i)} \\ \vdots \\ \theta_{n(i)} \\ \theta_{sr(i)} \end{pmatrix} = \begin{pmatrix} \theta_{e(i)} \cdot h_{ee(i)} + \theta_{1(i-1)} \frac{C_{heat,1}}{\Delta\tau} \\ 0 \\ \theta_{cav(i-1)} \frac{\kappa_{heat,cav}}{\Delta\tau} \\ 0 \\ \theta_{5(i-1)} \frac{C_{heat,5}}{\Delta\tau} \\ \vdots \\ \theta_{n(i-1)} \frac{C_{heat,n}}{\Delta\tau} \\ 0 \end{pmatrix}$$

For gable walls and ceiling construction, where there is no ventilated cavity a simpler version of a matrix can be formed (let it be denoted as matrix B_{left}):

$$\begin{pmatrix} h_{ee(i)} + \frac{C_1}{\Delta\tau} + h_{1,2} & -h_{1,2} & 0 & 0 & 0 & 0 & 0 & 0 \\ -h_{1,2} & h_{1,2} + \frac{C_2}{\Delta\tau} + h_{2,3} & -h_{2,3} & 0 & 0 & 0 & 0 & 0 \\ 0 & -h_{2,3} & h_{2,3} + \frac{C_3}{\Delta\tau} + h_{3,4} & -h_{3,4} & 0 & 0 & 0 & 0 \\ 0 & 0 & -h_{3,4} & h_{3,4} + \frac{C_4}{\Delta\tau} + h_{4,5} & -h_{4,5} & 0 & 0 & 0 \\ 0 & 0 & 0 & -h_{4,5} & h_{4,5} + \frac{C_5}{\Delta\tau} + h_{5,6} & -h_{5,6} & 0 & 0 \\ \vdots & \vdots \\ 0 & 0 & 0 & 0 & 0 & 0 & h_{n-1,n} + \frac{C_n}{\Delta\tau} + h_{n,n+1} & -h_{n,n+1} \\ 0 & 0 & 0 & 0 & 0 & 0 & -h_{n,n+1} & h_{n,n+1} + \alpha_{cr} + \alpha_{rr(i)} \end{pmatrix}$$

System of equations of such a construction, using matrices, can be then written as:

$$B_{\text{left}} \cdot \begin{pmatrix} \theta_{1(i)} \\ \theta_{2(i)} \\ \theta_{3(i)} \\ \theta_{4(i)} \\ \theta_{5(i)} \\ \vdots \\ \theta_{n(i)} \\ \theta_{sr(i)} \end{pmatrix} = \begin{pmatrix} \theta_{e(i)} \cdot h_{ee(i)} + \theta_{t(i-1)} \frac{C_1}{\Delta\tau} \\ \theta_{2(i-1)} \frac{C_2}{\Delta\tau} \\ \theta_{3(i-1)} \frac{C_3}{\Delta\tau} \\ \theta_{4(i-1)} \frac{C_4}{\Delta\tau} \\ \theta_{5(i-1)} \frac{C_5}{\Delta\tau} \\ \vdots \\ \theta_{n(i-1)} \frac{C_n}{\Delta\tau} \\ 0 \end{pmatrix}$$

In the next figure can be seen simplified version of the full left-side matrix composed from 6 partial matrices (according to the 5 envelope constructions and thermal buffering inner-attic construction) as can be seen above. Let the matrix will be denoted as $T_{\text{att, left}}$. Additionally in the final matrix there are two last rows that represent nodal balance equations for an attic air node and attic mean radiation temperature node. As both of the nodes link surface temperatures of all surrounding constructions, last two rows of the matrix are filled with convective and radiative surface heat transfer coefficients instead of zeros. If the more detailed form of the matrix would be presented, there would be seen that all the rows and columns of all A-F matrices instead of only one row and one column in the simplified version of the matrix below. In the detailed matrix would be seen, that the mentioned conductance terms in the last two rows are related to the particular last columns of each partial matrices A-F. The rest of the terms in last two rows of the matrix would be zeros. The same situation occurs in the last two columns, where there are added also a conductance terms to the rows belonging to the inner-attic surface nodal equations.

As the air temperature and mean radiation temperature do not directly affect each other, in the intersection of their rows and columns are zero terms.

$$\begin{pmatrix}
 \mathbf{A} & 0 & 0 & 0 & 0 & 0 & -\alpha_{cr,A} & -\alpha_{rr,A(i-1)} \\
 0 & \mathbf{B} & 0 & 0 & 0 & 0 & -\alpha_{cr,B} & -\alpha_{rr,B(i-1)} \\
 0 & 0 & \mathbf{C} & 0 & 0 & 0 & -\alpha_{cr,C} & -\alpha_{rr,C(i-1)} \\
 0 & 0 & 0 & \mathbf{D} & 0 & 0 & -\alpha_{cr,D} & -\alpha_{rr,D(i-1)} \\
 0 & 0 & 0 & 0 & \mathbf{E} & 0 & -\alpha_{cr,E} & -\alpha_{rr,E(i-1)} \\
 0 & 0 & 0 & 0 & 0 & \mathbf{F} & -\alpha_{cr,F} & -\alpha_{rr,F(i-1)} \\
 \\
 -\alpha_{cr,A}A_A & -\alpha_{cr,B}A_B & -\alpha_{cr,C}A_C & -\alpha_{cr,D}A_D & -\alpha_{cr,E}A_E & -\alpha_{cr,F}A_F & \alpha_{cr,A}A_A + \alpha_{cr,B}A_B + \alpha_{cr,C}A_C + \\
 & & & & & & \alpha_{cr,D}A_D + \alpha_{cr,E}A_E + \alpha_{cr,F}A_F + \\
 & & & & & & \dot{m}_{catt_att,A(i,y-1)} \cdot c_{pa} + \\
 & & & & & & \dot{m}_{catt_att,B(i,y-1)} \cdot c_{pa} + \\
 & & & & & & \dot{m}_{catt_att,C(i,y-1)} \cdot c_{pa} + \\
 & & & & & & \dot{m}_{catt_att,D(i,y-1)} \cdot c_{pa} + \\
 & & & & & & \dot{m}_{p,A(i,y-1)} \cdot c_{pa} + \dot{m}_{p,B(i,y-1)} \cdot c_{pa} + \\
 & & & & & & \dot{m}_{p,C(i,y-1)} \cdot c_{pa} + \dot{m}_{p,D(i,y-1)} \cdot c_{pa} + \\
 & & & & & & \dot{m}_{c_att(i,y-1)} \cdot c_{pa} + \\
 & & & & & & \kappa_{att} / \Delta\tau \\
 \\
 -\alpha_{rr,A(i-1)}A_A & -\alpha_{rr,B(i-1)}A_B & -\alpha_{rr,C(i-1)}A_C & -\alpha_{rr,D(i-1)}A_D & -\alpha_{rr,E(i-1)}A_E & -\alpha_{rr,F(i-1)}A_F & 0 & \alpha_{rr,A(i-1)}A_A + \alpha_{rr,B(i-1)}A_B + \\
 & & & & & & & \alpha_{rr,C(i-1)}A_C + \alpha_{rr,D(i-1)}A_D + \\
 & & & & & & & \alpha_{rr,E(i-1)}A_E + \alpha_{rr,F(i-1)}A_F
 \end{pmatrix}$$

The full system of equation in the matrix form is shown below. If such a form is put into the software, it solves all unknowns, ready to the next iteration step and consequently also time step.

$$\mathbf{T}_{att, left} \cdot \begin{pmatrix} \theta_{A(i)} \\ \theta_{B(i)} \\ \theta_{C(i)} \\ \theta_{D(i)} \\ \theta_{E(i)} \\ \theta_{F(i)} \\ \theta_{att(i)} \\ \theta_{rr(i)} \end{pmatrix} = \begin{pmatrix} A_{right} \\ B_{right} \\ C_{right} \\ D_{right} \\ E_{right} \\ F_{right} \\ \theta_{ecav,A(i,y-1)} \cdot \dot{m}_{catt_att,A(i,y-1)} \cdot c_{pa} + \theta_{ecav,B(i,y-1)} \cdot \dot{m}_{catt_att,B(i,y-1)} \cdot c_{pa} + \theta_{ecav,C(i,y-1)} \cdot \dot{m}_{catt_att,C(i,y-1)} \cdot c_{pa} + \theta_{ecav,D(i,y-1)} \cdot \dot{m}_{catt_att,D(i,y-1)} \cdot c_{pa} + \\ \theta_{ae(i)} c_{pa} \left(\dot{m}_{p,A(i,y-1)} + \dot{m}_{p,B(i,y-1)} + \dot{m}_{p,C(i,y-1)} + \dot{m}_{p,D(i,y-1)} \right) + \theta_{ai(i)} \dot{m}_{c_att(i,y-1)} \cdot c_{pa} + \theta_{att(i-1)} \kappa_{att} / \Delta\tau + Q_{c,gain(i)} \\ \alpha_{rr,A(i-1)}A_{1,A} + \alpha_{rr,B(i-1)}A_{1,B} + \alpha_{rr,C(i-1)}A_{1,C} + \alpha_{rr,D(i-1)}A_{1,D} + \alpha_{rr,E(i-1)}A_{1,E} + \alpha_{rr,F(i-1)}A_{1,F} + Q_{r,gain(i)} \end{pmatrix}$$

Thermal model – EAVE PARTS

As mentioned in some of the previous sections “EAVE PART” means the part of cathedralized (inclined) ceiling that is characterized by “length 2” in figures 17,18. The thermal and also moisture models compute each “eave part” using its own separate system of equations. However an approach to solve such a problem is similar to solving the attic-related system of equations presented in previous section (see 3.1.1 *Thermal model – “Thermal model – ATTIC”*).

3.1.2 Airflow model

The airflow model is directly bonded with the thermal model as the differences of an air temperature within the zones drive the airflow and mutually the airflow affects temperatures. Therefore there is, in the model, an iteration loop in every time step to find a balance between the two quantities. There are two separate airflow models - model of an airflow within the roof deck cavity and more complex model of an inter-zonal airflow between the interior, attic and eave cavity (ecav) spaces. The process of building-up the airflow models was mostly based on the Walker and Forest model presented in [34, 31].

Preliminary calculations:

- **Wind pressure coefficients - C_p**

Wind pressure coefficients on a building surfaces (and ventilation openings) are calculated according to [34]. However there was found an error in presented equation 18, which was fixed after an email consultation with Dr. Walker (author of the study) 20.7.2016.

Model presents a functions of surface averaged wind pressure coefficients on facades and roofs regarding wind direction. The coefficients are presented for a detached (isolated) and also undetached house with different roof slopes (however all for gable roofs). In the model presented in this doctoral study the wind pressures on the soffit vents (openings to the attic space) and eave vents of the roof-deck cavities are considered equal to the pressures acting on the facades below the particular eave. The peak (ridge) openings of the attic space as well as the top openings of the ventilated roof-deck cavities are considered to be exposed to the averaged pressure acting of the gable roof segment. Wind pressures on gable walls are considered to be equal to the pressures acting on the walls.

The empirical switching function (equation 18 in [34]) is, after consultation with the author simplified and changed to the form for roof slopes $\leq 30^\circ$ and > 30 respectively to form below. **It has to be pointed out, that quantity symbols presented in following two equations are in accordance with study [34] but not in accordance with symbols used in this doctoral thesis. Therefore they are also not numbered.**

$$F(\theta) = \cos \theta$$

$$F(\theta) = \cos^5 \theta$$

Airflow model – ROOF-DECK CAVITIES

As each roof-deck cavity consists of two parts, related to length 1 and length 2 (see schemes in figures 17,18), the model at first calculates the mean air temperature within the cavity as a weighted average of both lengths. Then the pressures across the eave and peak (ridge) openings are calculated with respect to the buoyancy and wind pressures. Finally the mass balance within the cavity is fulfilled resulting in the mass flow rate across the openings.

- **Wind-forced pressure difference across an opening**

Wind-forced pressure difference is calculated using following relation:

$$\Delta P_{U(i)} = C_{P(i)} \cdot S_U^2 \cdot \rho_{ae(i)} \cdot \frac{U_{o(i)}^2}{2} \quad (\text{eq.4 in [34]}) \quad (51)$$

Shelter coefficient S_U is a coefficient that adjusts the wind pressure according to the wind shelters nearby the house (openings). Coefficient can be in range from 0 to 1, while “0” means totally sheltered surface (e.g. façade of roof) where no wind pressure is taking place and “1” that there is no wind shelter nearby an object. Shelter coefficient is more closely described in study [34] and related studies.

Exterior air density is calculated in each time step as follows:

$$\rho_{ae(i)} = 1.293 \cdot \left(\frac{273.15}{\theta_{ae(i)} + 273.15} \right) \quad (52)$$

Wind speed at an orifice height is calculated from the reference wind speed at 10 m height and terrain coefficients.

$$U_{o(i)} = U_{10(i)} k_{wind} z_o^{a_{wind}} \quad (\text{pg. 230 in [57]}) \quad (53)$$

More information about terrain coefficients can be found in [57].

- **Buoyancy-caused pressure difference across an opening**

Regarding the pressure difference caused by buoyancy (temperature differences) is characterized by pressure gradient factor of the zone ($P_{T(i)}$).

$$P_{T,cav(i,z)} = g_G \cdot (\rho_{ae(i)} - \rho_{cav(i,z)}) \quad (\text{eq.12 in [34]}) \quad (54)$$

- **Mass flow rate across the openings**

The mass flow rate across the roof-cavity openings is characterized by a power law:

$$\dot{m} = \rho_a \cdot I \cdot \Delta P^L \quad (55)$$

The flow coefficient I is calculated from reference coefficient I_{ref} as follows:

$$I = I_{\text{ref}} \cdot \left(\frac{\theta_{\text{a,flow}} + 273.15}{\theta_{\text{ref}} + 273.15} \right)^{3L-2} \quad (\text{eq.3 in [34]}) \quad (56)$$

Reference flow coefficient for an orifice flow is calculated from following relation:

$$I_{\text{ref}} = J_d \cdot A_o \cdot \sqrt{\frac{2}{\rho_{\text{a,ref}}}} \quad (\text{eq.2-39 in [31]; pg.277 in [59]; pg.225 in [57]}) \quad (57)$$

where J_d is a discharge coefficient for an orifice flow. Its value is considered to be 0.6 (according to (pg.55 in [31]; pg.276 in [59]; pg.225 in [57])). $\rho_{\text{a,ref}}$ is reference density of air flowing across the opening – in the model this density is calculated according to equation (52) considering reference air temperature $\theta_{\text{a,ref}} = 10^\circ\text{C}$.

The flow exponent L for an orifice flow is considered to be 0.5 which is a common value for orifice flow and refers to fully turbulent flow.

Total pressure difference across the flow opening is calculated as follows:

$$\Delta P_{(j)} = P_{\text{R,ext}} - P_{\text{R,cav}(j)} + \Delta P_{\text{U,o}} - z_o \cdot P_{\text{T,cav}} \quad (58)$$

where the $P_{\text{R,ext}}$ and $P_{\text{R,cav}(j)}$ are a reference pressures for an exterior and the cavity space respectively. The exterior reference pressure is considered to be 0 Pa, while the cavity reference pressure is an unknown variable.

It may seem that the only variable is the cavity reference pressure, which can be calculated as the only one unknown in the mass balance equation. However there are two more unknowns – the densities of a flowing air across each particular opening. Moreover also the flow coefficients are dependent on the air densities. If the air density would be considered constant, the solution will be straight forward. However in the developed model an iteration loop using a bisection method is used (such an iteration loop is denoted as (j)).

Iteration process is based on the mass balance, where we search for the reference pressure within the cavity to fulfil the balance (mass flow rates across all openings results in zero). For the bisection method a two similar functions have been stated (see eq. (59 and 60)). It can be seen quite complicated expression of the mass flow rates in second equation (see eq. 60). However there is a good reason for that. The value of total pressure difference across the opening includes a

sign. A positive sign means that the pressure wants to drive the air to flow into the zone (into the cavity), while negative sign means that the pressure wants to suck the air out of the cavity. Thus the sign plays a very important role for solving the problem and needs to be preserved. However if the value is negative, by powering it with the flow exponent L , it returns a complex number which is not relevant. Therefore the pressure has to be powered as an absolute value. To keep also the sign

that is bonded with the value, the division $\frac{\Delta P_{(j)}}{|\Delta P_{(j)}|}$ is introduced within the equation since the only

result of such a ratio is the sign. This expression of the function can be moreover quite easily derived (see eq.(65)), instead of using, for instance, the “sign” function for keeping the sign within the value. This approach is adopted from [56].

$$f_{PR,cav(j)} = \dot{m}_{e,cav(j)} + \dot{m}_{p,cav(j)} \quad (59)$$

$$f_{PR,cav,Xa(j)} = \rho_{a,e,cav(j)} \cdot I_{e,cav(j)} \cdot \left(\frac{P_{R,ext} - X_{a(j)} + \Delta P_{U,e,cav} - z_{e,cav} \cdot P_{T,cav}}{P_{R,ext} - X_{a(j)} + \Delta P_{U,e,cav} - z_{e,cav} \cdot P_{T,cav}} \right) \cdot |P_{R,ext} - X_{a(j)} + \Delta P_{U,e,cav} - z_{e,cav} \cdot P_{T,cav}|^L - \quad (60)$$

$$\rho_{a,p,cav(j)} \cdot I_{p,cav(j)} \cdot \left(\frac{P_{R,ext} - X_{a(j)} + \Delta P_{U,p,cav} - z_{p,cav} \cdot P_{T,cav}}{P_{R,ext} - X_{a(j)} + \Delta P_{U,p,cav} - z_{p,cav} \cdot P_{T,cav}} \right) \cdot |P_{R,ext} - X_{a(j)} + \Delta P_{U,p,cav} - z_{p,cav} \cdot P_{T,cav}|^L$$

When the first function (59) would be extended to the form of the function (60), it would be seen, that both are almost identical. The only difference is that the $P_{R,cav(j)}$ in the first equation is replaced by the $X_{a(j)}$, which is a variable created for purpose of the iteration process. In fact there are two variables ($X_{a(j)}$ and $X_{b(j)}$), whose initial values states the estimated maximal and minimal value that the unknown variable ($P_{R,cav(j)}$) can be. In this problem, the values in first step are considered as $X_{a(1)} = 2000$ Pa and $X_{b(1)} = -2000$ Pa, while for the unknown reference pressure a following relation is valid in each iteration loop:

$$P_{R,cav(j)} = X_{a(1)} + \frac{X_{b(j)} - X_{a(j)}}{2} \quad (61)$$

Results of both functions are than multiplied and if the result is negative, for the next loop a following conditions apply:

$$\begin{aligned} X_{a(j+1)} &= X_{a(j)} \\ X_{b(j+1)} &= P_{R,cav(j)} \end{aligned} ,$$

if the result is positive values for next iteration loop are determined as:

$$\begin{aligned} X_{a(j+1)} &= P_{R,cav(j)} \\ X_{b(j+1)} &= X_{b(j)} \end{aligned} .$$

Airflow model – ATTIC-RELATED ZONES

A quite different approach is used in solving an airflow within the attic-linked system of zones. An approach is inspired by the [34] and [56].

- **Mass balance solver**

The system of mass balance equations is used to solve an airflow through the attic-related zones. Although the equations are not linear, the system of such an equations can be solved by an iteration loop, where in each step a linear system is solved [56]. For such a purpose a Newton-Raphson method is used.

As the unknown variable is a reference pressure of the zone, the general relation of the Newton-Raphson method for one zone is:

$$P_{R(j+1)} = P_{R(j)} - \frac{f(P_{R(j)})}{f'(P_{R(j)})} \quad (62)$$

where (j) is the iteration loop number.

If the zone has just two openings to the exterior, the function f has a following form:

$$\begin{aligned} f(P_{R,z(j)}) = & \\ I_{o1} \cdot \frac{(P_{R,ext} - P_{R,z(j)} + \Delta P_{U,o1} - z_{o1} \cdot P_{T,z})}{|P_{R,ext} - P_{R,z(j)} + \Delta P_{U,o1} - z_{o1} \cdot P_{T,z}|} \cdot |P_{R,ext} - P_{R,z(j)} + \Delta P_{U,o1} - z_{o1} \cdot P_{T,z}|^L + & \quad (63) \\ I_{o2} \cdot \frac{(P_{R,ext} - P_{R,z(j)} + \Delta P_{U,o2} - z_{o2} \cdot P_{T,z})}{|P_{R,ext} - P_{R,z(j)} + \Delta P_{U,o2} - z_{o2} \cdot P_{T,z}|} \cdot |P_{R,ext} - P_{R,z(j)} + \Delta P_{U,o2} - z_{o2} \cdot P_{T,z}|^L & \end{aligned}$$

Such a function can be more compactly as:

$$\begin{aligned} f(P_{R,z(j)}) = & \\ I_{o1} \cdot (P_{R,ext} - P_{R,z(j)} + \Delta P_{U,o1} - z_{o1} \cdot P_{T,z}) \cdot |P_{R,ext} - P_{R,z(j)} + \Delta P_{U,o1} - z_{o1} \cdot P_{T,z}|^{L-1} + & \quad (64) \\ I_{o2} \cdot (P_{R,ext} - P_{R,z(j)} + \Delta P_{U,o2} - z_{o2} \cdot P_{T,z}) \cdot |P_{R,ext} - P_{R,z(j)} + \Delta P_{U,o2} - z_{o2} \cdot P_{T,z}|^{L-1} & \end{aligned}$$

The derivative of the function is than:

$$\begin{aligned}
f'(P_{R,z(j)}) = & \\
& -I_{o1} \cdot L \cdot (P_{R,ext} - P_{R,z(j)} + \Delta P_{U,o1} - z_{o1} \cdot P_{T,z})^2 \cdot |P_{R,ext} - P_{R,z(j)} + \Delta P_{U,o1} - z_{o1} \cdot P_{T,z}|^{L-3} - \quad (65) \\
& I_{o2} \cdot L (P_{R,ext} - P_{R,z(j)} + \Delta P_{U,o2} - z_{o2} \cdot P_{T,z})^2 \cdot |P_{R,ext} - P_{R,z(j)} + \Delta P_{U,o2} - z_{o2} \cdot P_{T,z}|^{L-3}
\end{aligned}$$

It can be seen, that the terms within the brackets remained the same and thus the function and its derivative can be written in an even more compact form as:

$$f(P_{R,z(j)}) = I_{o1} \cdot \Delta P_{o1(j)} \cdot |\Delta P_{o1(j)}|^{L-1} + I_{o2} \cdot \Delta P_{o2(j)} \cdot |\Delta P_{o2(j)}|^{L-1} \quad (66)$$

$$f'(P_{R,z(j)}) = -I_{o1} \cdot L_{o1} \cdot \Delta P_{o1(j)}^2 \cdot |\Delta P_{o1(j)}|^{L-3} - I_{o2} \cdot L_{o2} \cdot \Delta P_{o2(j)}^2 \cdot |\Delta P_{o2(j)}|^{L-3} \quad (67)$$

For a system of interconnected zones a similar relation of Newton-Raphson method (as for one equation that can be seen in equation (62)) can be expressed:

$$P_{R(j+1)} = P_{R(j)} - \frac{f(P_{R(j)})}{J(P_{R(j)})} \quad (68)$$

\mathbf{P}_R is a vector of all unknown reference pressures, \mathbf{f} is a vector of mass balance functions related to each zone and \mathbf{J} is a Jacobian matrix including partial derivatives of the functions regarding the unknown reference pressures.

To use a linear system solver, a left and right side of the system should be separated. It can be performed as follows (suggested in [56]):

$$J(P_{R(j)}) \cdot \text{corr}_{(j+1)} = -f(P_{R(j)}) \quad (69)$$

where:

$$\text{corr}_{(j)} = P_{R(j+1)} - P_{R(j)} \quad (70)$$

An example can be than explained. For instance, if only two zones would be connected – one ecav space and the attic space, both of them having one additional opening to the exterior (ecav space having eave opening – e, and attic space having peak opening – p), the following relation would be performed in order to solve the system.

$$\begin{pmatrix} \frac{\partial f_{\text{ecav}(j)}}{\partial P_{\text{R,ecav}}} & \frac{\partial f_{\text{ecav}(j)}}{\partial P_{\text{R,att}}} \\ \frac{\partial f_{\text{att}(j)}}{\partial P_{\text{R,ecav}}} & \frac{\partial f_{\text{att}(j)}}{\partial P_{\text{R,att}}} \end{pmatrix} \cdot \begin{pmatrix} \text{CORR}_{\text{ecav}(j+1)} \\ \text{CORR}_{\text{att}(j+1)} \end{pmatrix} = \begin{pmatrix} f_{\text{ecav}(j)} \\ f_{\text{att}(j)} \end{pmatrix} \quad (71)$$

Which can be extended to final form:

$$\begin{pmatrix} -I_{\text{eatt}} \cdot L \cdot \Delta P_{\text{eatt_ecav}(j)}^2 \cdot |\Delta P_{\text{eatt_ecav}(j)}|^{L-3} & I_{\text{eatt}} \cdot L \cdot \Delta P_{\text{eatt_ecav}(j)}^2 \cdot |\Delta P_{\text{eatt_ecav}(j)}|^{L-3} \\ -I_{\text{e}} \cdot L \cdot \Delta P_{\text{e}(j)}^2 \cdot |\Delta P_{\text{e}(j)}|^{L-3} & \\ I_{\text{eatt}} \cdot L \cdot \Delta P_{\text{eatt_att}(j)}^2 \cdot |\Delta P_{\text{eatt_att}(j)}|^{L-3} & -I_{\text{eatt}} \cdot L \cdot \Delta P_{\text{eatt_att}(j)}^2 \cdot |\Delta P_{\text{eatt_att}(j)}|^{L-3} \\ & -I_{\text{p}} \cdot L \cdot \Delta P_{\text{p}(j)}^2 \cdot |\Delta P_{\text{p}(j)}|^{L-3} \end{pmatrix} \cdot \begin{pmatrix} \text{CORR}_{\text{ecav}(j+1)} \\ \text{CORR}_{\text{att}(j+1)} \end{pmatrix} =$$

$$\begin{pmatrix} I_{\text{eatt}} \cdot \Delta P_{\text{eatt_ecav}(j)} \cdot |\Delta P_{\text{eatt_ecav}(j)}|^{L-1} + I_{\text{e}} \cdot \Delta P_{\text{e}(j)} \cdot |\Delta P_{\text{e}(j)}|^{L-1} \\ I_{\text{eatt}} \cdot \Delta P_{\text{eatt_att}(j)} \cdot |\Delta P_{\text{eatt_att}(j)}|^{L-1} + I_{\text{p}} \cdot \Delta P_{\text{p}(j)} \cdot |\Delta P_{\text{p}(j)}|^{L-1} \end{pmatrix}$$

After the calculation the “new” values of reference pressures are obtained by adding the corrections to the “old” values. The iteration loop continues until a prescribed conditions are not fulfilled. In this model the iteration continues until the largest correction “CORR” of all the reference pressures is not greater than 1E-6 Pa.

3.1.3 Moisture model

As the Fourier's law of heat conduction (eq.1) and Fick's first law of diffusion (eq.3) are in their form very similar, the calculation core of the moisture model is based on the same scheme as the thermal model. However there is no airflow calculated and no radiation transfer, which makes the model simpler. On the other hand, there are a few other problems that makes the model also more complicated compared to the thermal model. At first, some materials (especially wood) have highly moisture-depend properties that should be expressed more precisely to get an appropriate results (in contrast with thermal model parameters such as heat capacity or thermal conductivity where often a constant values are sufficient enough). Particularly the moisture capacity and vapour permeability are representatives of such a moisture-dependent properties. Second common problem with moisture model is the dealing with an amount of condensate or frost. The approach to both problems is described in following sections.

Preliminary calculations

- **Saturated vapour pressure and concentration**

At first, for an evaluation of relative humidity and amount of condensate, it is needed to state partial vapour pressures at saturation or alternatively a saturated vapour concentration (saturated absolute humidity), which characterizes maximal amount of water vapour that can be present within an air of specific temperature and pressure. Those saturated amounts are stated for all nodes and all time steps as the temperatures of all computational nodes are already known from thermal model. In the model is used an equation where only temperature dependence on such a quantity is considered. Thus for partial vapour pressure and temperature ≤ 0 °C :

$$p_{v,\text{sat}}(\theta_a) = 4.689 \cdot \left(1.486 + \frac{\theta_a}{100} \right)^{12.3} \quad (72)$$

For temperature < 0 °C :

$$p_{v,\text{sat}}(\theta_a) = 288.68 \cdot \left(1.098 + \frac{\theta_a}{100} \right)^{8.02} \quad (73)$$

Although there should be held a limits for temperature ranges in which the previous equations are valid (min -20 °C and max +30 °C), the model does not take such a limits into account, since it is assumed, that the limits are exceeded just ion short time periods. However it was revealed that in such a periods can be, for instance in the roof-deck cavities, reached temperatures up to 60 °C – in that cases it would be more sufficient to use a better approximation of the saturated vapour pressure in those high temperature ranges.

Although the more common is a usage of partial vapour pressures, the model works with concentrations (absolute humidity) as more practically imaginable quantity. Relation between the two quantities is as follows:

$$v_{\text{sat}} = \frac{p_{v,\text{sat}}}{R_v \cdot (\theta_a + 273.15)} \quad (74)$$

- Moisture capacities of the air nodes (of the zones)

Specific moisture capacity of an air within the zone is calculated as follows:

$$\xi_a = \frac{p_{v,sat} \cdot R_a}{R_v \cdot p_{atm}} \quad (75)$$

Then a moisture capacity of the air within the zone is:

$$\kappa_{moist} = V_a \cdot \rho_a \cdot \xi_a \quad (76)$$

Moisture model - ATTIC

- Moisture capacities of the material nodes

For most materials is their moisture capacity considered as constant value (see Tab.5). However for wood based a sorption isotherm of spruce wood is used for a quantification of the moisture capacity in each time step. An isotherm for 23 °C measured at UCEEB CTU in Prague is used. An A-D-L model (Aranovich–Donohue scheme combined with classic Langmuir model) was adopted as suggested in [54]). An adsorption branch of the isotherm was used for the quantification of specific adsorption capacity regardless of the moisture evolution history (no hysteresis and scanning curves considered). The isotherm used has a following form:

$$u_{wood} = \frac{u_{m_sor} \cdot b_{sor} \cdot RH_{wood}}{(1 + b_{sor} \cdot RH_{wood}) \cdot (1 - RH_{wood})^{n_sor}} \quad (77)$$

where u_{m_sor} , b_{sor} and n_sor are parameters of the isotherm that for wood was quantified as:

$$u_{m_sor} = 0.2784 \text{ kg/kg}; b_{sor} = 1.15; n_sor = 0.17. \quad (78)$$

Specific sorption capacity of wooden based layers is then calculated as a derivative of sorption isotherm:

$$\xi_{wood(i)} = \frac{du_{wood(i-1)}}{dRH_{wood(i-1)}} \quad (79)$$

thus:

$$\xi_{wood(i)} = \frac{u_{m_sor} \cdot b_{sor} \cdot (1 - RH_{wood(i-1)})^{(-n_sor-1)} \cdot (b_{sor} \cdot n_sor \cdot RH_{wood(i-1)}^2 + (n_sor - 1) \cdot RH_{wood(i-1)} + 1)}{(b_{sor} \cdot RH_{wood(i-1)} + 1)^2} \quad (80)$$

Moisture capacity of material node is then calculated similarly as heat capacity (eq.8) as follows:

$$C_{\text{moist}} = d\rho\xi \quad (81)$$

- Vapour permeances

Similarly as moisture capacities, vapour permeances are mostly considered as constant values (for most of materials). However for a wood based materials (particularly wood and OSB, that are in the integrated in model material database) the water vapour resistance factor μ is variable. The reason is that especially wood (perpendicularly to the fibres) changes its permeability considerably according to its moisture content. Since the roof truss and sheathing is usually made out of such a materials it is appropriate to describe its permeability more precisely (instead of using a constant value). Based on literature survey and our measurement performed at UCEEB CTU for wood and OSB respectively is considered:

$$RH_{\text{spruce}} \leq 0.2; \quad \mu_{\text{spruce}} = 400$$

in higher values a linear interpolation between values is considered:

$$0.2 < RH_{\text{spruce}} \leq 0.35; \quad \mu_{\text{spruce}} = (0.35 - RH_{\text{spruce}}) \frac{400 - 130}{0.35 - 0.2} + 130$$

$$0.35 < RH_{\text{spruce}} \leq 0.6; \quad \mu_{\text{spruce}} = (0.6 - RH_{\text{spruce}}) \frac{130 - 30}{0.6 - 0.35} + 30$$

$$0.6 < RH_{\text{spruce}} \leq 0.85; \quad \mu_{\text{spruce}} = (0.85 - RH_{\text{spruce}}) \frac{30 - 6}{0.85 - 0.6} + 6$$

$$RH_{\text{spruce}} > 0.85; \quad \mu_{\text{spruce}} = 6$$

For an OSB board:

$$RH_{\text{OSB}} \leq 0.3; \quad \mu_{\text{OSB}} = 120$$

$$0.3 < RH_{\text{OSB}} \leq 0.8; \quad \mu_{\text{OSB}} = (0.8 - RH_{\text{OSB}}) \frac{120 - 40}{0.8 - 0.3} + 40$$

$$RH_{\text{OSB}} > 0.8; \quad \mu_{\text{OSB}} = 40$$

Vapour permeances are than calculated similarly to the thermal conductances (eq.9) as:

$$k = \frac{\delta_v}{d} \quad (82)$$

where:

$$\delta_v = \frac{\delta_{va}}{\mu} \quad (83)$$

By substitution there can be written more common relation:

$$k = \frac{\delta_{va}}{\mu \cdot d} = \frac{\delta_{va}}{s_d} \quad (84)$$

If a total permeance of more different layers have to be calculated an s_d -value is calculated as follows (similarly to eq.10):

$$s_{d,tot} = \sum_{l=1}^n s_{d(l)} = \mu_1 \cdot d_1 + \mu_2 \cdot d_2 + \dots + \mu_n \cdot d_n \quad (85)$$

The vapour permeability of still air (δ_{av}) is considered to be constant having a value of $25 \cdot 10^{-6}$ m²/s. Note that the subscript includes a symbol V, which represents an air permeability value for a mass transfer calculated using a vapour concentrations instead of partial vapour pressures. The relation between the two air permeabilities for different driving forces (difference of vapour concentrations and difference of partial vapour pressures) is as follows:

$$\delta_{va} = \delta_{pa} R_v T_a \quad (86)$$

Although in the model a constant value is used, equation (87) presents a Schirmer's relation (can be found in [55]), that can be used for more precise quantification.

$$\delta_{pa} = \frac{2.306 \times 10^{-5} \cdot p_0}{R_v T_a p_{atm}} \left(\frac{T_a}{273.13} \right)^{1.81} \quad (87)$$

- **Surface moisture transfer coefficients**

All convective surface moisture transfer coefficients β are calculated according to the convective heat transfer coefficient on particular surfaces following relation (88).

$$\beta = \frac{\alpha_c}{\rho_a c_{pa}} \quad (88)$$

- **Nodal equations**

Similarly to heat transport nodal equations that are based on energy balance, nodal equations in moisture model are based on mass balance.

General mass balance relation for every node is:

$$\sum_{k=1}^n G_{in(i),k} = \sum_{j=1}^m G_{out(i),j} + \frac{\kappa_{moist} \cdot (RH_{(i)} - RH_{(i-1)})}{\Delta \tau} \quad (89)$$

Since all calculation are performed using a vapour concentration as the unknown variable, the equation can be written also in following form:

$$\sum_{k=1}^n G_{in(i),k} = \sum_{j=1}^m G_{out(i),j} + \frac{\kappa_{moist} \cdot \left(\frac{v_{(i)}}{v_{sat(i)}} - \frac{v_{(i-1)}}{v_{sat(i-1)}} \right)}{\Delta \tau} \quad (90)$$

For even more simple version of the relation it can be considered that new saturated concentration ($v_{sat(i)}$) is very close to the old one ($v_{sat(i-1)}$). Thus the final form used in the model is as follows:

$$\sum_{k=1}^n G_{in(i),k} = \sum_{j=1}^m G_{out(i),j} + \frac{\kappa_{moist} \cdot (v_{(i)} - v_{(i-1)})}{v_{sat(i-1)} \cdot \Delta \tau} \quad (91)$$

- **Expression of unknowns**

Expression of unknown vapour concentrations are similar to the expression of the unknowns within the thermal model (equations (46) – (49)). Thus for a general node “z” in different positions within the model it is stated:

- Material nodes

$$v_{z-1(i)}(-k_{z-1,z}) + v_{z(i)}\left(k_{z-1,z} + \frac{C_{\text{moist},z(i-1)}}{v_{\text{sat},z(i-1)} \cdot \Delta\tau} + k_{z,z+1}\right) + v_{z+1(i)}(-k_{z,z+1}) = v_{z(i-1)} \cdot \frac{C_{\text{moist},z(i-1)}}{v_{\text{sat},z(i-1)} \cdot \Delta\tau} \quad (92)$$

- Zonal nodes

$$\begin{aligned} \sum_{k=1}^n v_{s,k(i)}(-\beta_k \cdot A_k) + v_{z(i)}\left(\sum_{k=1}^n (\beta_k \cdot A_k) + \sum_{l=1}^o \left(\frac{\dot{m}_{l,(i)}}{\rho_a}\right) + \frac{\kappa_{\text{moist},z(i-1)}}{v_{\text{sat},z(i-1)} \cdot \Delta\tau}\right) + \\ + \sum_{l=1}^o v_{a,l(i)}\left(\frac{-\dot{m}_{l,(i)}}{\rho_a}\right) = v_{z(i-1)} \cdot \frac{\kappa_{\text{moist},z(i-1)}}{v_{\text{sat},z(i-1)} \cdot \Delta\tau} + G_{\text{gain}(i)} \end{aligned} \quad (93)$$

- Interface nodes

$$v_{z-1(i)}(-k_{z-1,z}) + v_{z(i)}(k_{z-1,z} + k_{z,z+1}) + v_{z+1(i)}(-k_{z,z+1}) = 0 \quad (94)$$

- Surface nodes

$$\begin{aligned} v_{z-1(i)}(-k_{z-1,z}) + v_{z(i)}(k_{z-1,z} + \beta_{z,\text{zone_air}}) + \\ + v_{\text{zone_air}(i)}(-\beta_{z,\text{zone_air}}) = 0 \end{aligned} \quad (95)$$

- **Creating the system of equations using matrices**

Since the nodal equations are similar to the equations related to the thermal model, the same calculation scheme is used for the calculation of unknown vapour concentrations (see also section 3.1.1 *Thermal model* – pg.75).

- **Amount of condensate**

After the new vapour concentrations are calculated the model has to adjust some of the values. Some of them can be found oversaturated (i.e. $v_{(i)} > v_{\text{sat}(i)}$) that are not physically acceptable and indicates that some amount of water vapour changes its phase to liquid or solid. Such an amount of water has not to be lost as the mass balance should still be valid. There are several different approached to deal with such a problem. In the model presented in this study such an amount is stored in virtual “water tanks” that are bonded with each individual calculation node. Water in liquid or solid phase then remains in the tank until there are conditions suitable for its evaporation. When the evaporation from the tank takes place, the model has to also adjust the calculated vapour concentration values as the water from the tank rises up or saturates the calculation node. The particular set of equations that solves such a situations follows.

If the oversaturated concentration value is found ($v_{\text{prelim}(i)} > v_{\text{sat}(i)}$), it is set as saturated ($v_{(i)} = v_{\text{sat}(i)}$).

The increase of water amount in the particular water tank is then, for material nodes:

$$\Delta\omega_{C(i)} = \frac{C_{\text{moist}(i)}}{v_{\text{sat}(i-1)}} \cdot (v_{\text{oversat}(i)} - v_{\text{sat}(i)}) \quad (96)$$

and for air zone nodes:

$$\Delta\omega_{\kappa(i)} = \frac{\kappa_{\text{moist}(i)}}{v_{\text{sat}(i-1)}} \cdot (v_{\text{oversat}(i)} - v_{\text{sat}(i)}) \quad (97)$$

Then the new amount of water tank is:

$$\omega_{(i)} = \omega_{(i-1)} + \Delta\omega_{(i)} \quad (98)$$

Similarly when there is found lower than saturated value of vapour concentration in the node where there is some amount of water in the tank present, and if the amount is enough to saturate the node, the model sets the concentration value as saturated and evaporates an appropriate amount of water from the tank following next equation.

For material node:

$$\Delta\omega_{C(i)} = \frac{C_{\text{moist}(i)}}{v_{\text{sat}(i-1)}} \cdot (v_{\text{undersat}(i)} - v_{\text{sat}(i)}) \quad (99)$$

For zonal node:

$$\Delta\omega_{\kappa(i)} = \frac{\kappa_{\text{moist}(i)}}{v_{\text{sat}(i-1)}} \cdot (v_{\text{undersat}(i)} - v_{\text{sat}(i)}) \quad (100)$$

As the difference $\Delta\omega_{(i)}$ has now a negative sign, new amount of water in the tank respects equation (98) as well as in case of condensate formation.

Last case is when there is not enough water in the tank to saturate the vapour concentration. In that case the calculated vapour concentration would be adjusted respecting the previous relations as shown in relations 101 and 102. However it was not performed within the model and more simple calculation (eq.103) was used since was considered that such a cases are quite rare during the calculations.

For material node

$$v_{(i)} = = \frac{\Delta\omega_{C(i)} \cdot v_{\text{sat}(i-1)}}{C_{\text{moist}(i)}} + v_{\text{sat}(i)} \quad (101)$$

And for zonal node

$$v_{(i)} = = \frac{\Delta\omega_{\kappa(i)} \cdot v_{\text{sat}(i-1)}}{\kappa_{\text{moist}(i)}} + v_{\text{sat}(i)} \quad (102)$$

Final form of the new concentration calculation when there is not enough water within the tank to saturate it.

$$v_{(i)} = \frac{v_{(i)} + v_{\text{sat}(i)}}{2} \quad (103)$$

By thorough analysis of the condensation and evaporation part of the model it can be revealed that despite the effort the mass balance is not fully respected during such a processes. This analysis is however not a part of this thesis.

It should be also mentioned that there are no water tanks bonded to the surface of interface nodes and thus the model cannot quantify any amount of condensate on such a nodes. Although there can be found some relations of surface condensate amount (e.g. [47]), this relation is not a mass balance relation that should be valid for all nodes within the system, and thus it would make even larger error in the overall mass balance of the system. The model created in this study can thus only say the time period when surface relative humidity is equal to 100 %.

Moisture model – EAVE PARTS

Also the eave parts of the moisture model are calculated following the same approach as in previous section. Therefore its description is not independently presented.

3.2 Verification

Mathematical model was put to a set of simple tests to verify its proper functioning and detect possible errors. Tests were performed from the simplest to the most complex ones. Thermal model was at first tested without any airflow through the zones. Consequently a combination of thermal and airflow models was put to the test and finally an independent moisture model was tested as well. In total a 29 tests were performed.

All tests were accomplished successfully enough for the intended purposes of the model.

Full report from the verification can be found in “Appendix B”.

3.3 Validation

3.3.1 Thermal model validation

Thermal model was validated using data from one of previous experiments performed at University Centre for Energy Efficient Buildings under CTU in Prague. Experiment was performed using a box containing heat source, that was placed in climatic chamber with varying temperature. Box had dimensions ca. 0.75 x 0.75 x 1.2 m and was made out of gypsum board, XPS and plywood (see Fig. 21,22). Envelope constructions were precisely connected and overlapped for maximal elimination of heat losses through the joints. Heat source inside the box was well defined providing combination of convective and radiative parts of heat transfer. A set of temperature sensors was installed inside the box in different positions and on all surfaces (see Fig. 21). Data was recorded in 2-minutes time step. Box was placed inside the climatic chamber that all its outer surfaces were wind-washed by the conditioned air. Heat source was set to keep the mean inner air temperature at 20 °C, but was repeatedly switched on and off.

Results of comparison between measured and calculated data are depicted in figure 23. It can be seen quite reliable correlation between measured and calculated courses. Comparison was made for average air temperature and average surface. For basic statistical comparison was adopted an approach made in IEA Annex 41 project [53], where 13 models were compared with measured data. Comparison was performed using box-whisker plots (see Fig.24), (see also following section 3.3.2 *Moisture model validation*).



Fig. 21: left: test box in front of climatic chamber; right: open test box with hygro-thermal sensors and heat source

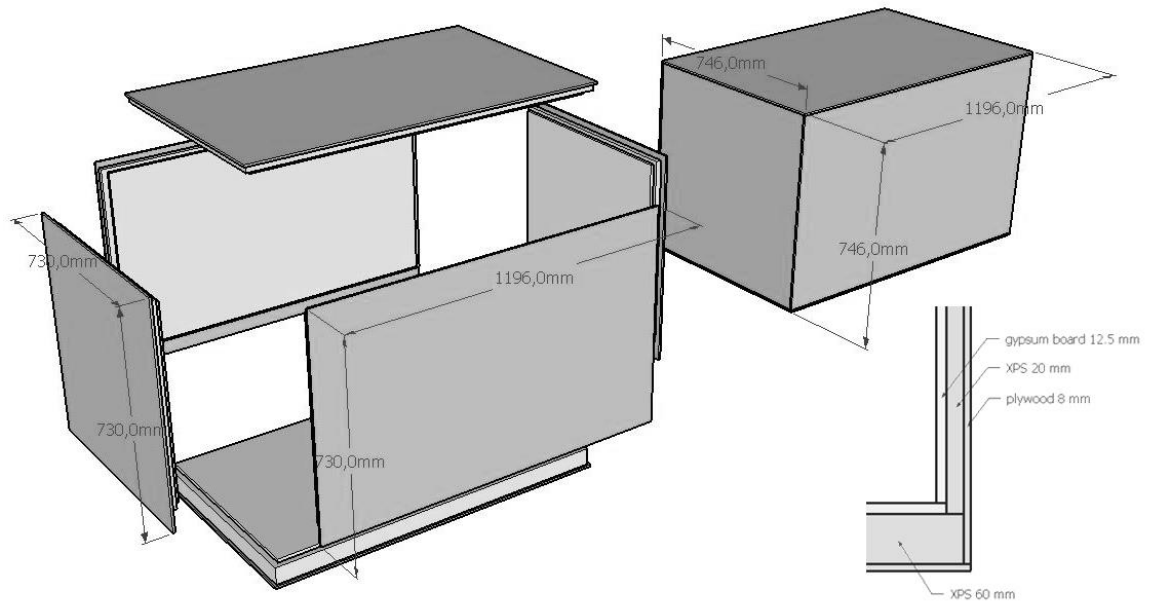


Fig. 22: Geometry of test box

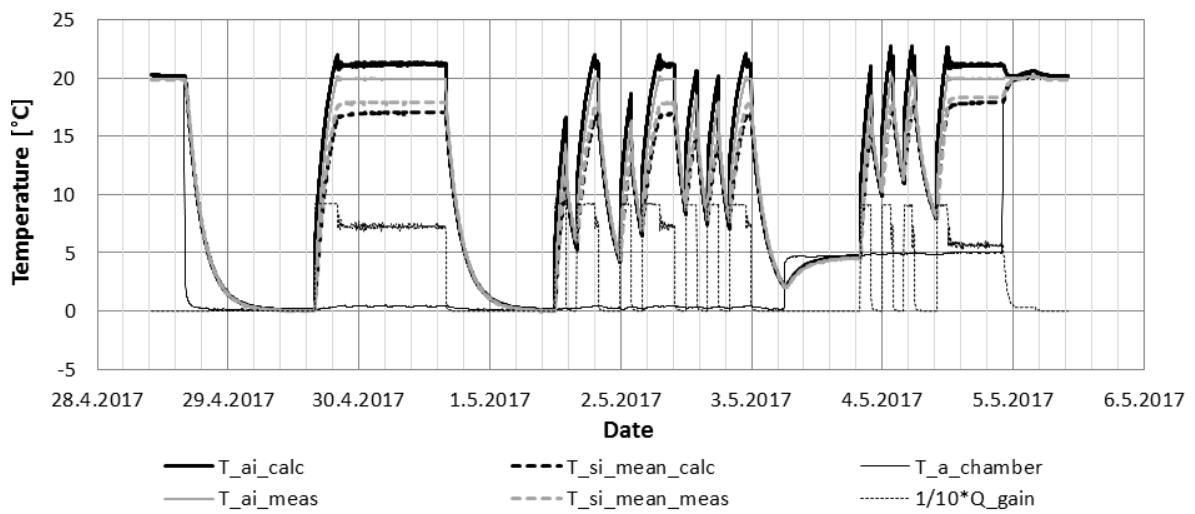


Fig. 23: Measured and calculated mean air and surface temperatures in the test box, ambient temperature (in climatic chamber) and one tenth of imposed heat gain.

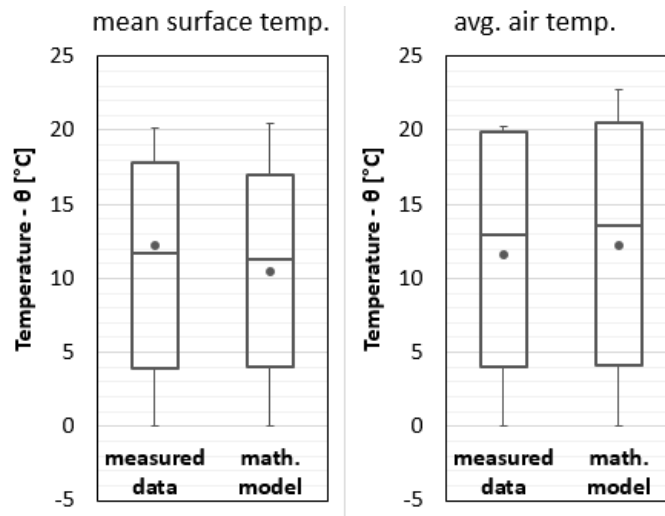


Fig. 24: Box-whisker plot of comparison between measured and calculated values of temperature

Tab. 6: Statistical data comparison between measured and calculated data from validation of the thermal model

	<i>mean surface temp.</i>		<i>avg. air temperature</i>	
	measured data	math. model	measured data	math. model
avg. value	12.22	10.46	11.60	12.22
maximal value	20.11	20.42	20.24	22.71
minimal value	-0.01	0.08	0.00	0.08
75% percentile	17.87	17.00	19.88	20.55
median	11.67	11.29	12.90	13.60
25% percentile	3.91	4.02	4.01	4.13

It can be found quite a good agreement between the measured and calculated data of surface and also air temperatures. It can be seen that the calculated mean surface temperature is slightly lower than the measured one. Oppositely the calculated average air temperature is placed slightly higher compared to the measurement. It implies that if the ratio of convective and radiative parts of the heat transfer would be adjusted, even better fit could be reached. All in all it can be stated, that thermal model is successively validated.

3.3.2 Moisture model validation

Moisture model was validated using data presented in project Annex41 - Subtask 1 (common exercise 3 – step 1 and 2) [53]. Calculated data of relative humidity was compared to data measured in test room during steps 1 and 2 (according to the original study). In step 1, all walls and ceiling of the room were covered with aluminium foil and flooring was made out of PVC (so no sorption within the space). In step 2 the foil was removed from the walls, allowing sorption to the 12.5 mm thick plasterboards. Walls had an area of 50 m² while volume of the room was 50 m³. Ventilation air change rate was held at 0.66 ach and temperature at 20 ± 0.2 °C. Inner moisture load was controlled simulating daily operation of 4-member family. Material properties of gypsum board were provided.

Comparison of measured and calculated data can be seen in figures 25 and 26. At first sight can be seen quite good correlation. It can be seen, how much the plasterboard layer on the walls inhibits the daily range of relative humidity.

As already mentioned in previous section, in the original project Annex 41 [53] was used a graphical presentation of statistical comparison using box-whisker plots. By adopting the same approach at figure 27 can be seen a comparison of measured and calculated data. Table 7 presents values of the charts. It can be seen that numerical model calculates slightly higher values in range of approximately 2-3 %. Average deviation of the comparison of “step 1” is ca. 2.5 %RH and in “step 2” ca. 2.7 %RH.

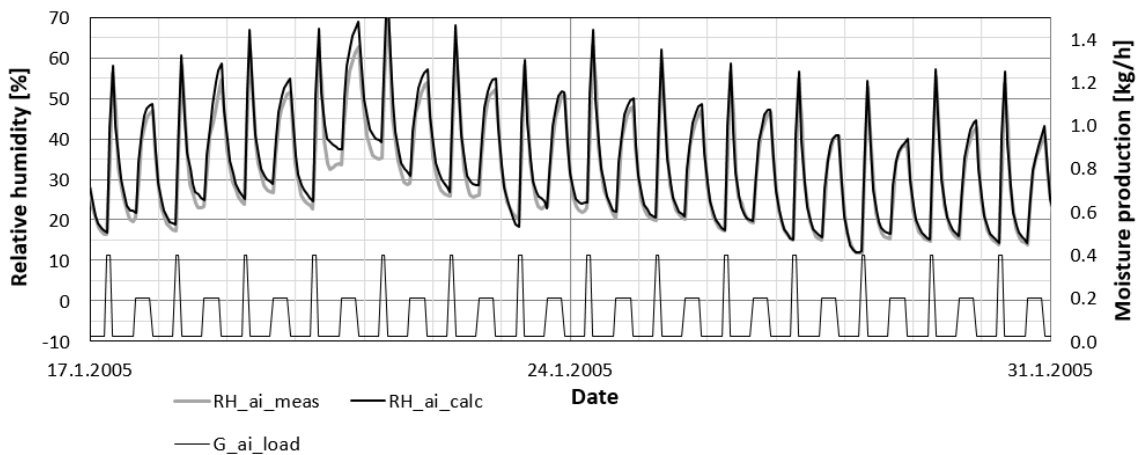


Fig. 25: Measured and calculated courses of relative humidity in test room (step1 according to [53])

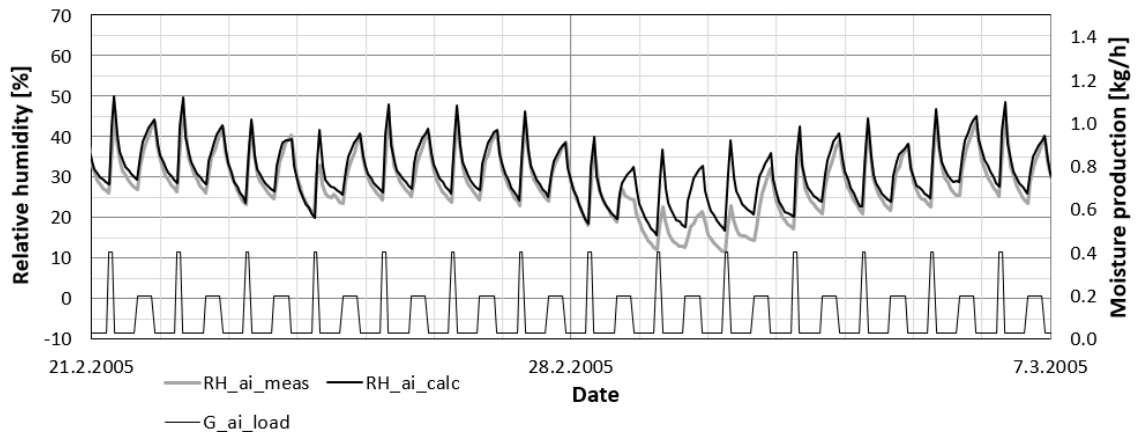


Fig. 26: Measured and calculated courses of relative humidity in test room (step2 according to [53])

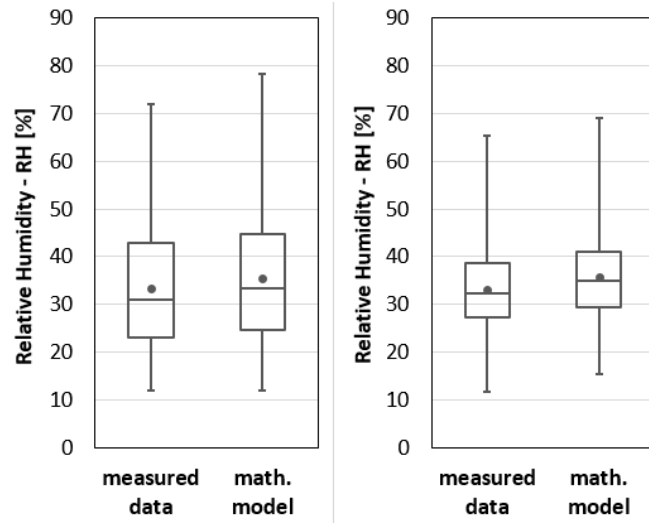


Fig. 27: Box-whisker plot of comparison between measured and calculated values of relative humidity

Tab. 7: Statistical data comparison between measured and calculated data from validation of the moisture model

	<i>step 1</i>		<i>step 2</i>	
	measured data	math. model	measured data	math. model
avg.value	33.2	35.3	33.1	35.7
maximal value	71.9	78.2	65.4	69.0
minimal value	11.8	12.0	11.6	15.5
75% percentile	42.9	44.8	38.6	40.9
median	31.0	33.3	32.3	34.9
25% percentile	23.1	24.6	27.3	29.5

3.3.3 Cavity-airflow model validation

Validation of an airflow model of ventilated roof-deck cavity was performed using data from experimental roof (see Fig.28). Although the real cavity is not ideal as it contains battens and contra-battens which affects the airflow pattern and also there are some air leakages through the roofing forced by wind acting on the roof, it can be seen that calculated data fits quite accurately to the measurement. Anemometer was installed in the level of contra-battens, where the main air stream is assumed and in the middle of the battens spacing. At first sight it can be seen, that measured data are placed higher compared to calculated ones. This difference can be attributed to a lot of factors, including model inaccuracy, but also positioning of the airflow sensors. Such a factors were not further analysed and the model was stated as sufficiently accurate for an intended purposes.

Statistical evaluation follows the same scheme described in previous sections (see Fig.30 and Tab.8).



Fig. 28: Experimental roof at UCEEB CTU

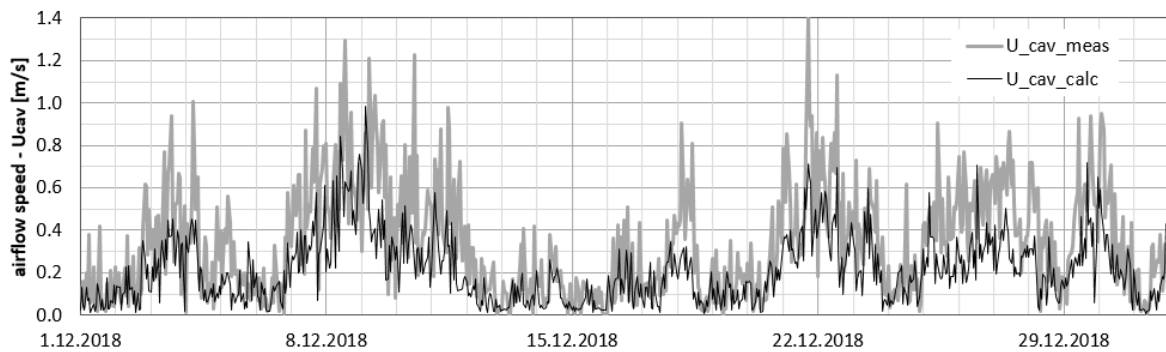


Fig. 29: Measured and calculated data of an airflow within the roof-deck cavity

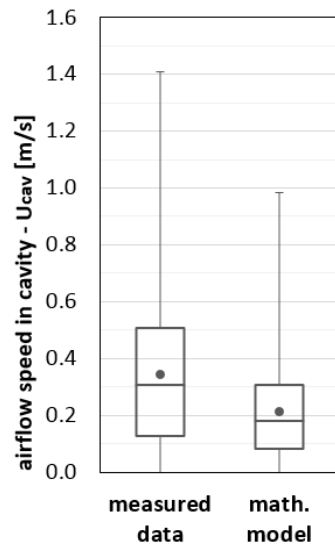


Fig. 30: Box-whisker plot of comparison between measured and calculated values of airflow speed in ventilated roof-deck cavity

Tab. 8: Statistical data comparison between measured and calculated data from validation of the airflow model

	measured data	math. model
avg.value	0.34	0.21
maximal value	1.41	0.98
minimal value	0.00	0.00
75% percentile	0.51	0.31
median	0.31	0.18
25% percentile	0.13	0.08

3.4 Conclusions

Numerical model was successively developed verified and validated.

Although the model represents a very useful tool for further cold attic analyses, it has still some parts that can be improved:

- Model is divided in few implicitly computed matrices instead of just one matrix. The linkages between the matrices are solved explicitly which is a potential source inaccuracy and other problems. It is so due to the fact that the eave parts of the model were implemented later during the model development process.
- The mean radiation temperature within the attic space is represented by just one value (area weighted mean of all inner-attic surfaces) instead of 6 values differing for each surface that the mean rad. temperature communicates with (energy wise).
- The surface and also interstitial condensation-related approach can be deeply studied and the model consequently improved.

4 Conclusions and outlook

The goal of this thesis was at first to find out whether it is possible to state one or more cold attic design suitable (moisture-safe) for whole or prevailing part of the HCT (humid cold and temperate) climate.

At first a thorough review of previous studies was carried out.

Few major problems were found towards the subject.

- 1) It is most likely that the studies dealing with hygro-thermal performance of cold attics were performed mostly in an areas where a moisture problems were recorded. Therefore it is possible that there is not well-distributed sample set across the whole HCT climate and consequent lack of information from other than the problematic areas. In an areas where there was no study found, is possibly a low number of moisture-related problems by using traditional attic designs (as it is also in Czech Republic, where an attic ventilation is usually enough for keeping the attic moisture-safe).
- 2) Within an analysed credible studies there were many different attic setups (designs) tested. After grouping those tested designs into “similar” groups, it was found that there are not enough samples (attic designs) in particular groups to draw any statistically relevant conclusions (see also section 2.3.3 *Grouping of similar designs*). Moreover the evaluated moisture safeness of designs within an each individual group were found to mostly not correspond (i.e. two similar designs in one group - one evaluated as moisture-safe while the other moisture-risky – see section 2.3.5 *Comparison of similar attic designs* and Tab. 4).
- 3) When looking at the suggested groups of similar attic designs, it was found that the groups of possible current and future best-practice are mostly empty (there were mostly no such a designs tested within the studies), (see section 2.3.5 *Comparison of similar attic designs*). Therefore this gap represents a well-defined room for potential future studies.

Despite the previous statements during the thorough analysis of previous cold attic studies, there were found many important general recommendations for moisture-safe cold attic design in HCT climate. Also there were stated some exception areas, where a different approach toward a suitable cold attic design should be used. Also the comparison of traditional European and North American roof decks, in terms of their affection of moisture-related problems, were stated and discussed (see section 2.3. *Discussion*).

It can be roughly summarized that:

It seems that moisture-safe cold attic design for an inland areas of HCT climate can be the ventilated cold attic with air- and vapour-tight ceiling construction. Preferable would be a double-skin roof deck with vapour permeable underlay felt. When such a roof-deck construction is used, also an unventilated cold attic design can perform similarly well.

In more humid maritime (coastal) areas of HCT climate is potentially advantageous to use an unventilated attic design with vapour permeable double-skin roof deck and tight ceiling. The more northern (colder climate) the more it is suitable to use a ventilated attic design.

For the purposes of further cold attic analysis a numerical HAM model was build-up in software Matlab 2018b. The model was successfully verified and validated. Full report from of the verification process can be found in *Annex B*. Validation was performed using three different reference measurements related to the thermal, moisture, and airflow parts of the model (see section *3.3 Validation*).

References

Selected cold attic studies

- [1] F.B. Rowley, A.B. Algren, C.E. Lund, (1941), Condensation of Moisture and its Relation to Building Construction and Operation, University of Minnesota, Retrieved from the University of Minnesota Digital Conservancy, <http://hdl.handle.net/11299/124254>.
- [2] D.M. Burch, G.A. Tsongas and G.N. Walton, (1996), Mathematical Analysis of Practices to Control Moisture in the Roof Cavities of Manufactured Homes, NISTIR 5880, National Institute of Standards and Technology, Gaithersburg, MD.
- [3] I. Samuelson, (1998), Hygrothermal performance of attics, J. Therm. Envel. Building Sci. Vol. 22, pp.132-145.
- [4] Ojanen, T., (2001), Thermal and moisture performance of a sealed cold-roof system with a vapor-permeable underlay, Proceedings Exterior Envelopes of Whole Buildings VIII, Clearwater Beach, Florida, December 2-7.
- [5] Kalagasidis, A.S. and Mattsson, B., (2005). Modelling of moisture conditions in a cold Attic space, 26th AIVC Conference, Brussels, Belgium.
- [6] A. Holm, K. Lengsfeld, (2006), Hygrothermal performance of unfinished attics (ventilated roofs) e An experimental study, in: Proceedings of the 3rd International Building Physics Conference e Research in Building Physics and Building Engineering, pp. 451e457.
- [7] Hagentoft CE., Sasic Kalagasidis A., Thorin M., Nilsson, (2008), Could growth control in cold attics through adaptive ventilation, 8th Nordic Symposium on Building Physics, Copenhagen, June 16-19, 2008.
- [8] Essah E, Sanders C, Baker P, Kalagasidis AS, (2009), Condensation and moisture transport in cold roofs: effects of roof underlay, Build Res Inform 2009;37(2): 117e28.
- [9] P. Roppel, M. Lawton, (2014), Attic Ventilation and Moisture Research Study e Final Report, no. June, Homeowner Protection Office, Burnaby, BC, Canada, p. 149.

Other cold attic studies

- [10] Arfvidsson, J. and Harderup, L-E, (2005), Moisture Safety in Attics Ventilated by Outdoor Air, The 9th Symposium in Building Physics, Island.
- [11] S. Uvsløkk, (2005), Moisture and temperature conditions in cold lofts and risk of mould growth, in: Proceedings of the 7th Symposium on Building Physics in the Nordic Countries, p. 8.
- [12] Hagentoft C-E, Sasic Kalagasidis A., (2010), Mould Growth Control in Cold Attics through Adaptive Ventilation: Validation by Field Measurements. 12th International Conference on Performance of the Exterior Envelopes of Whole Buildings, Clearwater Beach, Florida.

- [13] P. Johansson, G. Bok, A. Ekstrand-Tobin, (2011), Mould Growth in Attics and Crawlspace, 9th Nordic Symposium on Building Physics - NSB 2011, p.891-898.
- [14] A. Desjarlais et al., (2012), Energy and Moisture Performance of Attic Assemblies,” RCI Building Envelope Technology Symposium, Phoenix AZ, Oct 22-23.
- [15] Nik M.V., Sasic Kalagasidis A., Kjellström, E., (2012), Assessment of hygrothermal performance and mould growth risk in ventilated attics in respect to possible climate changes in Sweden, *Building and Environment* (55), p. 96-109.
- [16] Essah, E., (2012), Domestic cold pitched roofs in the UK: - effects of using different roof insulation materials, *International Journal of Ventilation*, 11 (3). Pp. 281-286, ISSN 2044-4044. (<http://centaur.reading.ac.uk/29836/>)
- [17] L.-E. Harderup and J. Arfvidsson, (2013), Moisture Safety in Cold Attics with Thick Thermal Insulation, *J. Archit. Eng.*, 2013, 19(4): 265-278, DOI: 10.1061/(ASCE)AE.1943-5568.0000067.
- [18] Hagentoft CE, Sasic Kalagasidis A., (2014), Moisture safe cold attics - Assessment based on risk analyses of performance and cost. Nordic Symposium on Building Physics. Lund, Sweden.
- [19] D. Prahl and M. Shaffer, (2014), Moisture Risk in Unvented Attics Due to Air Leakage Paths, US. Department of Energy, Energy Efficiency & Renewable Energy.
- [20] S. O. Mundt-Petersen*, L.-E. Harderup, (2015), Predicting hygrothermal performance in cold roofs using a 1D transient heat and moisture calculation tool, *Building and Environment* Vol. 90 , p.215-231.
- [21] S.P. Bjarløv, C.J. Johnston, M.H. Hansen, (2016), Hygrothermal conditions in cold, north facing attic spaces under the eaves with vapour-open roofing underlay in a cool, temperate climate. *Building and Environment*, Vol. 95, p.272-282.
- [22] A. Nielsen, M. Morelli, (2017), Measured temperature and moisture conditions in the roof attic of a one-and-a-half story house, 11th Nordic Symposium on Building Physics, *Energy Procedia*, Vol. 132, pp.789-794.
- [23] K. Kurkinen, (2017), Case Study of a Cold Attic in a Pitched Roof with Minimal Ventilation. 11th Nordic Symposium on Building Physics. *Energy Procedia*, Vol. 132, pp. 466-471.
- [24] H. Ge, R. Wang, D. Baril, (2018), Field measurements of hygrothermal performance of attics in extreme cold climates. *Building and Environment*, Vol. 134, pp.114–130. <https://doi.org/10.1016/j.buildenv.2018.02.032>
- [25] T. Hansen, E.B. Moeller, (2019), Hygrothermal performance of cold ventilated attics above different horizontal ceiling constructions – Field survey. *Building and Environment*, Vol. 165, 106380. <https://doi.org/10.1016/j.buildenv.2019.106380>

Other

- [26] Federal Housing Administration. (1942). Property Standards and Minimum Construction Requirements for Dwellings. Washington, DC, Federal Housing Administration.

- [27] Burch, D.M. and Thomas, W.C., (1992), An Analysis of Moisture Accumulation in a Wood Frame Wall Subjected to Winter Climate, Proceedings of Thermal Performance of the Exterior Envelopes of Buildings V, ASHRAE/DOE/BTECC Conference, Dec. 7-10, Clearwater Beach, FL.
- [28] Rose, W.B., and A.A. TenWolde, (2002), Venting of Attics and Cathedral Ceilings, ASHRAE Journal 44 (10): 26–33, ASHRAE. Atlanta, GA.
- [29] Attic ventilation design strategies for manufactured homes, Manufactured Housing Research Alliance, October 21, (2002).
- [30] Federal Housing Administration. (1942). Property Standards and Minimum Construction Requirements for Dwellings. Washington, DC, Federal Housing Administration.
- [31] Walker, I. S., (1993), Prediction of ventilation, heat transfer and moisture transport in attics, ProQuest Dissertations and Theses; University of Alberta.
- [32] Walker, I. S., and T. W. Forest, (1995), Field Measurements of Ventilation Rates in Attics. Building and Environment, Vol. 30, No. 3, pp. 333-347.
- [33] I. S. Walker and D. J. Wilson, (1998), Field Validation of Algebraic Equations for Stack and Wind Driven Air Infiltration Calculations, Published in ASHRAE HVAC&R Research Journal, Vol. 4, No. 2, April 1998.
- [34] Walker, I.S., Forest, T.W. and Wilson, D.J., (2005) An Attic-Interior Infiltration and Interzone Transport Model of a House. Building and Environment, Vol. 40, Issue 5, pp. 701-718.
- [35] F.B. Rowley, A.B. Algren, and C.E. Lund, (1939), Condensation of Moisture and its Relation to Building Construction and Operation. ASHRAE Transactions, 44 (1115).
- [36] A. Janssens (1998), Reliable Control of Interstitial Condensation in Light-Weight Roof Systems: Calculation and Assessment Methods, Doctoral Thesis, KU Leuven.
- [37] J. Lstiburek, (2006), Understanding Attic Ventilation. Building Science Digest 102. (Rev. 12/2013).
- [38] J. Lstiburek, (2011), A Crash Course in Roof Venting. https://www.buildingscience.com/sites/default/files/migrate/pdf/PA_Crash_Course_Roof_Venting_FHB.pdf
- [39] Hens, H., Applied Building Physics: Boundary Conditions, Building Performance and Material Properties, (2012), ISBN:9783433029626
- [40] Solař, J., Problematika nadměrné vlhkosti u střešních pláštů šikmých a strmých střech, é TZB-info, 2012. (in Czech)
- [41] Solař, J., Příčiny nadměrné vlhkosti dřevěných stavebních prvků v budovách, TZB-info, 2014. (in Czech)
- [42] C.-E. Hagentoft, (2011), Probabilistic Analysis of Hygrothermal Conditions and Mould Growth Potential in Cold Attics. Impact of Weather, Building System and Construction Design Characteristics, XII DBMC, Porto, PORTUGAL, 2011.

- [43] Hagentoft C-E., Kalgasidis A.S., (2016), Drying potential of cold attic using natural and controlled ventilation in different Swedish climates. 8th International Cold Climate HVAC 2015 Conference, Procedia Engineering, Vol. 146, p.2–7.
- [44] M. Belusko, F. Bruno, W. Saman, (2011), Investigation of the thermal resistance of timber attic spaces with reflective foil and bulk insulation, heat flow up. Applied Energy, Vol. 88, p. 127–137.
- [45] Gullbrekken L. et al., (2016), Norwegian Pitched Roof Defects. Buildings 2016, 6, 24; doi:10.3390/buildings6020024.
- [46] MATLAB 2018b, The MathWorks, Inc., Natick, Massachusetts, United States.
- [47] Hagentoft Carl-Eric, Introduction to Building Physics, Studentlitteratur AB, (2001), ISBN: 9789144018966.
- [48] Staněk, K., Úloha 1 – Větraná dutina, Podklady pro cvičení ST2B, textbook CTU in Prague, (2012).
- [49] Engineering ToolBox, (2001). [online] Available at: <https://www.engineeringtoolbox.com> [13.1.2020].
- [50] R.J. Ross (Edi.), (2010), Wood Handbook: Wood as an Engineering Material. General Technical Report FPL–GTR–190, Forest Products Laboratory, USDA.
- [51] Serge Ferrari A G, page from website (<https://www.stamisol.com/en/about-stamisol/history.html>), [18.1.2020].
- [52] website of Passive House Institute – PHI, [22.1.2020], (https://passiv.de/en/02_informations/02_passive-house-requirements/02_passive-house-requirements.htm)
- [53] International Energy Agency (IEA), Energy Conservation in Buildings & Community Systems Programme (ECBCS): Annex 41 – Common Exercise 3, 2003 – 2007. Available online: http://www.kuleuven.be/bwf/projects/annex41/protected/Common_Exercises/Documentation_of_Common_Exercises.htm

Moisture

- [54] Zhang, P., Li Wang, (2010), Extended Langmuir equation for correlating multilayer adsorption equilibrium data. Separation and Purification Technology, Vol. 70, p.367-371.
- [55] Schirmer, R., ZVDI, Beiheft Verfahrenstechnik, Nr. 6, S. 170, (1938).

Airflow

- [56] Feustel H.E., et al., (1990), Fundamentals of the Multizone Air Flow Model – COMIS, Technical Note 29, Air Infiltration and Ventilation Centre, University of Warwick Science Park, (IEA programme), ISBN: 0-946075-44-1.

- [57] Liddament M. W., (1996), AIVC Guide: A guide to Energy Efficient Ventilation. Air Infiltration and Ventilation Centre, University of Warwick Science Park, (IEA programme), ISBN 0 946075 85 9.
- [58] M. Orme, N. Leksmono, (2002), AIVC Guide 5: Ventilation Modelling Data Guide. (IEA programme), ISBN 0 946075 85 9.
- [59] Building science for building enclosures, John F. Straube, Eric F. P. Burnett, Building Science Press, (2005), ISBN: 0-9755127-4-9.
- [60] A. Bejan, (not sure about the original book – it is a found chapter), (.pdf document created 2003, edited 2008), Chapter 5, Forced Convection: Internal Flows. Department of Mechanical Engineering and Materials Science, Duke University, Durham, North Carolina.
- [61] website of “The National Air Barrier Association - NABA” [22.1.2020] available at: https://www.naba.ca/air_barriers/materials.php

Mould growth

- [62] Vereecken, E., Roels, S., (2012), Review of mould prediction models and their influence on mould risk evaluation. Build Environ. 51: 296-310.
- [63] Hukka, A, Viitanen, H.A., (1999), A mathematical model for mould growth on wooden material. Wood Sci. Technol. 33(6): 475-485.
- [64] Viitanen, J., Ojanen, T., (2007), Improved model to predict mold growth in building materials. In: Proceeding of thermal performance of the exterior envelopes of whole buildings X (on CD).
- [65] Adan, O.C.G., Samson, R.A., (eds.), (2011): Fundamentals of mould growth in indoor environments and strategies for healthy living. The Netherlands, Wageningen Academic Publishers. ISBN: 978-90-8686-135-4, e-ISBN: 978-90-8686-722-6, DOI: 10.3920/978-90-8686-722-6.
- [66] Rychtera, M., Němcová-Machová, B., Genovová, E., (1974), Atmospheric microbial corrosion of technical materials and its prediction. Prague, Czech Republic, Academia. Edice: Rozpravy ČSAV, Series techn. Sciences. You're. 3 (Řada techn. věd. Seš. 3) (Vol. 84/1974). (in Czech)
- [67] Sedlbauer, K., (2001), Prediction of mold fungus formation on the surface of and inside building components. Dissertation, Stuttgart University, 247 pp.
- [68] Platt, S.D., et al., (1989), Damp housing, mould growth, and symptomatic health state. Brit. Med J. 298(6689): 1673-1678.
- [69] Piecková, E., Jesenská, Z., (1999), Microscopic fungi in dwellings and their health implications. Ann. Agric. Environ. Med., Vol.6, p.1-11.
- [70] Johansson, P., (2012), Critical moisture conditions for mould growth on building materials. Thesis. Lund University, 119 pp.

[71] Dix, N.J., Webster, J., (1995), Fungal ecology. London: Chapman & Hall, ISBN: 978-94- 010-4299-4 (Print) 978-94-011-0693-1 (Online), 549 pp.

[72] Shigo, A.L., (1975), Biological of decay and wood quality. In: Biological transformation of wood by microorganisms (W. Liese, ed.), Springer-Verlag, Berlin and New York, p.1-15.

Köppen-Geiger climate classification

[73] Kottek, M., et al., (2006), World map of the Köppen-Geiger climate classification updated, Meteorol. Zeitschr., 15(3), p.259–263.

[74] Peel MC, Finlayson BL & McMahon TA, (2007), Updated world map of the Köppen-Geiger climate classification. Hydrol. Earth Syst. Sci., Vol. 11, p.1633-1644.

[75] Rubel, F., and M. Kottek, (2010), Observed and projected climate shifts 1901-2100 depicted by world maps of the Köppen-Geiger climate classification. Meteorol. Z., Vol. 19, p.135-141. DOI: 10.1127/0941-2948/2010/0430.

[76] Geiger, R., (1954), Klassifikation der Klimate nach W. Köppen, [Classification of climates after W. Köppen]. Landolt-Börnstein – Zahlenwerte und Funktionen aus Physik, Chemie, Astronomie, Geophysik und Technik, alte Serie. Berlin: Springer. 3. pp. 603–607.

[77] Geiger, R., (1961), Überarbeitete Neuauflage von Geiger, R.: Köppen-Geiger / Klima der Erde. (Wandkarte 1:16 Mill.) – Klett-Perthes, Gotha.

[78] Köppen, W., (1900), Versuch einer Klassifikation der Klimate, vorzugsweise nach ihren Beziehungen zur Pflanzen-welt. Geographische Zeitschrift 6, 569-611, 657-679.

[79] A. Merkel, web site: (<https://en.climate-data.org/info/sources/>), AM Online Projects.

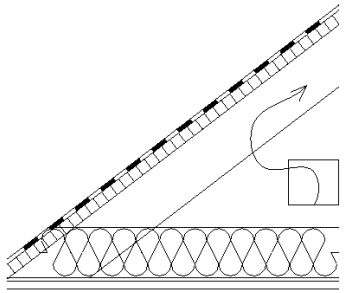
Appendices

Appendix A – Overview of analysed attic designs

Rowley et al. (1941) – USA. [1]

Full-scale experimental house inside a conditioned room was used to study condensation of moisture and its relation to building construction and operation. Beside other constructions a risk of condensation and frost accumulation in cold attics under sloped roof-deck were studied using different ventilation regimes and boundary conditions.

Design no: 1

<p>General information: <u>study type</u>: experimental <u>design</u>: full-scale bungalow (one storey + attic) placed in conditioned chamber $A_{ceil,real} = ca. 35 m^2$ $V_{att,real} = ca. 48 m^3$ <u>roof slope</u>: 45° <u>roof orientation</u>: not specified (in climatic chamber) <u>ventilation</u>: 3 gable openings, area of each 1:290 of attic floor area – thus ca. 1:100 in total <u>other</u>: attic stairwell leaky - test labelled “40-9-2” according to the original study</p>		<p><u>Roof-deck assembly</u>:</p> <ul style="list-style-type: none"> asphalt shingles pine shiplap 1x8" (25 mm) <p>$S_{d,r,deck} = ca. 200 m$</p> <p><u>Ceiling assembly</u>:</p> <ul style="list-style-type: none"> mineral wool between wooden joists 3 5/8" (92 mm) metal lath 3/4" (19 mm) plaster <p>$S_{d,ceil} = ca. 0.3 m$ $U_{ceil} = ca. 0.52 W/m^2/K$</p> <p>- leaky attic stair well $Q_{50,hatch} = ca. 20.6 I/s/50Pa$ - ceiling construction $Q_{50,ceil} = ca. 0.17 I/s/m^2/50Pa$ - equivalent ceiling air permeance $Q_{50,ceil,tot} = ca. 0.76 I/s/m^2/50Pa$</p>
<p>Indoor conditions:</p> <ul style="list-style-type: none"> 70 °F (21 °C) 40 %RH 	<p>Outdoor conditions:</p> <ul style="list-style-type: none"> around -7.9 °F (-22 °C) humidity not specified 	

Design no: 2 (test labelled “40-9-3” according to the original study)

- same as 1 with following exceptions :
 - o air-sealed attic stair well
 - o outdoor temperature changed to - 4.8 °F (-20 °C)

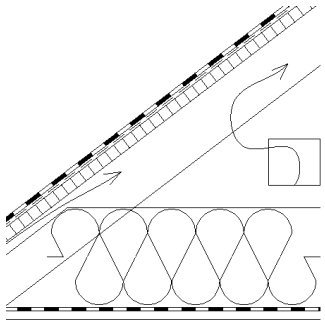
Design no: 3 (test labelled “40-9-4” according to the original study)

- same as 1 with following exceptions :
 - o air-sealed attic stair well
 - o no attic ventilation
 - o outdoor temperature changed to - 5.8 °F (-21 °C)

Design no: 4

Burch et al. (1996) – USA. [2]

An upgraded version of mathematical model called MOIST was used to analyse the effectiveness of practices of moisture control in cold attic spaces. Moisture content of plywood sheathing of north-sided roof-deck was studied using sensitivity analysis of selected attic parameters. Than a set of various attic designs in different locations in USA were compared.

<p>General information: <u>study type</u>: computational <u>design</u>: ceiling height 2.44 m $A_{\text{ceiling}} = 130 \text{ m}^2$ $V_{\text{att}} = \text{ca. } 35 \text{ m}^3$ (estimated from a figure)</p> <p><u>roof slope</u>: 14° <u>roof orientation</u>: south-north <u>ventilation</u>: gable end walls and roof constructions were fitted with vents of net free open area of 1:300 of the floor area, unintentional leakage area assumed as 1/10 of vents area (i.e. $ELA_{\text{r,deck}} = 434 \text{ cm}^2$) <u>else</u>:</p>		<p>Roof-deck assembly:</p> <ul style="list-style-type: none"> asphalt shingles (solar abs. = 0.8) asphalt roofing paper exterior-grade plywood 12 mm <p>$S_{d,\text{r,deck}} = \text{ca. } 200 \text{ m}$</p> <p>Ceiling assembly:</p> <ul style="list-style-type: none"> 180 mm glass fibre insulation – 3.9 $\text{m}^2\text{K/W}$ 0.15 mm kraft paper (vapour retarder) ($s_d = \text{ca. } 2.1 \text{ m}$, in 50 % RH) 13 mm gypsum board <p>$S_{d,\text{ceiling}} = \text{ca. } 2.6 \text{ m}$ $U_{\text{ceiling}} = \text{ca. } 0.24 \text{ W/m}^2\text{/K}$ $Q_{50,\text{ceiling}} = \text{ca. } 0.3 \text{ l/s/m}^2/50\text{Pa}$</p>
<p>Indoor conditions:</p> <ul style="list-style-type: none"> natural ventilation – 0.48 ach when wind speed $v = 4.9 \text{ m/s}$ and temperature difference $\Delta T = 16.7 \text{ K}$ non-humidified interior - relative humidity vary approx. between 20 / 60 % (summer / winter) 20-24 °C 	<p>Outdoor conditions:</p> <ul style="list-style-type: none"> Madison (WI), Portland (OR), Atlanta (GA); USA before 1996 	

Design no: 5

- same as 4 with following exceptions :
 - o location of the attic – Boston (MA); USA

Design no: 6

- same as 4 with following exceptions :
 - o no attic ventilation opening (ventilation just by leakages – ca. 1 ach at 2.5 m/s wind speed)
 - o location of the attic – just Madison (WI); USA

Design no: 7

- **same as 4 with following exceptions :**
 - humidified interior – min RH = 45 %
 - location of the attic – just Madison (WI); USA

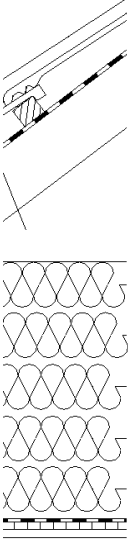
Design no: 8

- **same as 4 with following exceptions :**
 - totally air-tight ceiling
 - location of the attic – just Madison (WI); USA

Design no: 9

Samuelson (1998) - Sweden. [3]

Study deals with measurement of temperature and relative humidity in six attic designs differing in used thermal insulation at the ceiling level (mineral wool, cellulose fibres) and ventilation systems (non-ventilated, naturally and mechanically ventilated). Subsequently a team of researchers tried to fit their numerical models to measured data.

<p>General information: <u>study type</u>: experimental <u>design</u>: (8) 6 testing sections of an attic above a flat roof of office building each section: $A_{ceil} = ca. 23.5 m^2$ (estimated from a drawing) $V_{att} = ca. 28 m^3$ (estimated from a drawing) <u>roof slope</u>: approx. 1:2 (i.e. 26° - estimated from drawing) <u>roof orientation</u>: not specified <u>ventilation</u>: mechanically ventilated (2 ach) <u>else</u>: essentially totally airtight ceiling and a negative pressure kept on interior side of the ceiling (no moisture input to the attic from interior)</p>		<p>Roof-deck assembly:</p> <ul style="list-style-type: none"> • concrete tiles • PE film <p>$S_{d,r,deck} = ca. 10 m$</p> <p>Ceiling assembly:</p> <ul style="list-style-type: none"> • 500 mm mineral wool • PE foil • secondary spaced boarding • gypsum plants <p>$S_{d,ceil} = ca. 10 m$ $U_{ceil} = ca. 0.077 W/m^2/K$ $Q_{50,ceil} = 0 l/s/m^2/50Pa$ (since the interior underpressure provides no flow from interior into the attic)</p>
<p>Indoor conditions:</p> <ul style="list-style-type: none"> • office building • ca. 17 - 24 °C • 31-55 %RH • underpressure (related to attic space) 	<p>Outdoor conditions:</p> <ul style="list-style-type: none"> • Swedish weather (Borås) - 1994-1995 	

Design no: 10

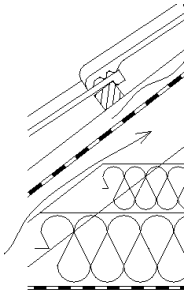
- same as 9 with following exceptions :
 - plywood instead of PE foil underlay was used
 - no attic ventilation
 -

Design no: 11

- same as 9 with following exceptions :
 - plywood instead of PE foil underlay was used
 - naturally ventilated - 50 mm openings by the eaves (i.e. ventilation rule ca.1:84)

Design no: 12
Ojanen (2001) - Finland. [4]

Experimental attic with five sections was used to compare a hygro-thermal performance of traditional Finish ventilated attic using plastic foil underlay and non-ventilated attic design with the use of highly permeable underlay foil. Concrete tiles and steel plates were compared in both options. Three different tests during three heating seasons were performed.

<p>General information: <u>study type</u>: experimental <u>design</u>: 5 attic sections (1.2 m) above 6 m wide bungalow (one storey) $A_{\text{ceil}} = 7.2 \text{ m}^2$ $V_{\text{att}} = 5.4 \text{ m}^3$ <u>roof slope</u>: 1:2 (ca. 26°) <u>roof orientation</u>: south-north <u>ventilation</u>: eaves (+ridge)</p> <p><u>other</u>: test period 1 (reference with concrete tiles)</p> <p>– air-tight ceiling and water vessels in the attics (controlled moisture load 1 g/h/m^2 - per ceiling area), corresponding to continuous air inflow 0.1 l/s/m^2 from interior space. It means total 7.2 g/h moisture load.</p>		<p>Roof-deck assembly:</p> <ul style="list-style-type: none"> • concrete tiles • ventilated cavity 50 mm • reinforced plastic foil <p>$S_{d,r,\text{deck}} = 10 \text{ m}$</p> <p>Ceiling assembly:</p> <ul style="list-style-type: none"> • 250 mm glass wool (150 + 100 mm batts) • perfectly airtight PE foil <p>$S_{d,\text{ceil}} = \text{ca. } 10 \text{ m}$ $U_{\text{ceil}} = \text{ca. } 0.15 \text{ W/m}^2/\text{K}$</p> <p>simulated moisture input $Q_{\text{ceil},\text{sim}} = \text{ca. } 0.1 \text{ l/s/m}^2$ <i>considering pressure difference 4 Pa it corresponds to:</i> $Q_{50,\text{ceil},\text{sim}} = \text{ca. } 0.54 \text{ l/s/m}^2/50\text{Pa}$</p> <p><i>real air permeance of the ceiling is possibly:</i> $Q_{50,\text{ceil}} = \text{ca. } 0.002 \text{ l/s/m}^2/50\text{Pa}$</p>
<p>Indoor conditions:</p> <ul style="list-style-type: none"> • 22 °C; 35 %RH 	<p>Outdoor conditions:</p> <ul style="list-style-type: none"> • Finish weather (Espoo)- 1998-1999 	

Design no: 13 (test period 1 – according to the study)

- **same as 12 with following exceptions :**
 - no attic ventilation openings (sealed attic)
 - vapour permeable flash-spun HDPE underlay foil
 - $S_d < 0.02 \text{ m}$;
 - airflow permeance $< 3.3 \cdot 10^{-6} \text{ m}^3/\text{s}/\text{m}^2/\text{Pa}$
 - $S_{d,r,\text{deck}} = 0.02 \text{ m}$
 - $Q_{50,r,\text{deck}} = \text{ca. } 0.33 \text{ l/s/m}^2/50\text{Pa}$

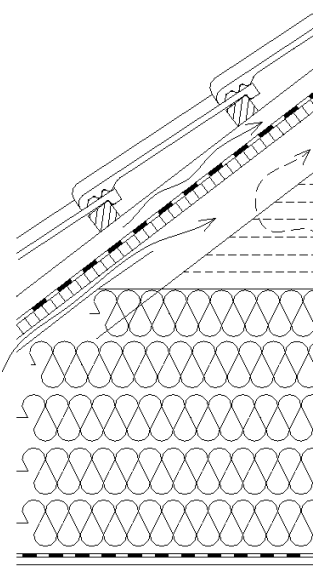
Design no: 14 (test period 2 – according to the study)

- **same as 13 with following exceptions :**
 - no simulated moisture gain (i.e. air-tight ceiling and roof deck)
 - real ceiling air permeance ca. $Q_{50,\text{ceil}} = \text{ca. } 0.002 \text{ l/s/m}^2/50\text{Pa}$
 - steel plate roofing above ventilated roof-deck cavity
 - 20 Pa indoor overpressure

Design no: 15

Kalagasidis and Mattsson (2005) - Sweden. [5]

Using numerical modelling the study investigated an impact of the wind and air infiltration from a living space to moisture conditions in cold attic. Ventilated and non-ventilated attic designs with tight and leaky ceilings in an open and city areas (regarding different wind speed conditions) were compared. The aim was to find out whether the ventilation of the attic may help in removing convectively transported moisture through the attic floor.

<p>General information: <u>study type</u>: computational <u>design</u>: “VCL” design – ventilated city-located with leaky ceiling (from 9 attic designs above one storey family house 8x12 m, eave height 2.5 m) $A_{ceil} = 96 \text{ m}^2$ $V_{att} = 110 \text{ m}^3$ <u>roof slope</u>: 30 ° <u>roof orientation</u>: south-north <u>ventilation</u>: ventilated – eave openings + leakages through gable ends ca. 0 - 8 ach, mean 2.2 ach <u>other</u>: airtightness of the house – 0.8 l/m²/s/50 Pa (3.5 ach)</p>		<p>Roof-deck assembly:</p> <ul style="list-style-type: none"> • concrete tiles • ventilated cavity • roofing felt • roof-decking (spruce) 19 mm <p>$S_{d,r,deck} = \text{ca. } 2.6 \text{ m}$</p> <p>Ceiling assembly:</p> <ul style="list-style-type: none"> • 500 mm loose-fill insulation • air barrier • gypsum board <p>$S_{d,ceil} = \text{ca. } 11 \text{ m}$ $U_{ceil} = \text{ca. } 0.077 \text{ W/m}^2/\text{K}$</p> <p>leaky ceiling: $Q_{50,ceil} = \text{ca. } 0.44 \text{ l/s/m}^2/50\text{Pa}$</p>
<p>Indoor conditions:</p> <ul style="list-style-type: none"> • 22 °C • 40 - 70 % RH (wintertime / summertime) • exhaust-supply ventilation (exhaust 120 m³/h – supply 90 % when the climate do not influence ventilation system) 	<p>Outdoor conditions:</p> <ul style="list-style-type: none"> • south-west coastal area of Sweden (mild winters and summers, heavy and lengthy rainy periods throughout the whole year) 	

Design no: 16 (design labelled “VOL” according to the original study)

- **same as 15 with following exceptions :**
 - o located in open area instead of in city which results in:
 - $n_{att,ceil,real} = \text{ca. } (-0.5) - 0.5 \text{ ach}$ (summer / winter respectively)
 - $n_{att,ext,real} = \text{ca. } 0 - 30 \text{ ach}$, mean 13.9 ach

Design no: 17 (design labelled “UCL” according to the original study)

- **same as 15 with following exceptions :**
 - o unventilated attic - $n_{att,ext,real} = \text{mean } 0.1 \text{ ach}$

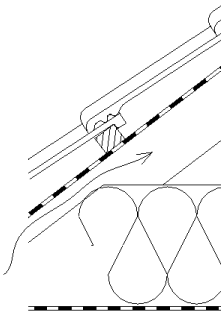
Design no: 18 (design labelled “UCT” according to the original study)

- **same as 15 with following exceptions :**
 - o unventilated attic - $n_{att,ext,real} = \text{mean } 0.1 \text{ ach}$
 - o tight ceiling - $Q_{50,ceil} = 0 \text{ l/s/m}^2/50\text{Pa}$

Design no: 19

Holm and Lengsfeld (2007) - Germany. [6]

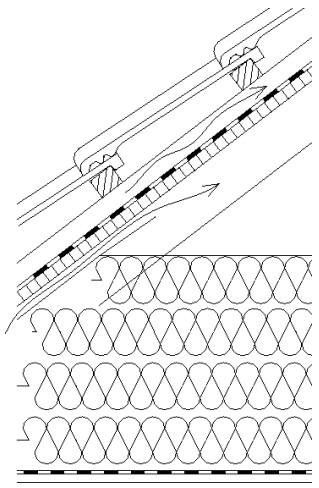
Experimental study from Germany compares condensation risk on the underside of vapour open underlay felt of three ventilated cold attic designs. Controlled airflow from interior to each attic space was introduced.

<p>General information: <u>study type</u>: experimental <u>design</u>: 3 ventilated attic spaces above one storey conditioned interior, each roof has area approx. 2.5x4 m $A_{ceil} = 10 \text{ m}^2$ $V_{att} = \text{ca. } 4.5 \text{ m}^3$ <u>roof slope</u>: 24 ° <u>roof orientation</u>: south-north <u>ventilation</u>: 3 mm slots at the eaves and 2 cm slot at the ridge <u>other</u>:</p> <ul style="list-style-type: none"> ceiling with controlled leakage from interior 135 m³/day (equivalent to possibly leaky staircase) 		<p>Roof-deck assembly:</p> <ul style="list-style-type: none"> concrete tiles battens (<i>no contra battens</i>) vapour open underlay (two different types) (permeance 925 ng/(Pa·s·m²)) <p>$S_{d,r.deck} = \text{ca. } 0.22 \text{ m}$</p> <p>Ceiling assembly:</p> <ul style="list-style-type: none"> thermal insulated <p><i>(thickness estimated from the figure to 0.3 m, estimated conductance of ceiling construction:</i> $U_{ceil, estim.} = 0.13 \text{ W/m}^2/\text{K}$ <i>)</i></p> <p><i>(no information about vapour- or air-barrier in the ceiling level – but as it was mentioned, that the air leakage across the ceiling was well controlled, it is assumed that there was some air- and vapour-barrier, and thus:</i> $S_{d,ceil, estim.} = \text{ca. } 10 \text{ m}$ <i>)</i></p> <p>well controlled 135 m³/day leakage (simulation of leaky attic staircase) – <i>by using power law with flow exponent 0.67 and by estimating some realistic pressure difference 4 Pa, it is assumed that airflow across simulated staircase</i> $Q_{50, staircase} = \text{ca. } 8.5 \text{ l/s}/50\text{Pa}$ <i>and no other leakage assumed, thus for the ceiling construction:</i> $Q_{50,ceil} = \text{ca. } 0.85 \text{ l/s}/\text{m}^2/50\text{Pa}$</p>
<p>Indoor conditions:</p> <ul style="list-style-type: none"> 20-22 °C 50-60 %RH 	<p>Outdoor conditions:</p> <ul style="list-style-type: none"> Germany (Holzkirchen) – Dec. 2003 – March 2004 	

Design no: 20

Hagentoft et al. (2008) – Sweden. [7]

Based on validated computational model a several cases of regular (leaky) and sealed roof designs with controlled (adaptive) ventilation were compared regarding mould growth risk within the attic space. Study also investigates cases with different tightness of the ceiling construction as well as of the attic space.

<p>General information: <u>study type</u>: computational <u>design</u>: $A_{\text{ceiling}} = 74.8 \text{ m}^2$ $V_{\text{attic}} = 80 \text{ m}^3$, $A_{\text{r.deck}} = 189 \text{ m}^2$ <u>roof slope</u>: 28° <u>roof orientation</u>: south-north <u>ventilation</u>: regular attic - $n_{50} = 130 \text{ h}^{-1}$ <u>other</u>:</p>		<p>Roof-deck assembly:</p> <ul style="list-style-type: none"> • concrete tiles • bitumen felt (vapour tight) • 22 mm wood <p>$S_{d,r.deck} = \text{ca. } 12 \text{ m}$</p> <p>Ceiling assembly:</p> <ul style="list-style-type: none"> • 400 mm mineral wool • 0.2 mm PE foil (vapour barrier) <p>$S_{d,ceiling} = \text{ca. } 10 \text{ m}$ $U_{ceiling} = \text{ca. } 0.1 \text{ W/m}^2/\text{K}$</p> <p>medium tight ceiling - $24 \text{ m}^3/\text{h}$ at 50 Pa p.dif.</p> <p>$Q_{50,ceiling} = \text{ca. } 0.09 \text{ l/s/m}^2/50\text{Pa}$</p>
<p>Indoor conditions:</p> <ul style="list-style-type: none"> • 30 %RH (if outdoor temperature -10°C); 60 %RH (if outdoor temperature 20°C) (corresponds to moisture supply 3g/m^3) • balanced ventilation 	<p>Outdoor conditions:</p> <ul style="list-style-type: none"> • Gothenburg region (Sweden) 	

Design no: 21

- same as 20 with following exceptions :
 - o ideally tight ceiling (i.e. $Q_{50,ceiling} = 0 \text{ l/s/m}^2/50\text{Pa}$)

Design no: 22

- same as 20 with following exceptions :
 - o well sealed attic – unintentional air change rate $n_{50,att} = 1 \text{ ach}$
 - o controlled (adaptive) ventilation of the attic (1 ach when running)

Design no: 23

- same as 20 with following exceptions :
 - o well sealed attic – unintentional air change rate $n_{50,att} = 1 \text{ ach}$
 - o increased controlled (adaptive) ventilation of the attic (5 ach when running)

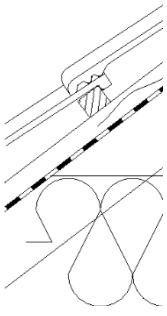
Design no: 24

- same as 20 with following exceptions :
 - o ideally tight ceiling (i.e. $Q_{50,ceiling} = 0 \text{ l/s/m}^2/50\text{Pa}$)
 - o sealed attic – unintentional air change rate $n_{50,att} = 7 \text{ ach}$
 - o controlled (adaptive) ventilation of the attic (1 ach when running)

Design no: 25

Essah et al. (2009) – U.K. [8]

Computational study based on non-validated model compares condensed quantities on different types of roofing underlays (high-resistance, relatively vapour-permeable and two highly permeable) within the cold attic located in UK. Study presents a results of four cases that differ in number of occupants, airtightness of ceiling and whole house and ventilation regime of the attic.

<p>General information: <u>study type</u>: computational <u>design</u>: 6.8 m x 9.7 m attic above two storey family house, eave height 5.1 m $A_{\text{ceil}} = 66 \text{ m}^2$, $V_{\text{att}} = 64.7 \text{ m}^3$ house airtightness $n_{50} = 5 \text{ ach}$ <u>roof slope</u>: 30° <u>roof orientation</u>: not specified <u>ventilation</u>: ventilated (20 mm openings along the eaves) – ca. 28 ach at 50 Pa p.dif. <u>other</u>:</p>		<p>Roof-deck assembly: (reference attic)</p> <ul style="list-style-type: none"> • tiles • ventilated cavity • bituminous felt (200 MNs/g; $s_d = 40 \text{ m}$) <p>$S_{d, \text{r.deck}} = 40 \text{ m}$</p> <p>Ceiling assembly:</p> <ul style="list-style-type: none"> • 250 mm of insulation • <i>no other information but we consider additional plasterboard</i> <p>$S_{d, \text{ceil}} = \text{ca. } 0.5 \text{ m}$</p> <p>$U_{\text{ceil}} = \text{ca. } 0.15 \text{ W/m}^2/\text{K}$</p> <p>$Q_{50, \text{ceil}} = 0 \text{ l/s/m}^2/50\text{Pa}$</p>
<p>Indoor conditions:</p> <ul style="list-style-type: none"> • determined from EN 15026:2007 • moisture load from 5 persons - ca (6 – 15) kg/day • <i>according to the standard – 20-25 °C; 40-70 %RH (high occupancy)</i> • $n_{50} = 5 \text{ ach}$ 	<p>Outdoor conditions:</p> <ul style="list-style-type: none"> • U.K. weather 	

Design no: 26

- **same as 25 with following exceptions :**
 - no intentional attic ventilation (leakages are several orders of magnitude lower compared to intentional leakages)
 -

Design no: 27

- **same as 25 with following exceptions :**
 - no intentional attic ventilation (leakages are several orders of magnitude lower compared to intentional leakages)
 - moisture dependent underlay foil ($s_d = 0.6\text{--}4.6 \text{ m}$)

Design no: 28

- **same as 25 with following exceptions :**
 - no intentional attic ventilation (leakages are several orders of magnitude lower compared to intentional leakages)
 - vapour permeable underlay foil ($s_d = 0.02$ m)

Design no: 29

- **same as 25 with following exceptions :**
 - no intentional attic ventilation (leakages are several orders of magnitude lower compared to intentional leakages)
 - vapour permeable underlay foil ($s_d = 0.02$ m)
 - ceiling leakage flow rate *ca. $Q_{50,ceil} = 0.6$ l/s/m²/50Pa*

Design no: 30

- **same as 25 with following exceptions :**
 - ceiling leakage flow rate *ca. $Q_{50,ceil} = 0.6$ l/s/m²/50Pa*

Design no: 31

- **same as 25 with following exceptions :**
 - vapour permeable underlay foil ($s_d = 0.02$ m)
 - ceiling leakage flow rate *ca. $Q_{50,ceil} = 0.6$ l/s/m²/50Pa*

Design no: 32

- **same as 25 with following exceptions :**
 - ceiling vapour tightness, $s_d = ca. 10$ m
 - whole house leakage flow rate $n_{50} = 2$ ach
 - ceiling leakage flow rate *ca. $Q_{50,ceil} = 0.24$ l/s/m²/50Pa*
 - attic ventilation by 10 mm openings along the eaves (*resulting in ca. 20 ach at 50 Pa pressure difference*)

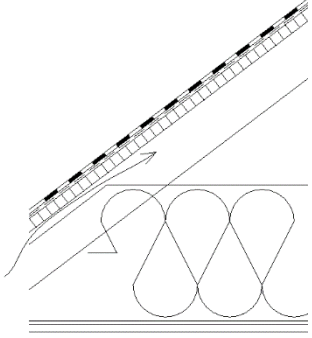
Design no: 33

- **same as 25 with following exceptions :**
 - ceiling vapour tightness, $s_d = ca. 10$ m
 - whole house leakage flow rate $n_{50} = 2$ ach
 - ceiling leakage flow rate *ca. $Q_{50,ceil} = 0.24$ l/s/m²/50Pa*
 - attic ventilation by 10 mm openings along the eaves (*resulting in ca. 20 ach at 50 Pa pressure difference*)
 - normal house occupancy (according to mentioned standard – 20-25°C; 30-60 %RH)

Design no: 34

Roppel and Lawton (2014) – Canada. [9]

In-situ measurement of four in cold maritime climate of Vancouver - Port Moody (British Columbia).

<p>General information: <u>study type</u>: in-situ measurement <u>design</u>: (test unit 1) east – west sloped roof orientation $A_{\text{ceiling}} = 57 \text{ m}^2$ $V_{\text{attic}} = 59 \text{ m}^3$ <u>roof slope</u>: <i>ca. 20° (estimated from figure)</i> <u>roof orientation</u>: east-west <u>ventilation</u>: ventilated by baffle vents <u>other</u>: leaky attic hatch</p>		<p>Roof-deck assembly:</p> <ul style="list-style-type: none"> • asphalt shingles • underlayment (<i>ca. 20 mm wooden based boards</i>) <p>$S_{d, \text{r.deck}} = \text{ca. } 200 \text{ m}$</p> <p>Ceiling assembly:</p> <ul style="list-style-type: none"> • 12" fibreglass blown insulation • PE foil • gypsumboard <p>leaky attic hatch</p> <p>$S_{d, \text{ceiling}} = \text{ca. } 10.5 \text{ m}$ $U_{\text{ceiling}} = \text{ca. } 0.12 \text{ W/m}^2/\text{K}$</p> <p>$Q_{\text{real}} (\text{tracer gas}) = \text{ca. } 23 \text{ m}^3/\text{h}$ $= 0.11 \text{ l/s/m}^2$</p> <p>$Q_{50, \text{ceiling}} = \text{ca. } 0.6 \text{ l/s/m}^2/50\text{Pa}$</p>
<p>Indoor conditions:</p> <ul style="list-style-type: none"> • average of winter 2011/2012 24.1 °C; 30.7 %RH 	<p>Outdoor conditions:</p> <ul style="list-style-type: none"> • Vancouver – Port Moody (BC), Canada – winter 2011/12 (winter 2011/2012 averages were 6.9 °C; 84.4 %RH) 	

Design no: 35

- **same as 34 with following exceptions :**
 - standalone roof deck built above mailbox – thus there were no ceiling or conditioned interior space. Lower surface of the roof deck were fully ventilated as was exposed to outdoor conditions
 - one sheathing plywood was installed with additional 25 mm extruded polystyrene on its upper side (both cases have the same results)

Appendix B – Verification of the model – full report

Thermal model

At first a verification of thermal model was performed using following assumptions and attic geometry:

- time step = 30 min
- ground temperature (T_g) and apparent sky temperature (T_{sky}) are set equal to the temperature of outdoor air (T_{ae})
- no solar gains considered
- attic volume (V_{att}) 70 m³
- area of each of four roof segments ($A_{1,2,3,4}$) set at 10 m²
- attic floor area (A_{floor}) 10 m²
- ceiling construction is made out of 50 mm thick gypsum board
- roof deck assembly consists of 50 mm thick gypsum board, 50 mm unventilated roof-deck cavity and 10 mm gypsum board on the external side
- volume of thermally active constructions that are present inside the attic space (V_{inside}) 0.25 m³ (i.e. 50 mm thick gypsum board with exposed area (A_{inside}) 5 m²)
- all ventilation openings to all zones and cavities are closed
- equivalent thermal conductivity of the air within the unventilated 50 mm cavities is considered to be $\lambda_{a,eq} = 0.4 \text{ W}/(\text{m}^2\text{K})$.

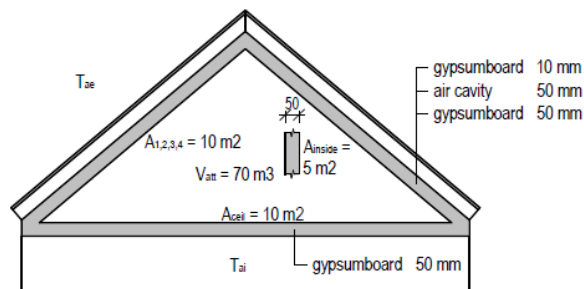


Fig. 31: Geometrical scheme of an attic space used for a verification of the thermal model

Although all ventilation openings are considered to be closed (no airflow), the solving airflow matrix must not be singular, and thus there has to be always at least one vent opened to each zone. One opening still results in no airflow as the model does not allow simultaneous inflow and outflow across one opening. However the iterative character of the airflow solver results in a slight „apparent“ flow across the north eave opening ($m_{e_1} = \text{ca. } -0.003 \text{ kg/s}$) which is an error of the model. The same error reflects also in the total mass balance of the zone (see Fig.34). This inaccuracy is associated with an iterative character of the airflow solver. Solver stops the iterative cycling when the maximal difference of all zonal reference pressures (PR_i) (unknown variables) is less than $1e-6 \text{ Pa}$. More precise results of mass flow rates can be reached by tightening this requirement.

Although the model has 6 zones, in the figure 33 can be seen no other course following the same error as m_{e_1} . That is because other openings that were left opened to other zones were just not shown in the chart, however they were checked and follow the same trend.

2) Different initial temperature

- Boundary conditions were kept at 20°C as well as in previous case, but initial temperatures of all nodes were set 0°C . No ventilation and no heat gains present.

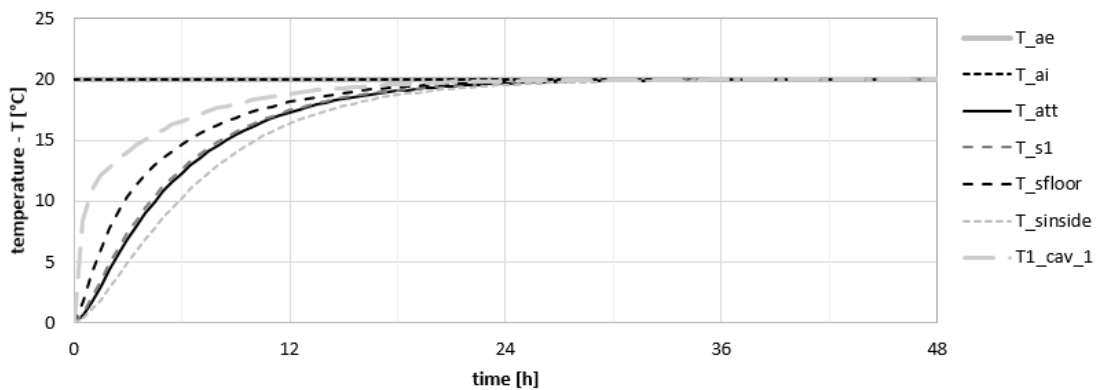


Fig. 35: Ver. Test 2 – Temperature courses

As can be seen, all courses start at 0°C and limit to boundary value 20°C . As the external layer of the roof deck is formed only by 10 mm gypsum board, the air temperature within the roof-deck cavity ($T1_{cav_1}$) has the steepest course (just one course out of four representing four roof-deck cavities is shown). Second and third steepest course represents a surface temperature of the attic floor (T_{sfloor}) and inner surface of the roof deck (T_{s1}). The temperature of the floor surface rises faster due to the lower thermal resistance of the ceiling construction compared to the construction of the roof deck. Air within the attic (T_{att}) is heated up only via convection from surrounding surfaces (no ventilation in this case) and therefore its course rises subsequently. Finally the surface of thermal mass located within the attic ($T_{sinside}$) is heated up by radiation between the surrounding surfaces and by the air within the attic. Therefore its temperature rise is slowest.

3) Enlarged volume of attic air

- Same case as 2) but considering ten times higher attic air volume ($V_{att} = 700 \text{ m}^3$).

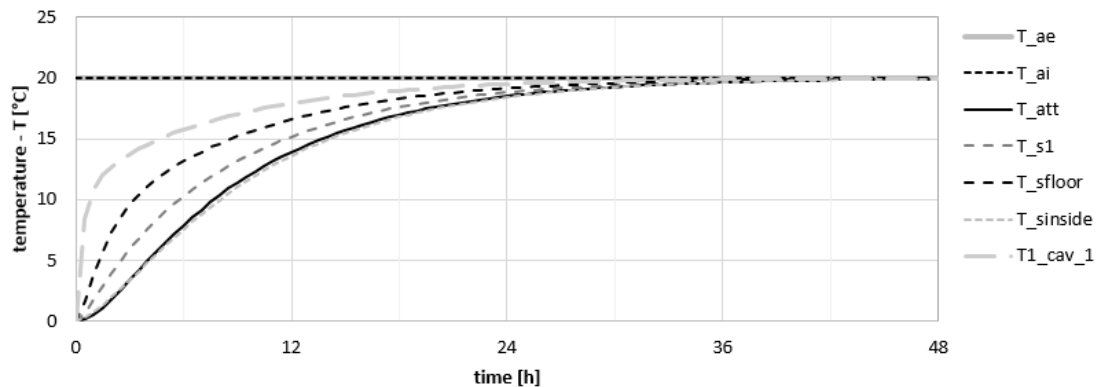


Fig. 36: Ver.Test 3 – Temperature courses

Compared to case 2) a slower response of temperature courses to the boundary conditions can be seen as the higher volume of the attic air means also higher thermal capacity of the zone. It can be also seen that surface temperature of the buffering mass ($T_{sinside}$), heated also by radiation, goes hand in hand with convectively heated attic air (T_{att}).

4) More mass of attic inner constructions

- Same case as 2) but considering ten times higher mass and exposed area of the inner attic buffering mass ($V_{inside} = 2.5 \text{ m}^3$; $A_{inside} = 50 \text{ m}^2$).

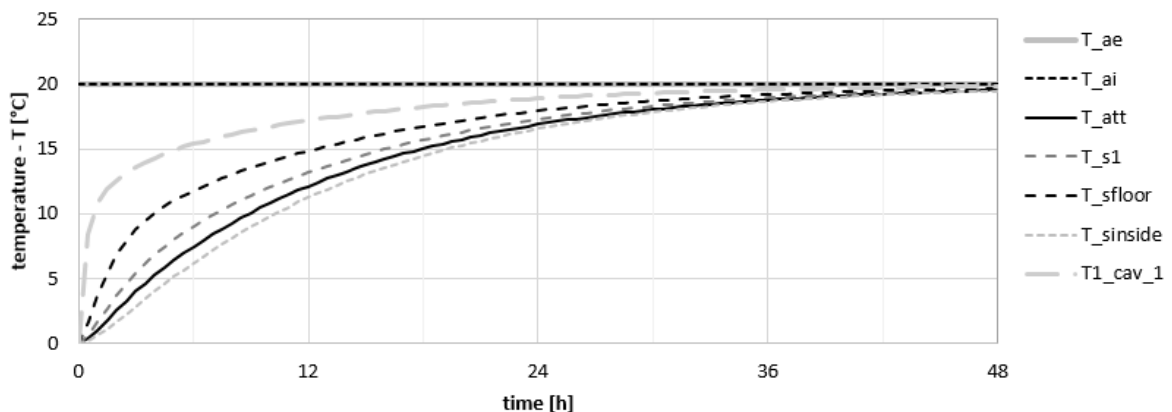


Fig. 37: Ver.Test 4 – Temperaturte courses

When compared to case 3) it can be seen, that ten times higher volume and exposed area of the thermal mass in the attic inhibits the rise of air temperature even more than ten times higher volume of the attic air. It corresponds to the total thermal capacities ($C_{air_700m^3} = \text{ca. } 0.9 \text{ MJ/K}$), ($C_{gypsum_2.5m^3} = \text{ca. } 2 \text{ MJ/K}$).

5) Higher thermal capacity of gypsum board

- Same case as 2) but considering two times higher thermal capacity of all gypsum mboard layers ($c_p = 2120 \text{ J/kgK}$).

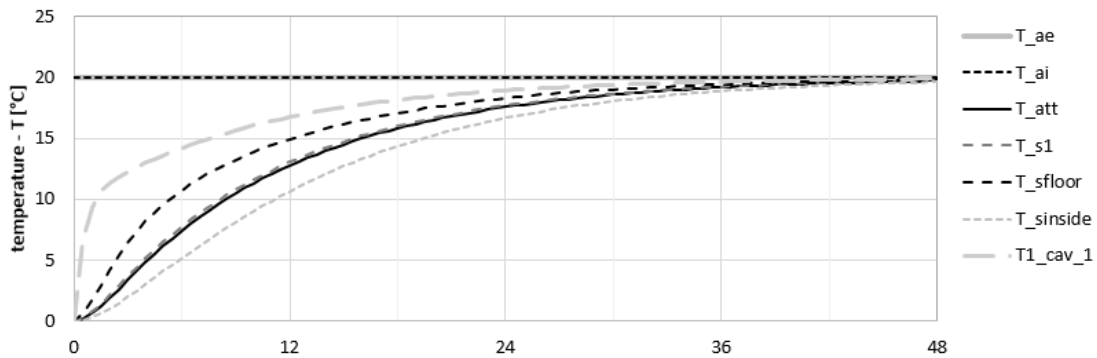


Fig. 38: Ver. Test 5 - Temperature courses

Comparing result with case 2) it can be nicely seen that proportions between the courses remained the same but with two times slower response to boundary conditions.

6) Roof segments are set as gable walls

- All roof segments were considered to become gable walls instead of roof decks. Walls were made out of 50 mm gypsum boards without any cavities and therefore form the same construction as the ceiling.

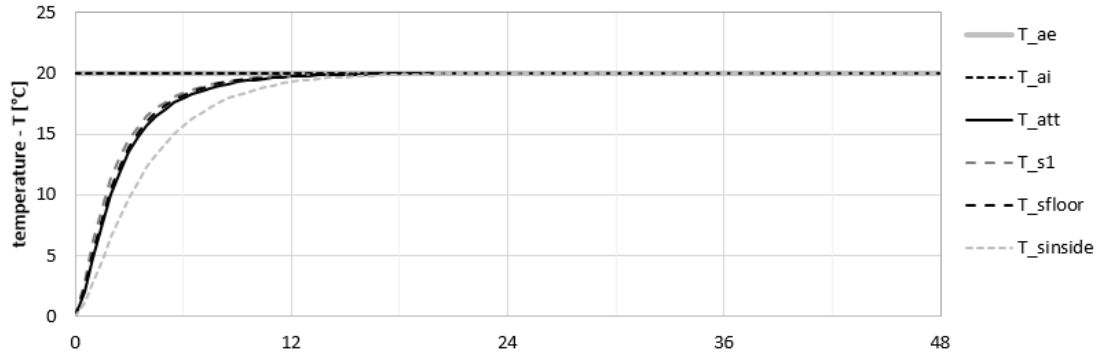


Fig. 39: Ver. Test 6 - Temperature courses

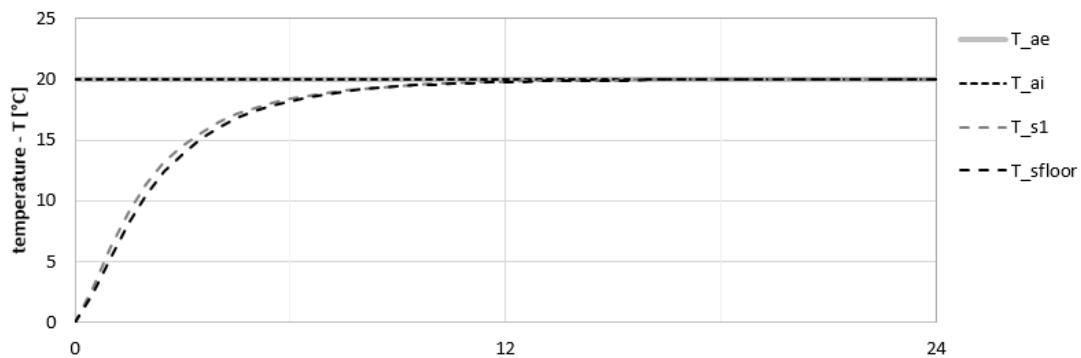


Fig. 40: Ver. Test 6 - Comparing different courses of (T_{s1}) and (T_{sfloor})

Compared to case 2) the temperatures reach the equilibrium faster thanks to lower heat resistance of gable walls compared to roof decks, where additional 50 mm air cavity and external 10 mm gypsum board layer is present.

Although the gable walls and the ceiling construction form (in this case) the same construction, it can be seen that their surface temperature courses are not fitting precisely one on another. Difference is caused by different convective and radiative surface heat transfer coefficients (SHTC).

To check if all constructions behaves identically, in the next test (case 7)) were all SHTC values set uniform for all surfaces.

7) Test of constructions

- Eleven versions of the same case as 6) were performed, but in each case using different areas of attic surrounding constructions. Total area off all constructions was in all cases maintained at 50 m².
 - At first all constructions were considered as gable walls (each construction with an area of 10 m²).
 - Than each gable wall area was separately set to 50 m² while all others were kept zero.
 - Subsequently all gable walls were changed back to roof decks, each with an area 10 m², as well as the ceiling construction.
 - Then each roof deck area was set separately to 50 m² while all others kept zero. Finally the ceiling construction was tested separately as well having the area 50 m².

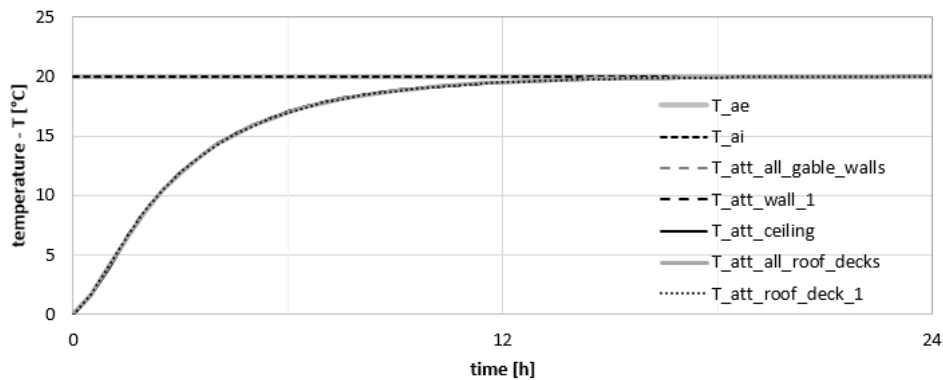


Fig. 41: Ver. Test 7 - Temperature courses

Even in a closer look (see fig. 41) can be seen, that all constructions and their combinations gives the same result (some courses are not shown in the chart to keep the figure and legend more clear). Before the execution of the calculation some modifications of the model were performed:

- 1) all convective and radiative SHTC were unified (all with value of $5 \text{ W/m}^2\text{K}$),
- 2) large openings to the ventilated roof-deck cavities and high windspeed (25 m/s) were performed to set the temperature in the cavity as fastest as possible close to the temperature of outdoor air,
- 3) the radiative part of heat exchange between the surfaces in the ventilated cavities was almost eliminated by setting the transfer coefficients equal to $0.0001 \text{ W/(m}^2\text{K)}$.

8) Heat source

- Same case as 2) but 200 W heat gain was performed within the attic. 60 % of the gain was assigned to the node of the attic air (convective part) and 40 % to the node of mean attic radiation temperature (radiative part).

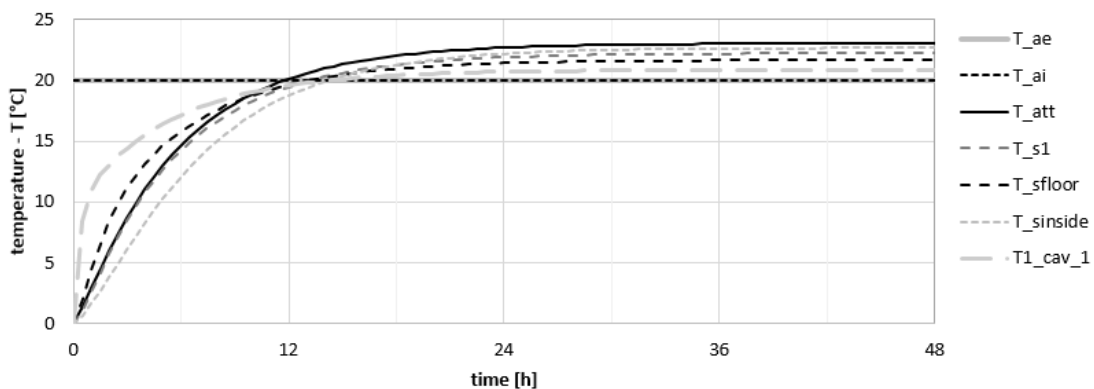


Fig. 42: Ver. Test 8 - Temperature courses

Heat source caused a rise of an attic air temperature above the temperature of boundaries. Surface temperature of the internal thermal mass ($T_{sinside}$) reached the second highest level as is surrounded only by the attic air. However there is still a radiation heat exchange of this surface with all other surfaces surrounding the attic space and since all these surfaces are always colder (cooled by the boundary temperatures), $T_{sinside}$ will not reach the attic air temperature.

9) Dynamic boundary conditions

- Same case as 2) but exterior and interior boundary temperatures are determined by diurnal sinusoidal function with mean value 20 °C and amplitude 5 °C.

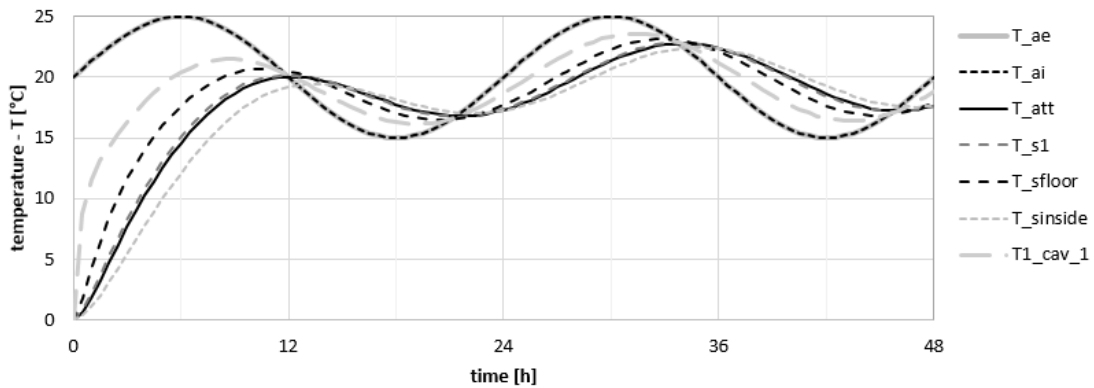


Fig. 43: Ver.Test 9 – Temperature courses

After first 48 hours is the diurnal average value of each temperature course the same as the average of boundaries. Calculated temperatures are dampened and shifted in time respecting their thermal capacities and positions. From the depicted courses, the highest amplitude has a temperature of air within the roof-deck cavity (T1_cav_1) and lowest temperature the surface of inner thermal mass (T_sinside). Precise analysis unfortunately revealed, that none of quasi-stationary diurnal average values is precisely equal to 20 °C. Maximal recorded difference was ca. 0.02 °C. This inaccuracy is caused mainly by radiation SHTCs - when all SHTCs were set uniform, maximal difference recorded was than ca. 0.0001 °C. It is possible that computational inaccuracy in the order of 0.02 °C can be essential in some special cases, but in most of building physics applications it can be still assumed as sufficiently low.

10) Constant but different boundary conditions

- Same case as 2) but exterior air temperature (and so ground and apparent sky temperature) was set equal to (-15) °C.

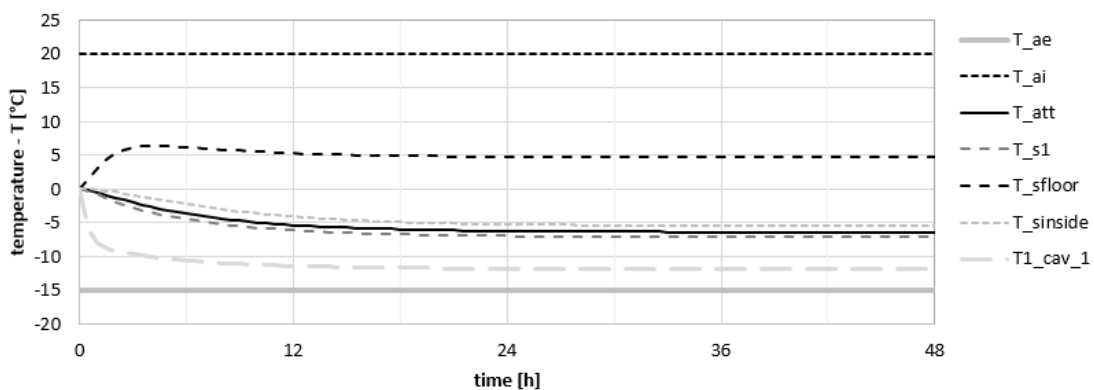


Fig. 44: Ver.Test 10 – Temperature courses

As can be seen in figure 44, temperature courses are logically distributed between the two boundary temperatures. Temperature course of the floor surface (T_{sfloor}) is located nearest the interior boundary (T_{ai}) and temperature of the air in roof-deck cavity ($T_{\text{T1_cav_1}}$) nearest to exterior boundary (T_{ae}). Ceiling construction has lower thermal resistance compared to roof deck, and thus a slight temperature rise during the first few hours can be seen. Although the roof deck has higher thermal resistance, total area of all four roof decks is four times higher than the area of the ceiling - that is the reason why floor surface temperature (T_{sfloor}) drops lower after reaching first peak.

11) Random exterior boundary

- Same case as 2) but exterior boundary temperature was set random between -10 and -20 °C to check stability of the model.

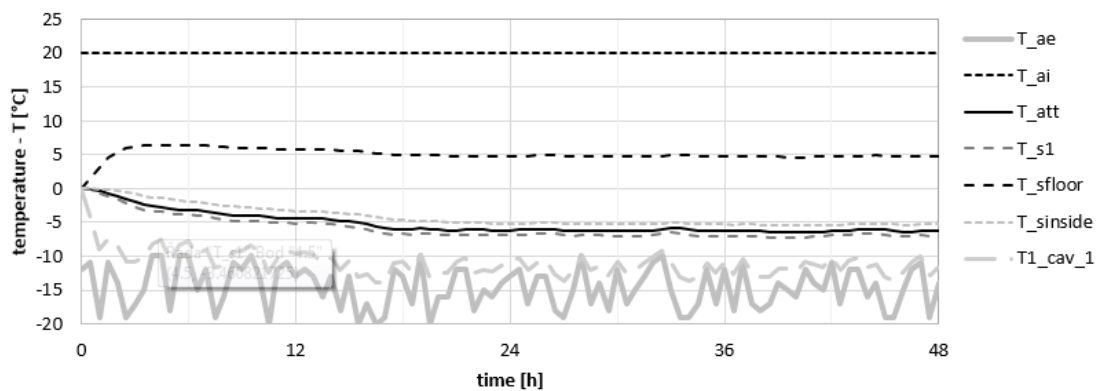


Fig. 45: Ver.Test 11 – Temperature courses

It can be seen that as the average exterior temperature is the same as in case 10) (i.e. -15 °C), temperature courses follow the same trends. It can also be seen that the courses are more stable the closer they are to the interior boundary. Even if the exterior temperature is changing between two time steps up to 10 °C, the model is stable.

Thermal + airflow model

This section presents a verification of the combination of thermal and airflow models. For this and following section an extended attic geometry is considered (see fig 46).

Constructions of the attic space remains the same as shown in figure 31 but lower parts of roof decks are prolonged and form a cathedral ceilings above interior space. This geometry also creates a new cavities that are placed in between the roof decks and pitched parts of the ceiling - these cavities represent an airflow ducts between outdoor environment and attic space (each cavity represents an independent zone and is in further text denoted as „ecav“ – eave cavity space). All ecav spaces are 50 mm thick as well as the roof-deck cavities. Width of all ecav spaces is 10 m as well as width of roof-deck cavities (as 10 m is a considered length of all four eaves).

Each zone has at least two orifices - at each boundary and interzonal connections. Roof-deck cavities have a lower opening “e_cav” (eave cavity opening) and higher opening “p_cav” (peak or ridge cavity opening). Each ecav space has a lower opening “e” (eave opening) and higher “eatt” opening (interface of ecav and attic space). Attic space has four “eatt” openings to four ecav spaces, four “p” (peak) openings and one opening on the interface with interior space - “c” (ceiling opening). Finally the interior space has a ceiling opening to attic zone and four window openings denoted as “w”.

As can be seen in figure 46, each roof deck is divided vertically in two parts (lengths) - part above attic space – „length 1“ and part above cathedral ceiling – „length 2“. In following computations both lengths are set equal to 2.5 m. In figure 46 can be also seen the heights of openings above ground level that are important in terms of thermal and also wind driven airflow. Slope of all roof-decks is 40°.

Although the scheme in figure 46 seems realistic, it should be mentioned that this attic geometry is, in fact, unreal - for instance considered areas and slopes of constructions surrounding the attic space cannot contain considered air volume. Also in terms of ventilation, the cavities are considered to have a constant width (horizontal dimension) in their entire vertical length – if considered four roof decks all with the same slope, it is obvious that this assumption cannot be fulfilled. Despite these facts the models verification can be successfully performed.

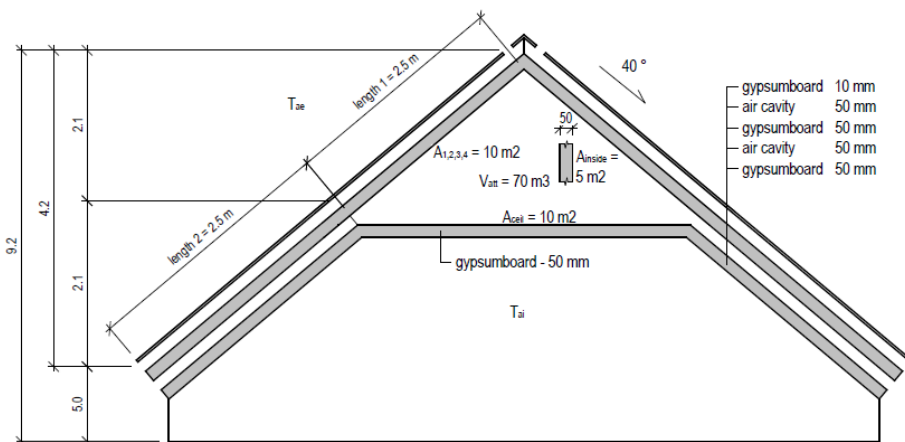


Fig. 46: Geometrical scheme of an attic space used for a verification of thermal + airflow model

12) Opened roof-deck cavities

- Same case as 10) but with opened roof-deck cavities. All other openings are considered to be closed – no attic ventilation. Total area of each cavity opening is 0.5 m² (0.05 m x 10 m).

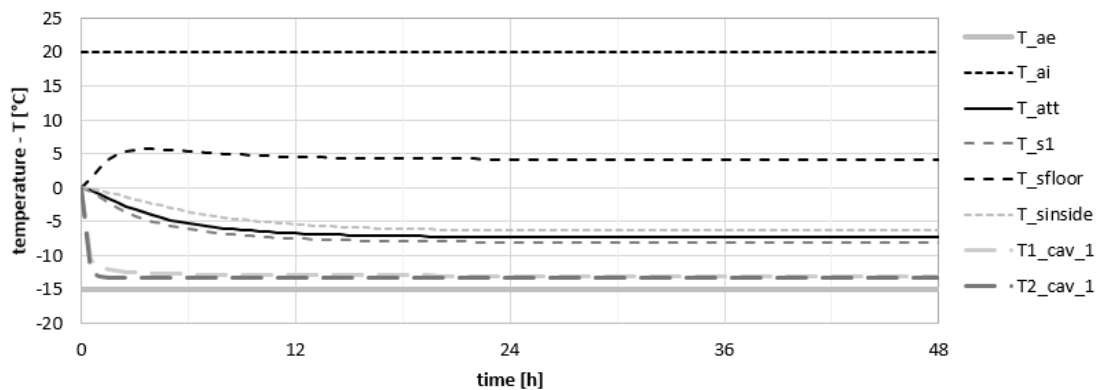


Fig. 47: Ver. Test 12 – Temperature courses

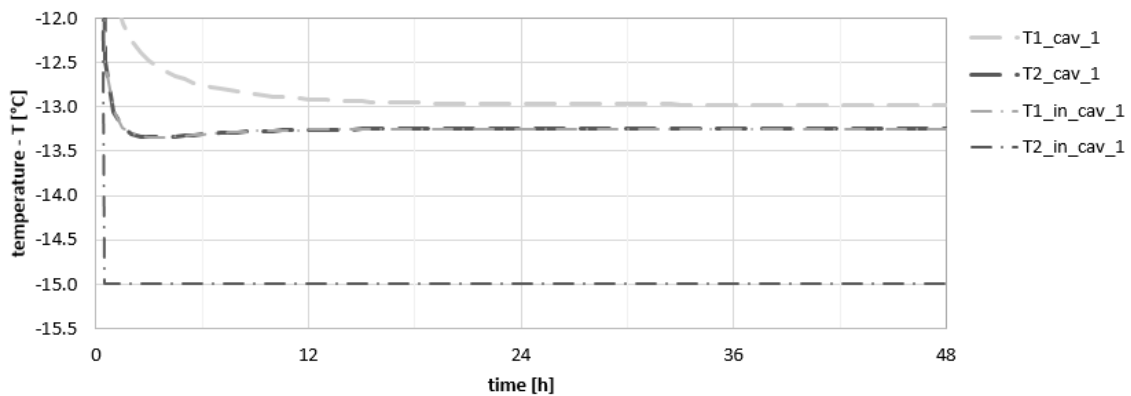


Fig. 48: Ver. Test 12 – Detail of differences of air temperatures within the roof-deck cavity

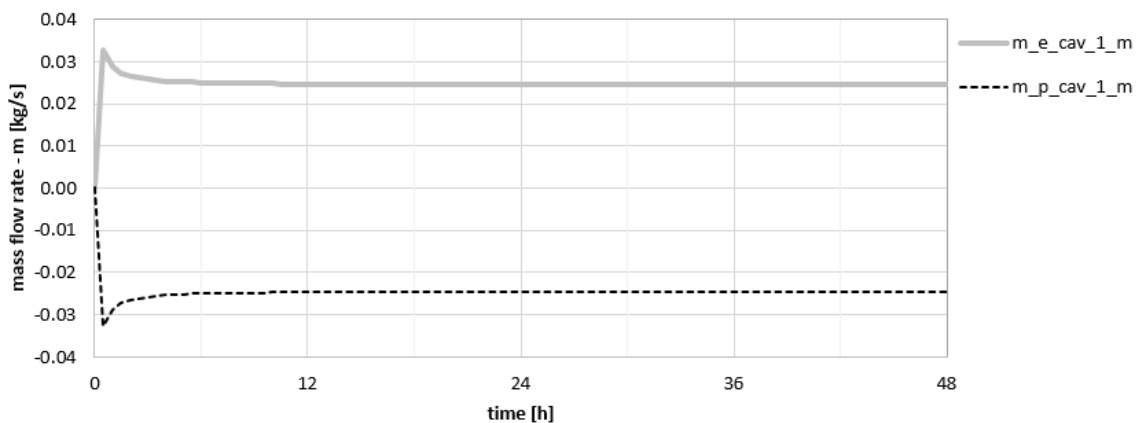


Fig. 49: Ver. Test 12 – Mass flow rates accross roof-deck cavity openings

As the roof-deck cavities are now ventilated by outdoor air all temperature courses are (compared to case 10)) shifted closer to the exterior boundary. Biggest difference is obviously recorded by the cavity temperatures (T1_cav_1 and T2_cav_1) where „T1_“ stands for the upper part of the cavity (in „length 1“) and „T2_“ for the lower part of the cavity (in „length 2“).

As the air within the cavity is moving upwards the temperature in the lower part ($T_{2_cav_1}$) is placed slightly lower than the temperature in the upper part ($T_{1_cav_1}$). In figure 47 can be seen the two temperature courses in a closer look. Two more courses can be seen in the figure - temperature of the air entering the lower part ($T_{2_in_cav_1}$) and temperature of the air entering the upper part of the cavity ($T_{1_in_cav_1}$). Since to the lower part comes the exterior air the incoming temperature is equal to the exterior boundary. Similarly the temperature of the air entering the upper part of the cavity is equal to the temperature of the air within the lower part of the cavity – it also proves that the air in the cavity is flowing upwards.

Figure 49 shows a mass flow rate across the eave and peak (ridge) openings. Inflow is denoted with plus sign and outflow with the minus sign. Courses again confirms that the air in the cavity is moving upwards. Also can be seen that the same amount of mass that is entering cavity via the eave opening ($m_{e_cav_1_m}$) leaving the cavity through the peak opening ($m_{p_cav_1_m}$) – index „_m“ at the end of the mass flow designation means, that the mass flow [kg/s*m] is related to one meter of cavity width (horizontal dimension of the cavity).

13) Opened roof-deck cavities with dynamic boundaries

- Interior and exterior boundary temperatures were determined by diurnal sinusoidal function with mean value 20 °C and amplitude 5 °C.

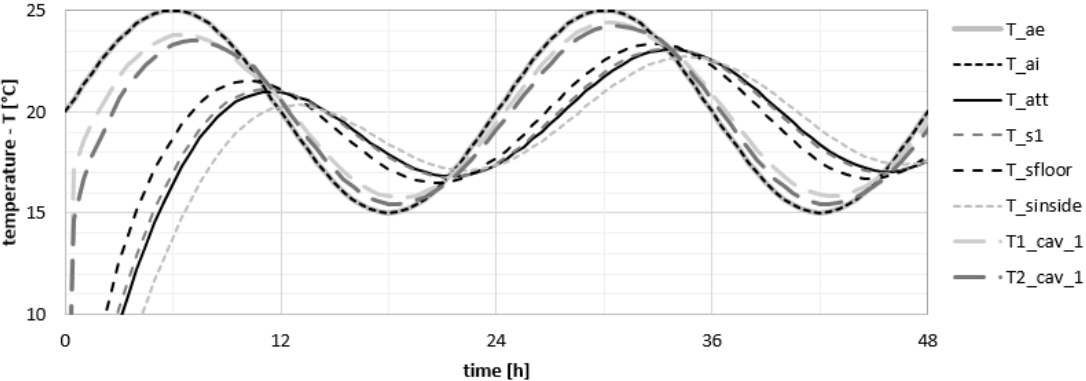


Fig. 50: Ver.Test 13 – Temperature courses

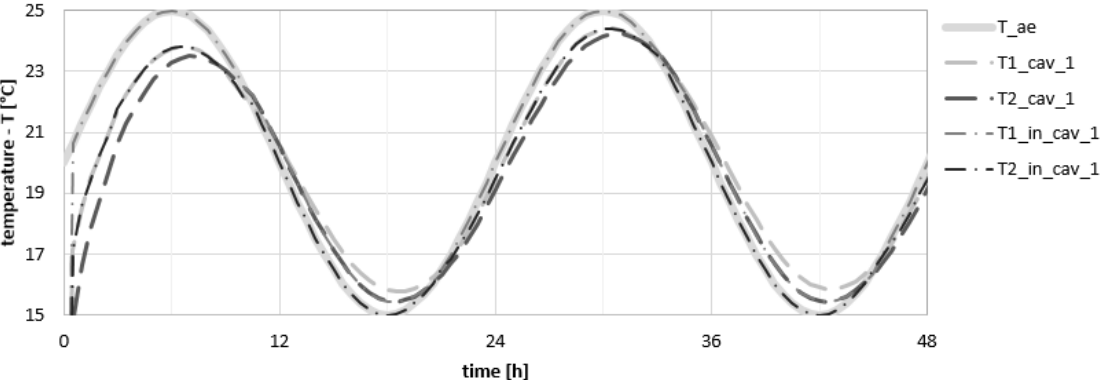


Fig. 51: Ver.Test 13 – Closer look at the roof-deck cavity temperature courses

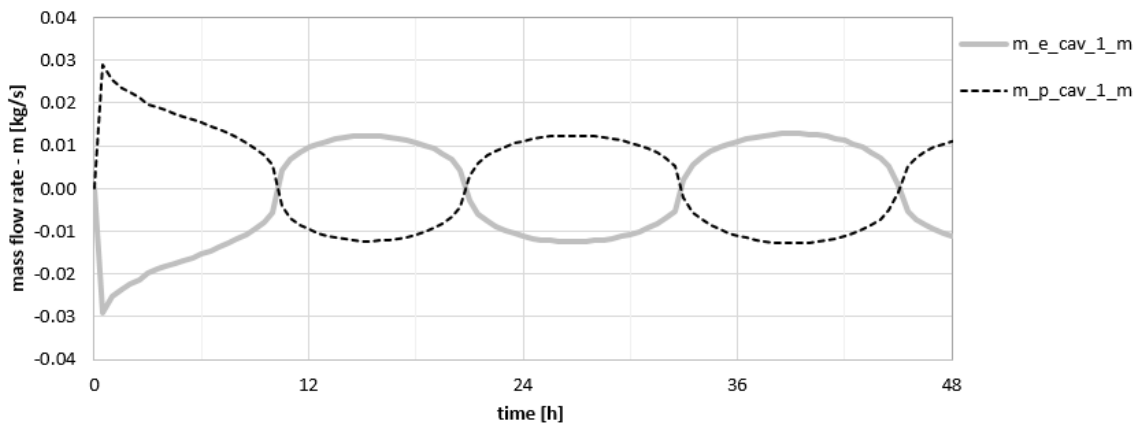


Fig. 52: Ver. Test 13 – Mass flow rates accros roof-deck cavity openings

As the air from exterior now flows through the roof-deck cavities the amplitudes of all courses are placed higher, compared to case 9).

In figure 51 can be seen more detailed view of the cavity temperatures. Regarding upper part of the cavity it can be seen, that when the outdoor air temperature is higher than an average temperaturte within the cavity, the air flows downwards and thus the incoming air in the upper part ($T1_{in_cav_1}$) is the exterior air. When the outdoor air temperature is lower, flow direction changes and the air from the lower part of the cavity is the incomming one to the upper part. Similar behaviour can be seen also looking at the courses of the lower part of the cavity.

In figure 52 can be clearly seen how the mass flow rate changes in time accros the eave and peak (ridge) openings of the roof-deck cavity. Positive values represent a mass flow rate into the cavity and negative values out of the cavity.

14) Wind on cavities

- All temperatures were set constant including the initial temperatures. Windspeed at the height of all openings was kept evenly equal to the reference windn speed at 10 m ($U_{10} = 3 \text{ m/s}$). Wind dirrection changes every time step by two degrees starting at 0° (wind normal to north side). Last value is 384° thus durint this experiment wind fully rounds the attic.

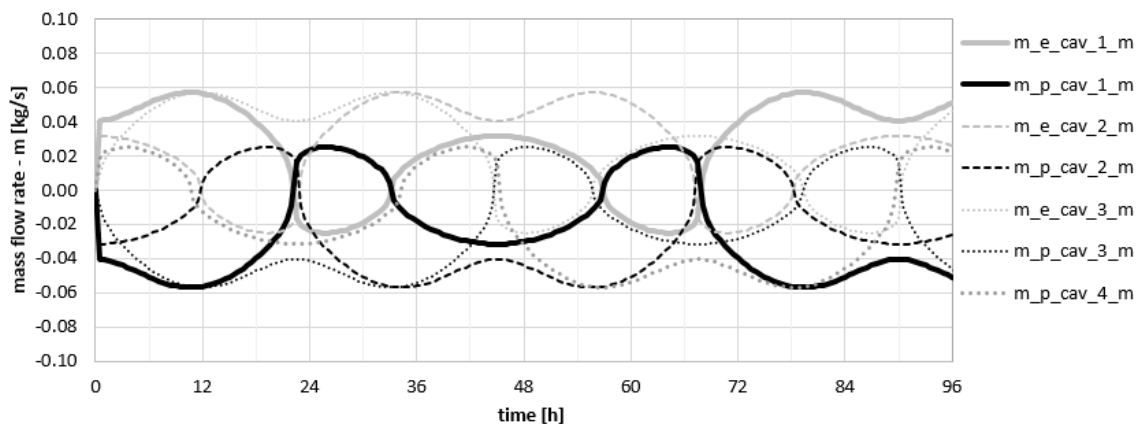


Fig. 53: Ver. Test 14 – Mass flow rates across openings of differently oriented roof-deck cavities (unifrom wind speed)

It can be seen a nicely shaped mass flow rate courses of differently oriented cavity openings. Courses mutually changing their position as the wind direction rounds the roof. These results are basically a consequence of the difference of wind pressure coefficients (C_p) (calculated based on [34]). For visual clarity the results of west cavity ($_4$) are not shown in the figure.

In the following figure can be seen results of the same test but using calculated wind speed at each height of the openings (this is the default set-up of the model). Compared to figure 53 it can be seen much flattened courses.

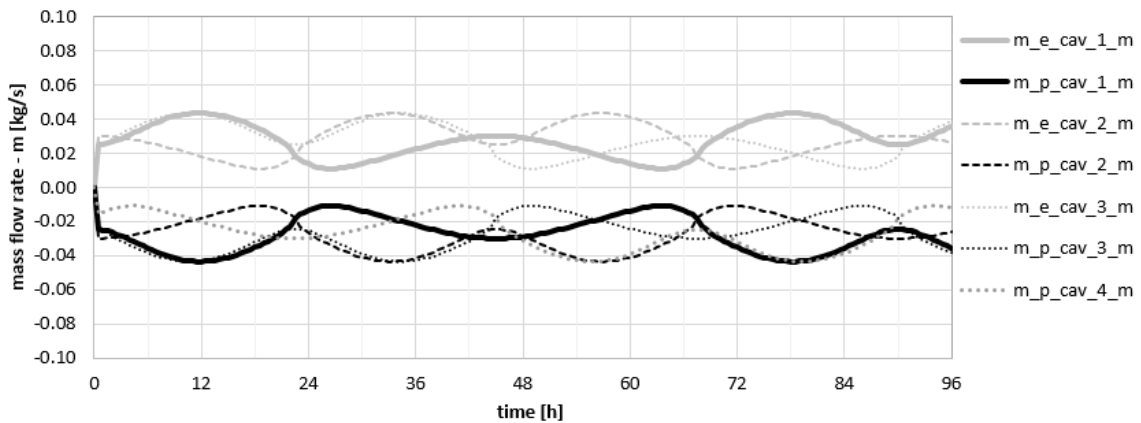


Fig. 54: Mass flow rates across openings of differently oriented roof-deck cavities (calculated wind speed)

In figure 55 can be seen a comparison of mass flow rates across differently oriented eave openings calculated using uniform (U_{10}) and calculated wind speed at different opening heights. North is the upwind side (denoted as „1“). Denoted as „2“, „3“ and „4“ are south, east and west respectively.

It can be surprising how different can the results be – especially the east cavity mass flow rate (denoted as „3“) that changes even the flow direction.

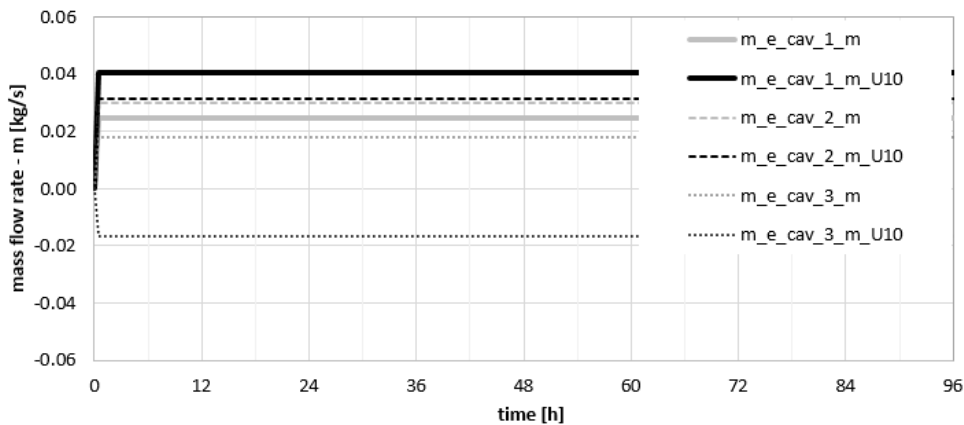


Fig. 55: Mass flow rates across eave openings of differently oriented cavities (uniform and calculated wind speed)

15) Opened all flow pathways, except ceiling vent + attic heat source

- All openings to the attic zone, interior zone and „ecav“ zones are open excepting the ceiling vent. Total free area of each opening is 0.05 m² including roof-deck cavity openings (note that the areas are ten times lower than in all other cases). Exterior and interior air temperature is kept constantly at (- 15) °C. Attic space is provided with heat gain 200 W.

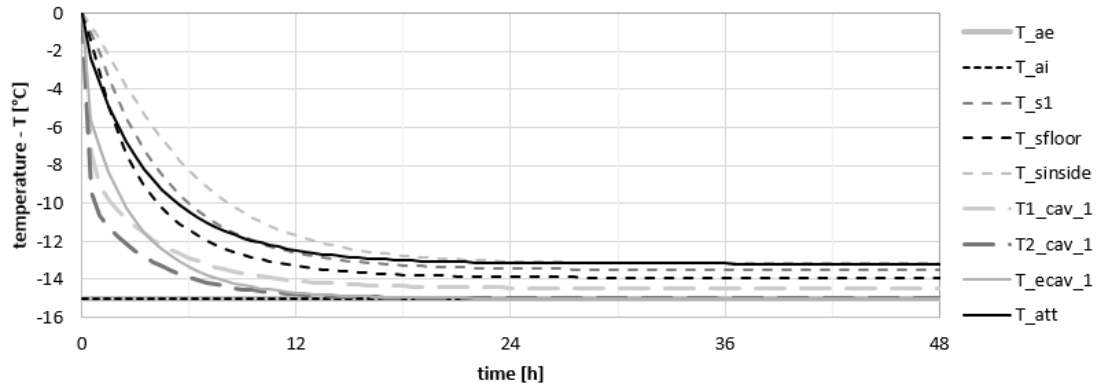


Fig. 56: Ver. Test 15 – Temperature courses

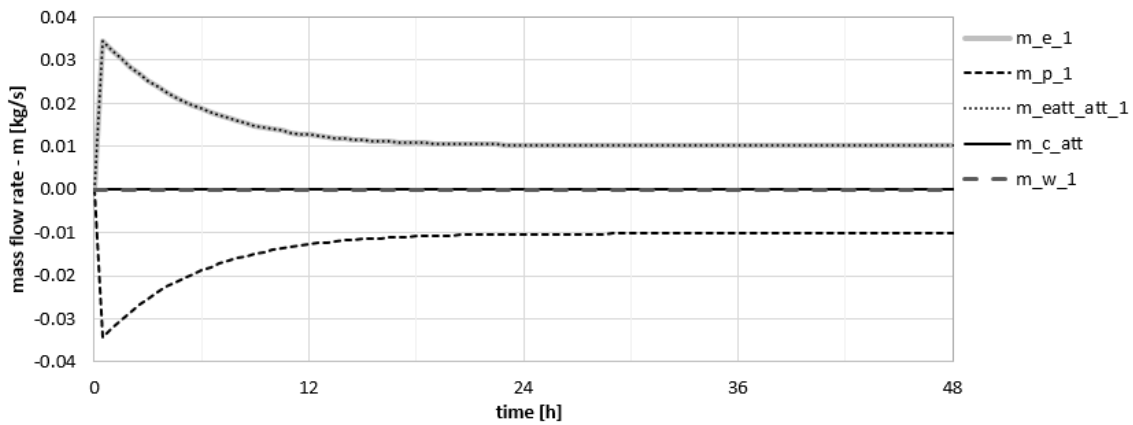


Fig. 57: Ver. Test 15 – Mass flow rate courses

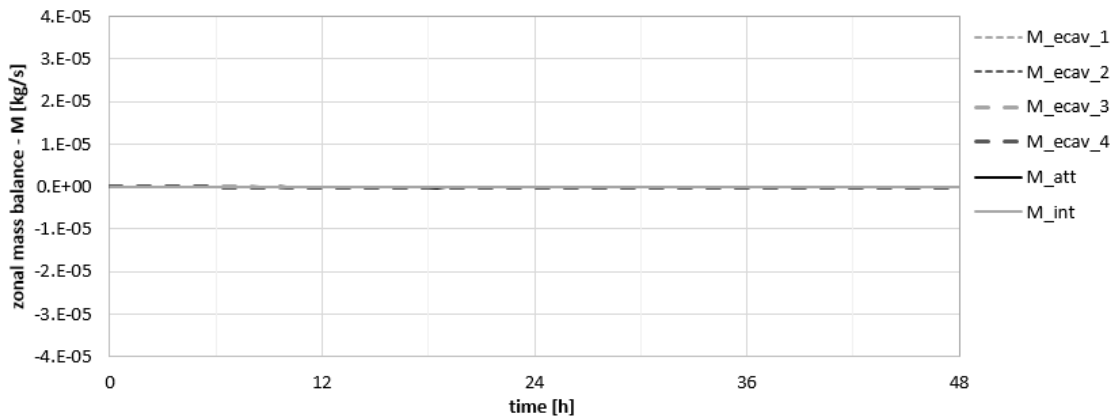


Fig. 58: Ver. Test 15 – Zonal mass balance

As the attic is heated, its temperature is placed highest (after reaching equilibrium) followed by others. Whereas the temperature within the attic is higher than the exterior boundary, the airflow through the attic takes place in upward direction. In Fig. 57 can be seen that flow across eave opening (m_{e_1}) is positive, which means inflow to ecav space. The same amount of air which

enters the ecav space is released to the attic via the eatt vent – from the attic point of view it is an inflow and thus $m_{eatt_att_1}$ is also positive following the same course as m_{e_1} . The mass that is released from the attic via the peak opening and so the m_{p_1} following the opposite trend.

As the ceiling opening is considered closed, there is no airflow present across it. And since there is neither wind pressure nor temperature difference across the windows, no mass flow is present even across these openings.

As there is an upward flow in the roof-deck cavity, the outdoor air is sucked into the lower part of it as well as into the ecav space. And since these two cavities are together surrounded from both sides by boundary temperatures (T_{ae} and T_{ai}) which are the same ($-15\text{ }^{\circ}\text{C}$), they reach equilibrium at the same level ($-15\text{ }^{\circ}\text{C}$) (see Fig. 56).

16) Opened all flow pathways, except ceiling vent + different boundaries

- Same case as 12) but now all flow pathways are opened except the ceiling vent – each opening has a total area 0.5 m^2 .

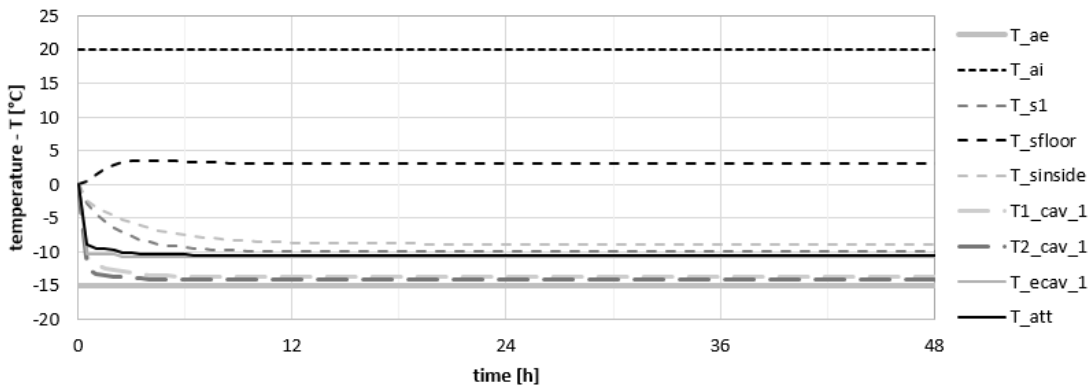


Fig. 59: Ver. Test 16 – Temperature courses

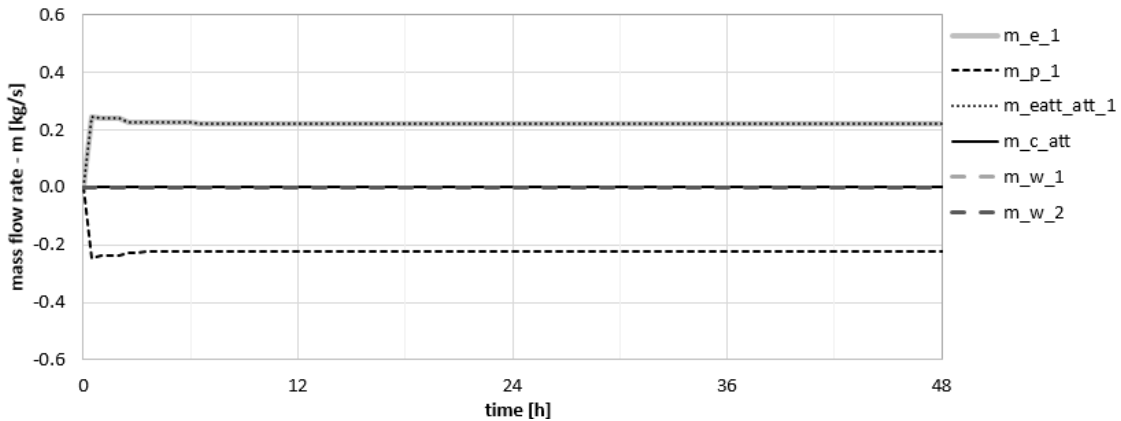


Fig. 60: Ver. Test 16 – Mass flow rate courses

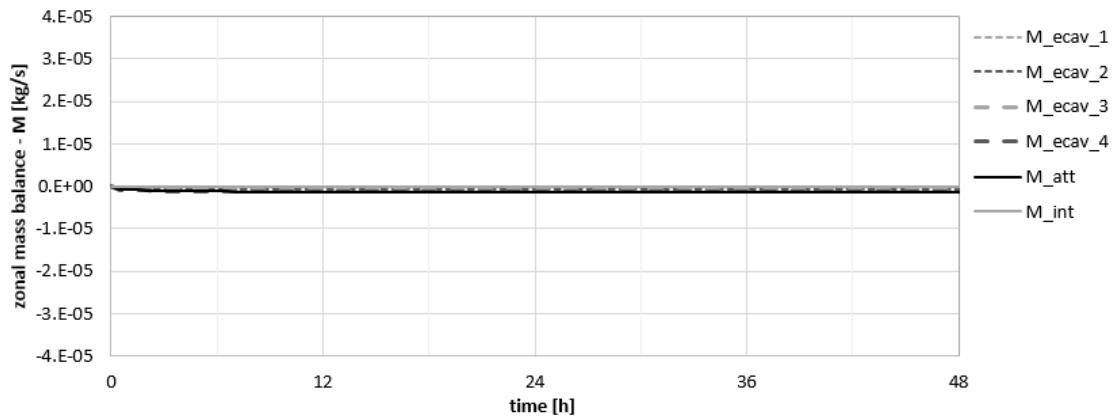


Fig. 61: Ver. Test 16 – Zonal mass balance

As the attic is now ventilated by outdoor air via the ecav ducts and peak openings, its temperature is closer to the exterior boundary (compared to case 12)).

Although there is now a temperature difference across the window openings, still no mass is present. That is because all openings are at the same level and therefore there is the same pressure acting on each of them which results in no flow.

In figure 62 can be seen mass flow rates in case that one of the openings (window 2) is placed one meter above the others. It can be seen that mass flow out of window 2 is now three times higher than the inflow of the other three windows, which corresponds to zonal mass balance.

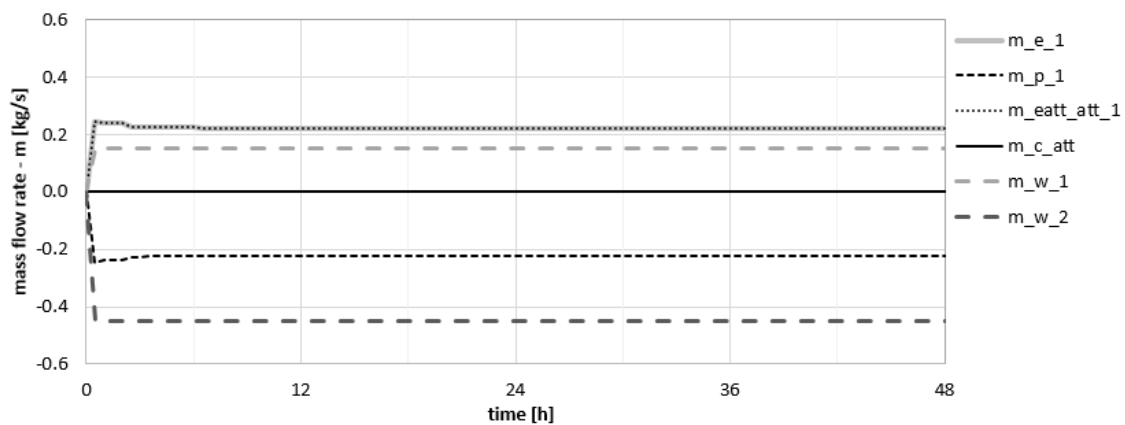


Fig. 62: Ver. Test 16 – Mass flow rate courses with different window 2 position

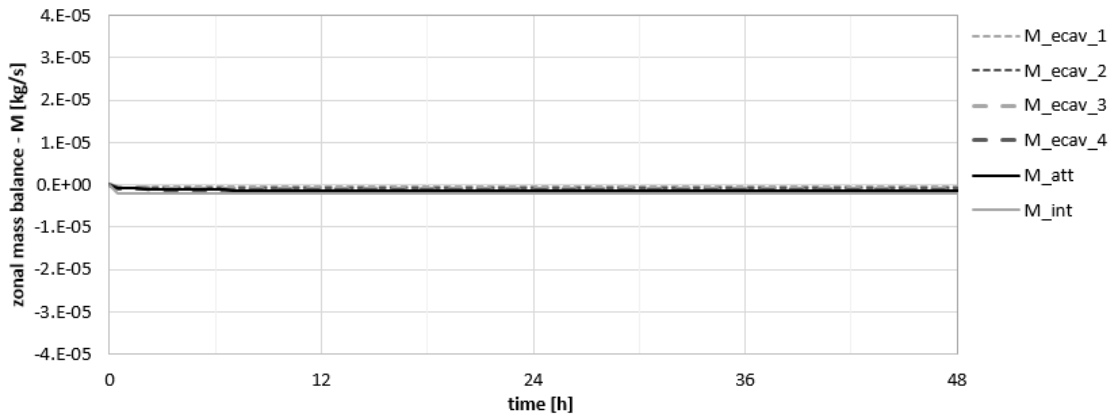


Fig. 63: Ver. Test 16 – Zonal mass balance with different window 2 position

17) Opened all flow pathways

- Same case as 16) except that all flow pathways are now opened including the ceiling vent
wich area is the only that differs with its value 0.1 m². All other openings have each the area
0.5 m².

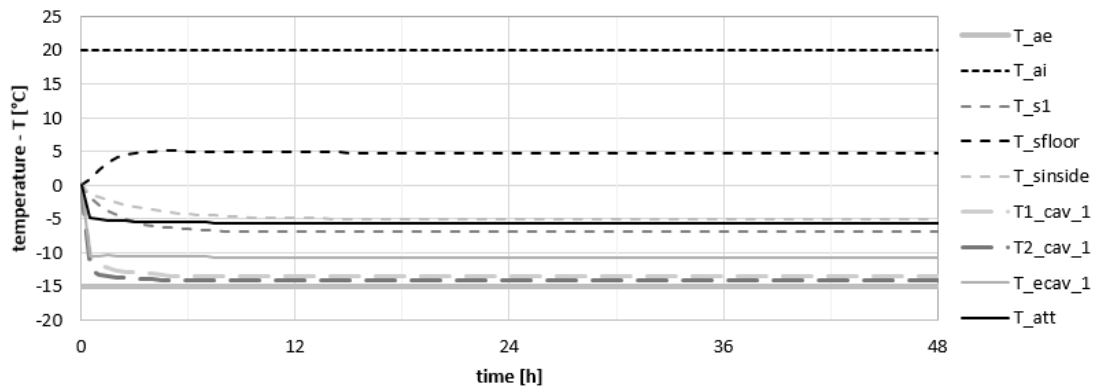


Fig. 64: Ver. Test 17 – Temperature courses

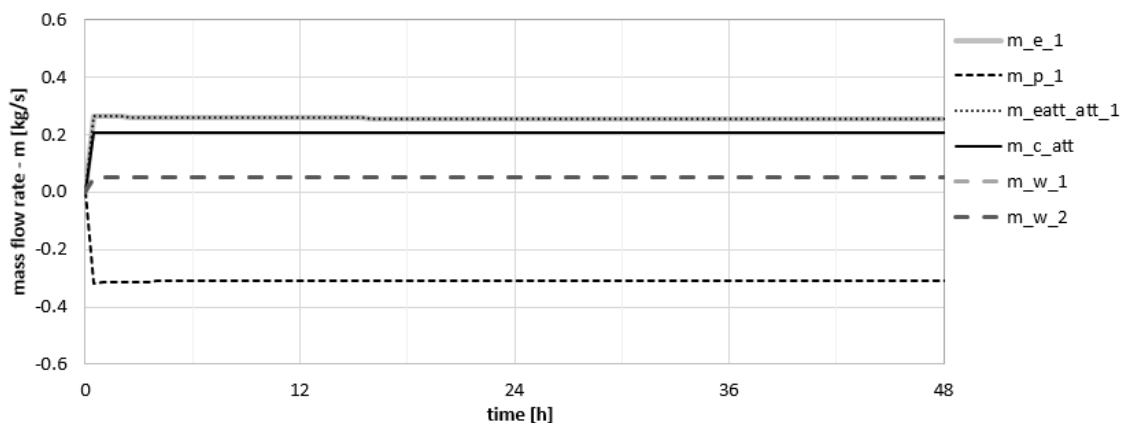


Fig. 65: Ver. Test 17 – Mass flow rate courses

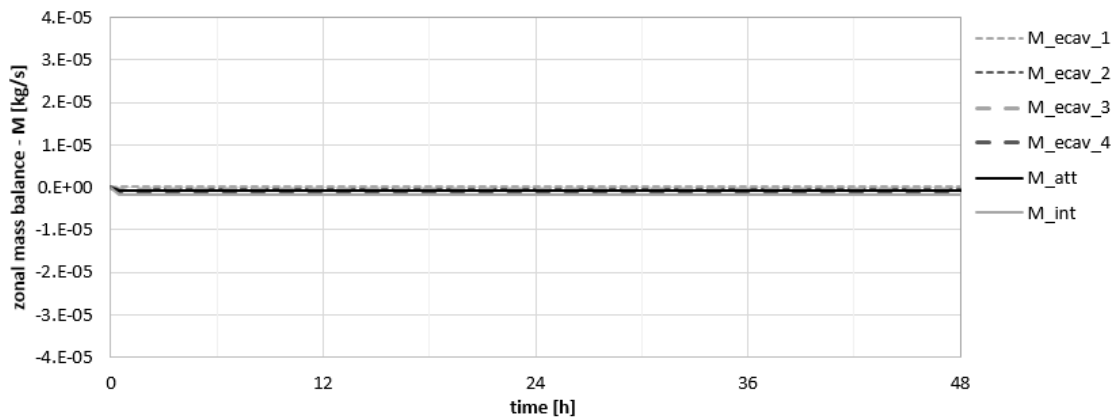


Fig. 66: Ver. Test 17 – Zonal mass balance

Compared to case 16) it can be seen that temperatures of the attic air and surrounding surfaces are placed higher which is caused by the inflow of warm air coming from the interior via the ceiling opening.

Looking at the mass flow rates it is obvious that the mass entering the attic space via the ceiling opening (m_{c_att}) is four times larger than to the mass entering the interior zone through one window (since the interior has four identical window openings). Mass that enters the attic space through the ceiling vent as well as masses incoming through the ecav ducts (m_{eatt_att}) leaves the space through the peak openings (m_p), and the mass balance is conserved.

18) Opened all flow pathways with dynamic boundaries

- Outdoor boundary temperature is determined by diurnal sinusoidal function with mean value 20 °C and amplitude 5 °C. Interior temperature is constantly held at 20 °C. All openings opened – ceiling opening 0.1 m², all others 0.5 m².

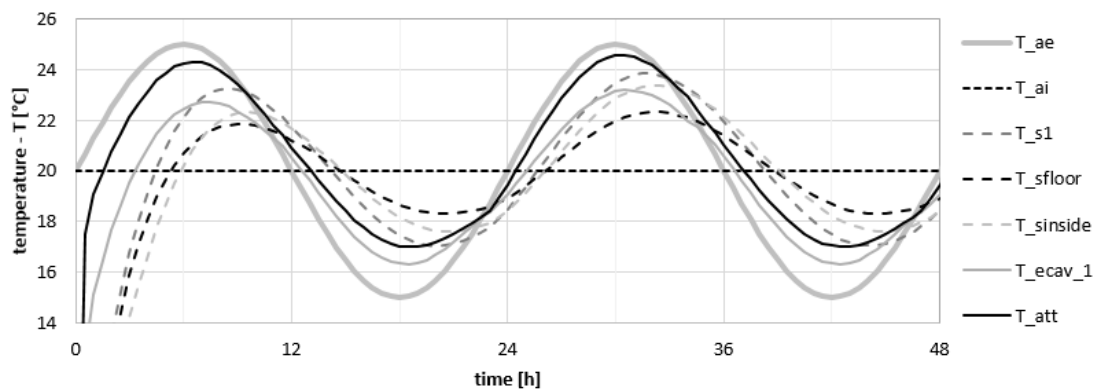


Fig. 67: Ver. Test 18 – Temperature courses

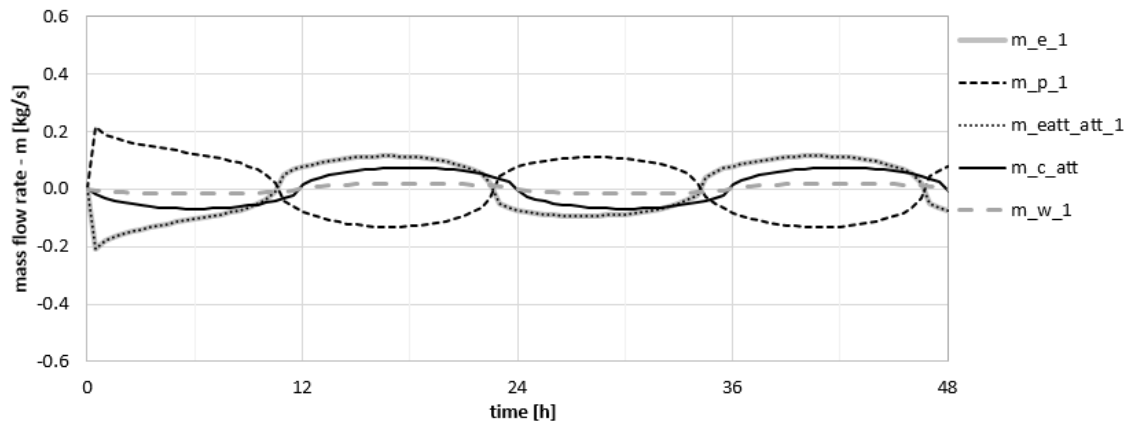


Fig. 68: Ver. Test 18 – Mass flow rate courses

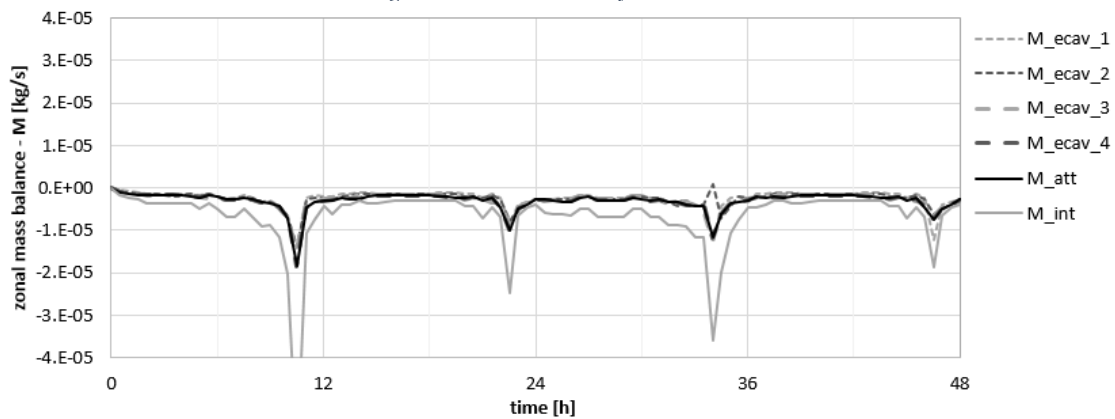


Fig. 69: Ver.test 18 – Zonal mass balance

In figures 67 and 68 can be clearly seen how the direction of the airflow through the zones changes with the change of temperatures. When the exterior air is warmer while the interior air is colder than the air within the attic, the direction of the overall airflow is downwards – air enters the attic via peak vents and then leaves the space partly through the acav ducts and partly through the ceiling. Air that enters the interior space through the ceiling vent leaves it through the windows.

An interesting moment occurs when the attic space has the highest temperature above outdoor and so the indoor spaces. In that situation the air within the attic wants to flow upwards while sucking the mass from exterior using the ecav ducts, but the indoor air has lower temperature than exterior one and thus it wants to leave the space through the lowest located opening (window openings). In those moments the air is sucked into the attic via the ecav ducts and than splitted in two parts, one leaving through the peak vents and one through the ceiling. First of these moments can be seen around the eleventh hour and repeats every 24 hours. An opposite situation occurs periodically after every twelve hours.

It can be seen higher inaccuracy of the zonal mass balance compared to all previous cases - (15), (16), (17).

19) Wind on the attic

- All initial and boundary temperatures are kept constantly at 20 °C. All openings opened – ceiling opening 0.1 m², all others 0.5 m². Reference wind speed (U_{10}) 3 m/s and wind direction changes every time step by 2° starting from 0° which means north is the first step upwind side.

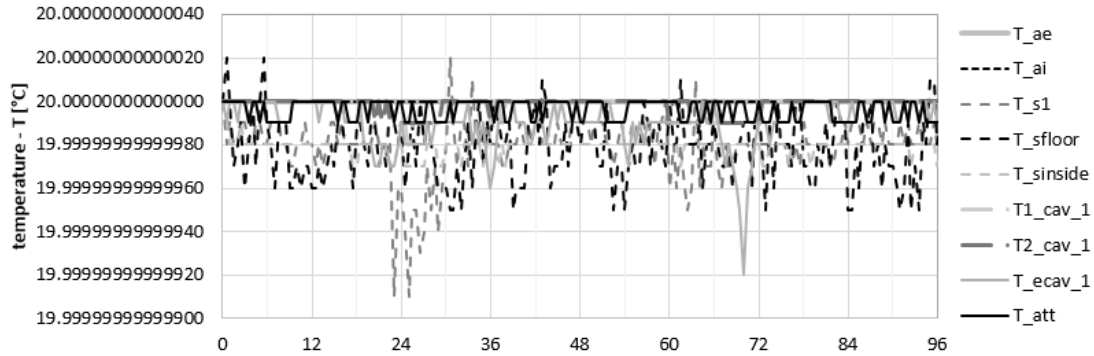


Fig. 70: ver.Test 19 – Temperature courses

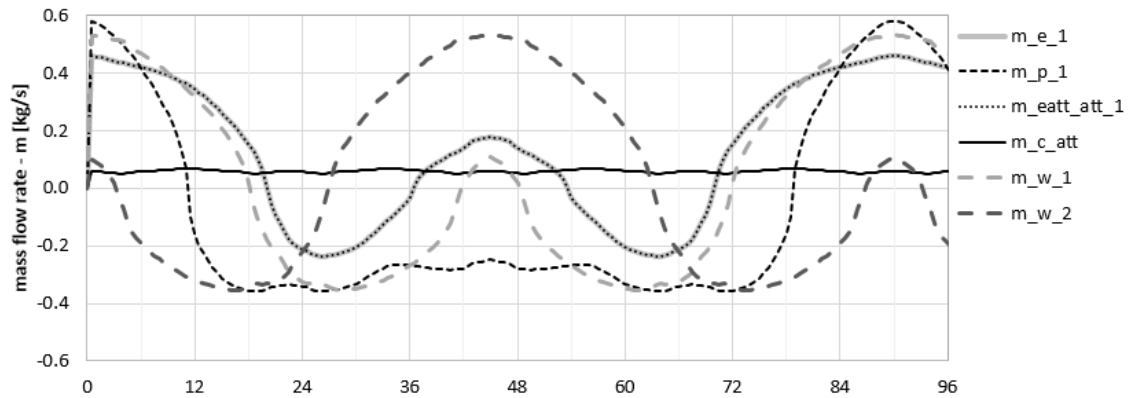


Fig. 71: Ver.Test 19 – Mass flow rate courses

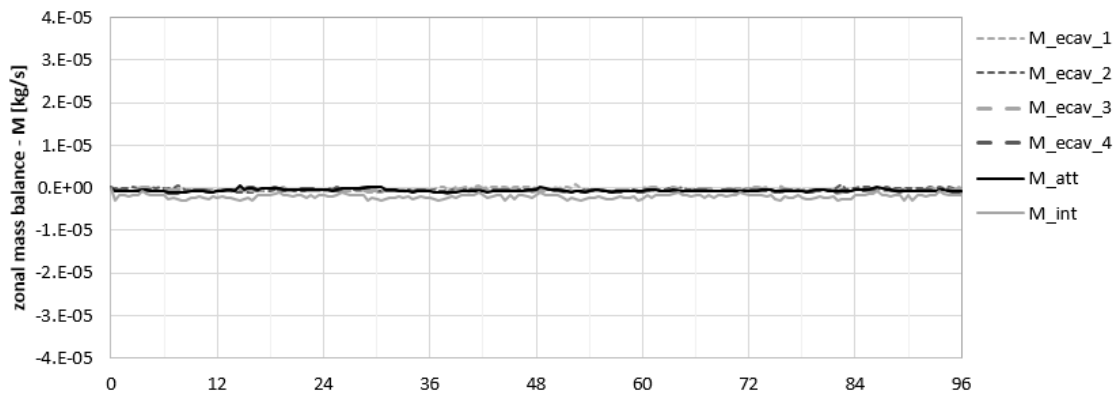


Fig. 72: Ver.Test 19 – Zonal mass balance

Again a nicely shaped courses of mass flow rates can be seen in figure 71. All temperatures are very precisely held at 20 °C. It can also be seen that zonal mass balance is much more stable compared to case 18).

Moisture model

For verification of the moisture model was used the same attic geometry as for the thermal model (see Fig. 31).

20) Steady state

- Constant temperature 20 °C and constant relative humidity 50 %.

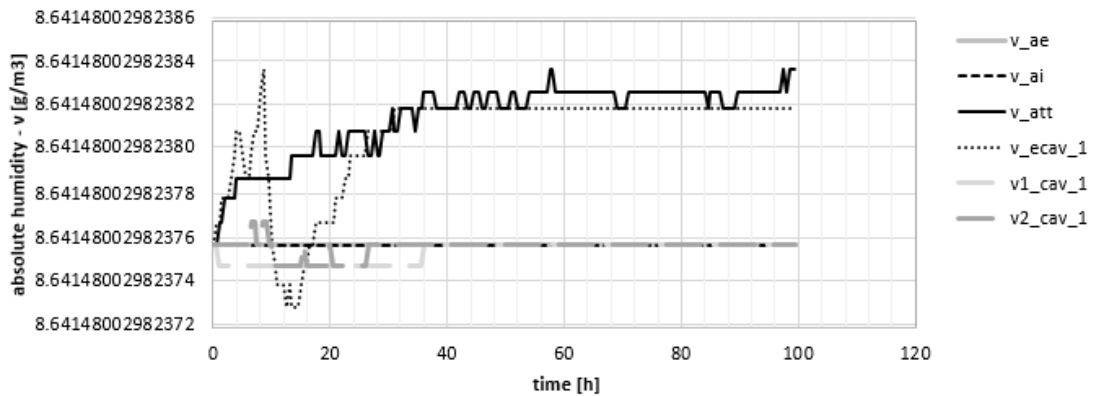


Fig. 73: Ver. Test 20 – Absolute humidity courses

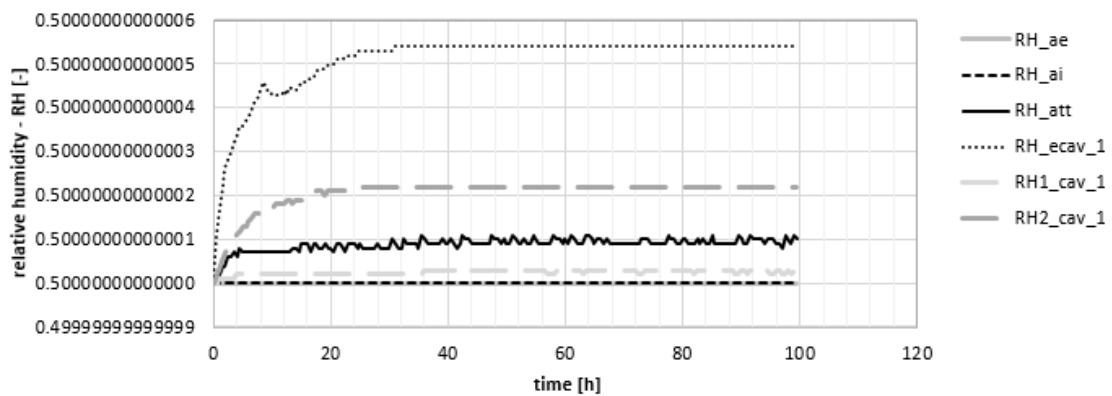


Fig. 74: Ver. Test 20 – Relative humidity courses

21) Different initial concentration

- Temperature 20 °C, initial relative humidity 30 % and boundaries kept at 50 % RH.

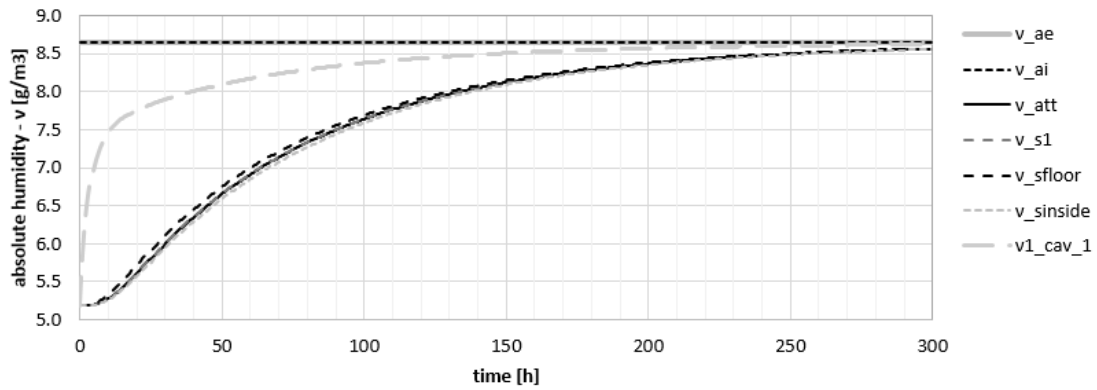


Fig. 75: Ver.Test 21 – Absolute humidity courses

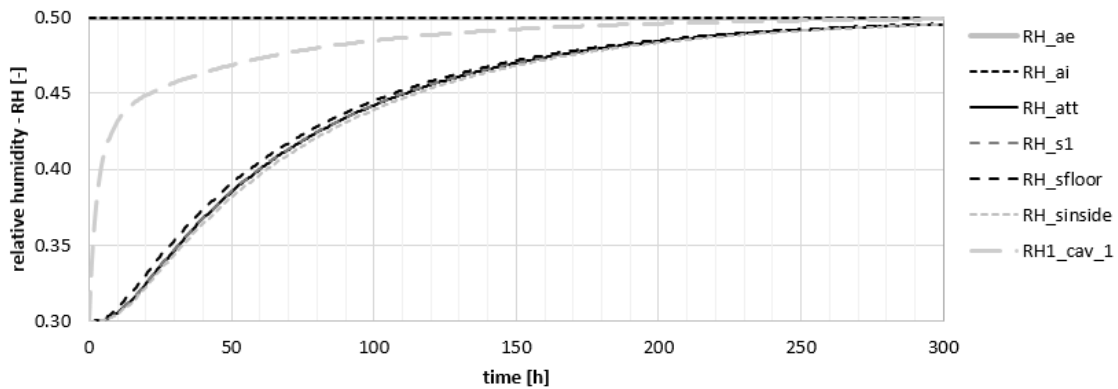


Fig. 76: Ver.Test 21 – Relative humidity courses

22) Enlarged volume of attic air

- Same case as 21) but considering ten times higher attic air volume ($V_{att} = 700 \text{ m}^3$).

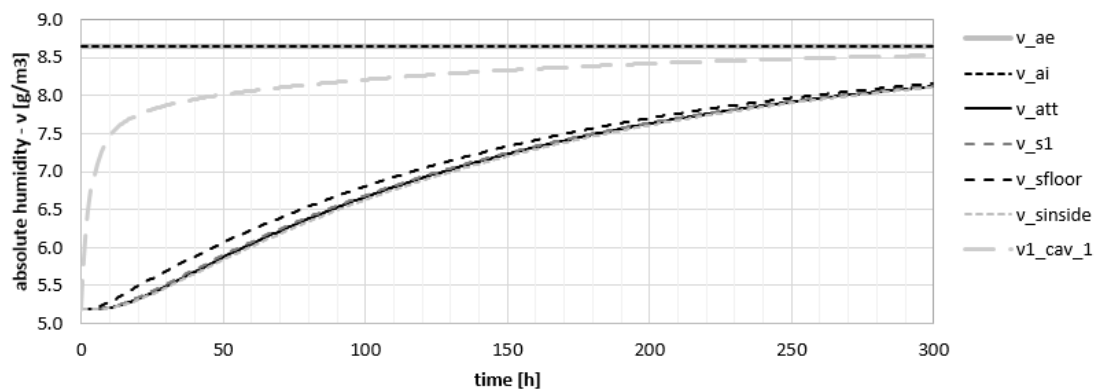


Fig. 77: Ver.Test 22 – Absolute humidity courses

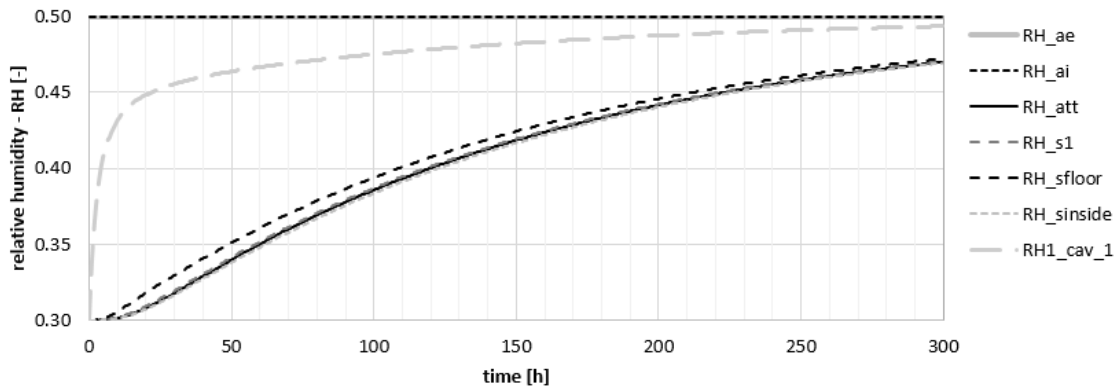


Fig. 78: Ver. Test 22 – Relative humidity courses

23) More mass of attic inner constructions

- Same case as 21) but considering ten times higher mass and exposed area of the inner attic buffering mass ($V_{\text{inside}} = 2.5 \text{ m}^3$; $A_{\text{inside}} = 50 \text{ m}^2$).

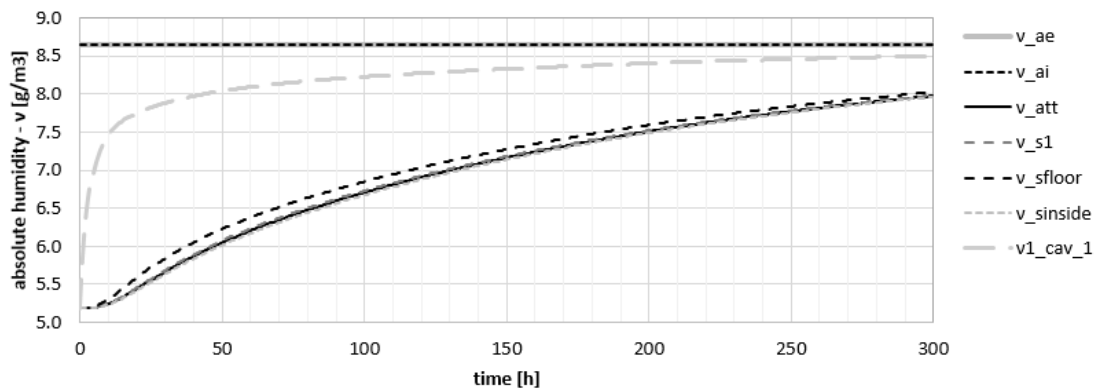


Fig. 79: Ver. Test 23 – Absolute humidity courses

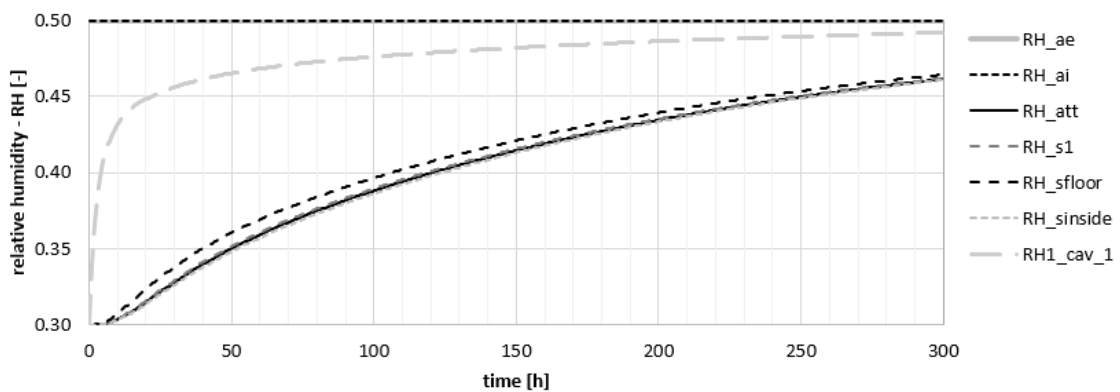


Fig. 80: Ver. Test 23 – Relative humidity courses

24) Higher moisture capacity of gypsum board

- Same case as 21) but considering two times higher moisture capacity of all gypsum board layers ($\xi = 0.016 \text{ kg/kg}$).

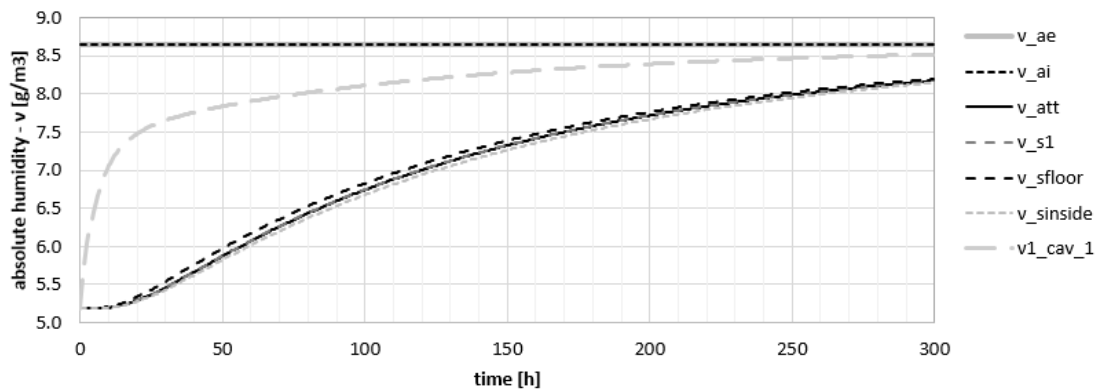


Fig. 81: Ver.Test 24 – Absolute humidity courses

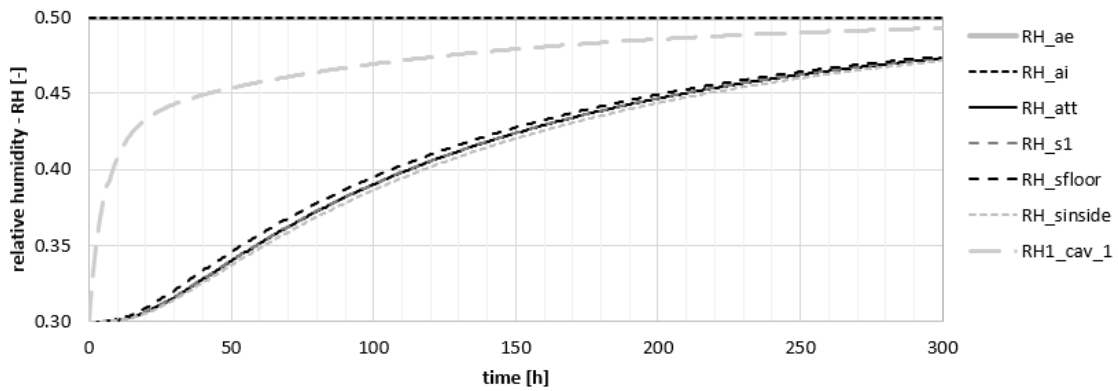


Fig. 82: Ver.Test 24 – Relative humidity courses

25) Roof segments are set as gable walls

- All roof segments were considered to become gable walls instead of roof decks. Walls were made out of 50 mm gypsum boards without any cavities and therefore form the same construction as the ceiling.

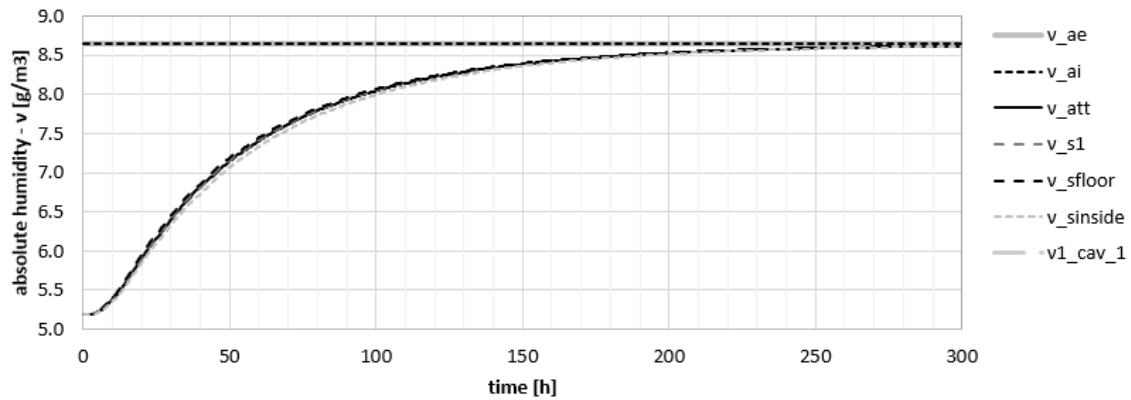


Fig. 83: Ver. Test 25 – Absolute humidity courses

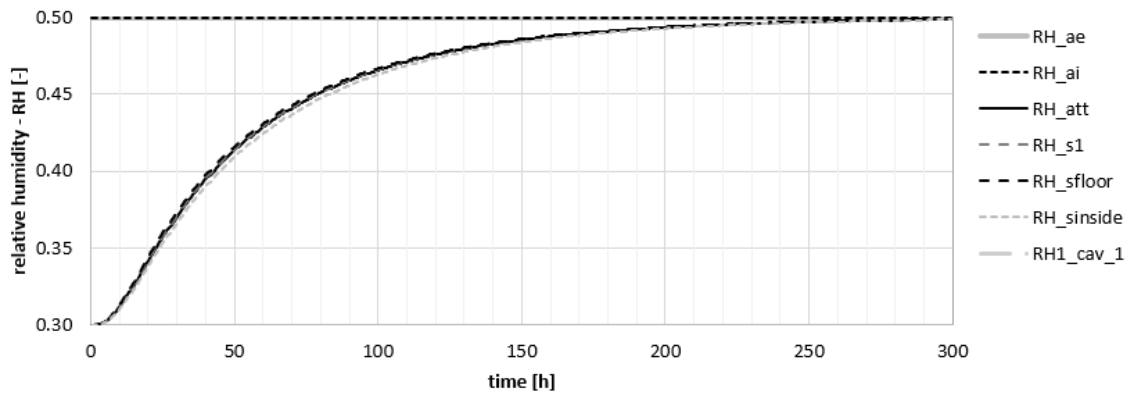


Fig. 84: Ver. Test 25 – Relative humidity courses

26) Test of constructions

- Eleven versions of the same case as 25) were performed, but in each case using different areas of attic surrounding constructions. Total area of all constructions was in all cases maintained at 50 m².
 - At first all constructions were considered as gable walls (each construction with an area of 10 m²).
 - Then each gable wall area was separately set to 50 m² while all others were kept zero.
 - Subsequently all gable walls were changed back to roof decks, each with an area 10 m², as well as the ceiling construction.
 - Then each roof deck area was set separately to 50 m² while all others kept zero. Finally the ceiling construction was tested separately as well having the area 50 m².

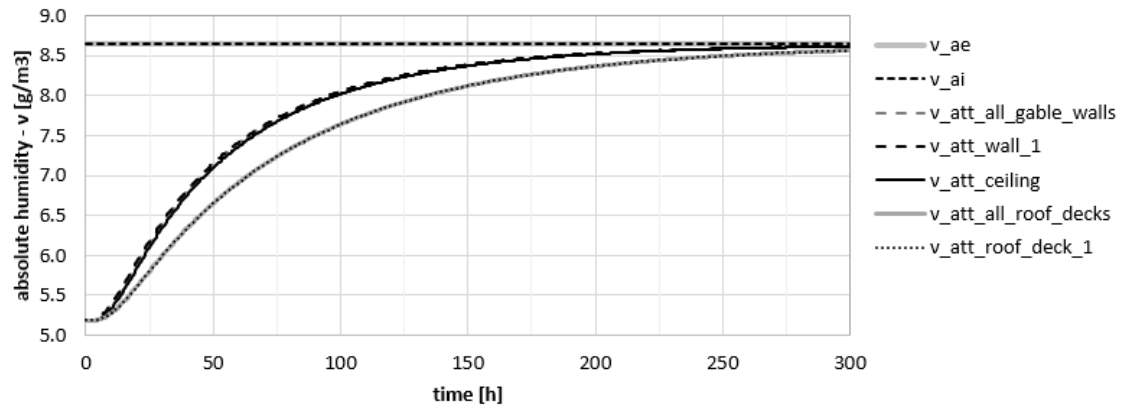


Fig. 85: Ver. Test 26 – Absolute humidity courses

27) Moisture source

- Same case as 21) but 0.03 g/s moisture gain was performed within the attic.

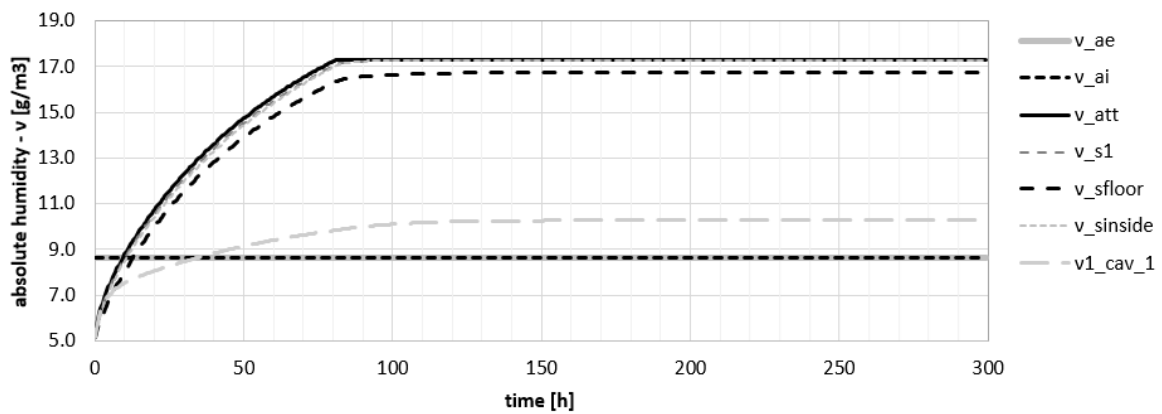


Fig. 86: Ver. Test 27 – Absolute humidity courses

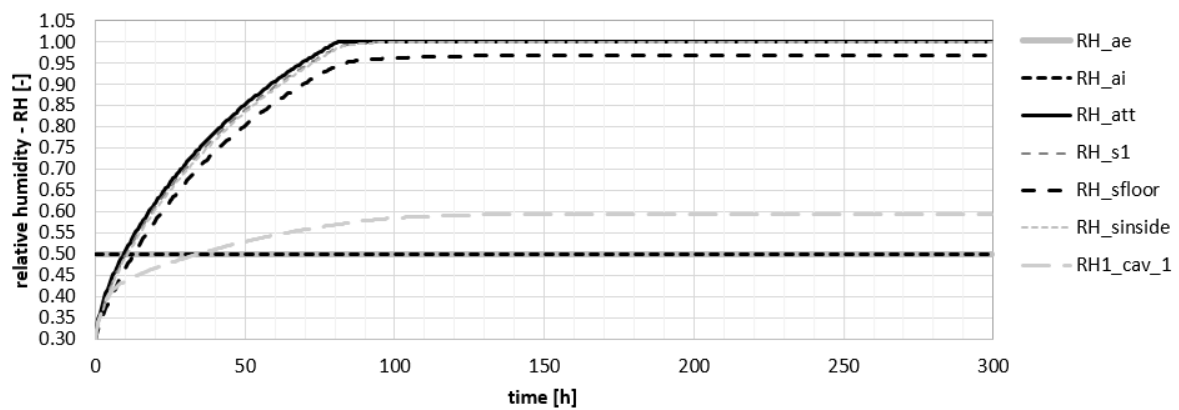


Fig. 87: Ver. Test 27 – Relative humidity courses

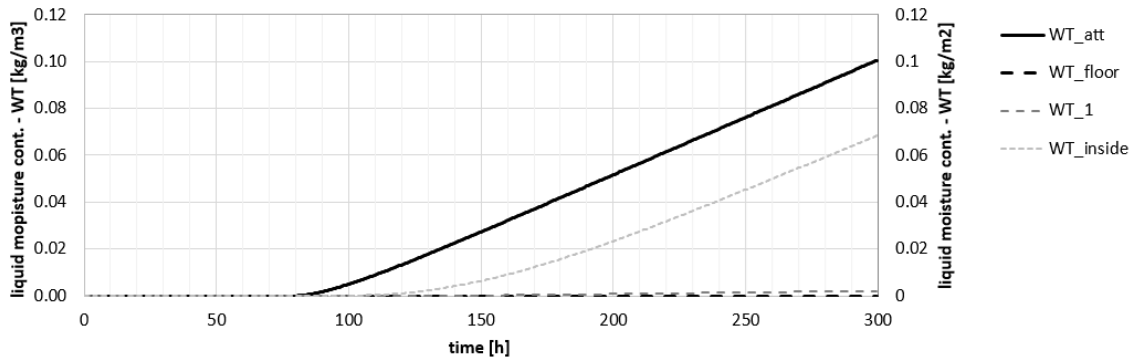


Fig. 88: Ver. Test 27 – liquid water content courses

28) Dynamic boundary conditions

- Same case as 2) but exterior and interior boundary relative humidity are determined by diurnal sinusoidal function with mean value 50 % and amplitude 20 %.

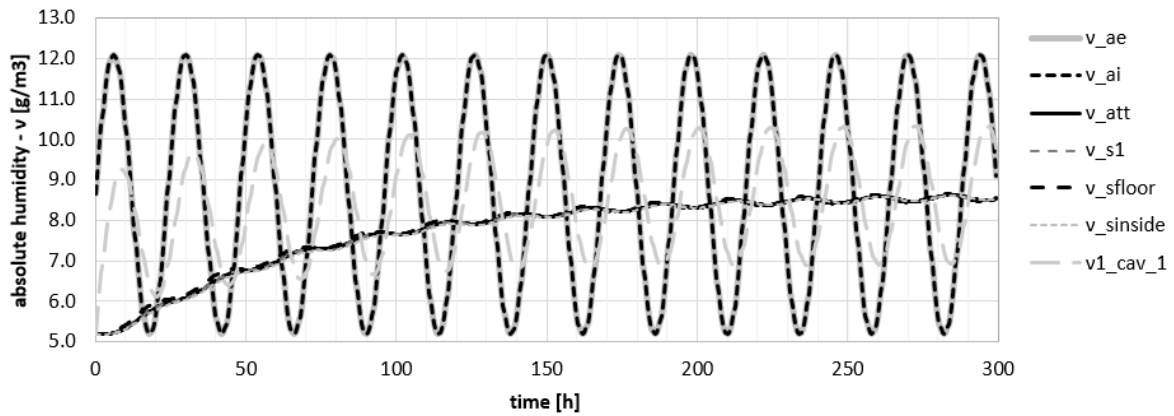


Fig. 89: Ver. Test 28 – Absolute humidity courses

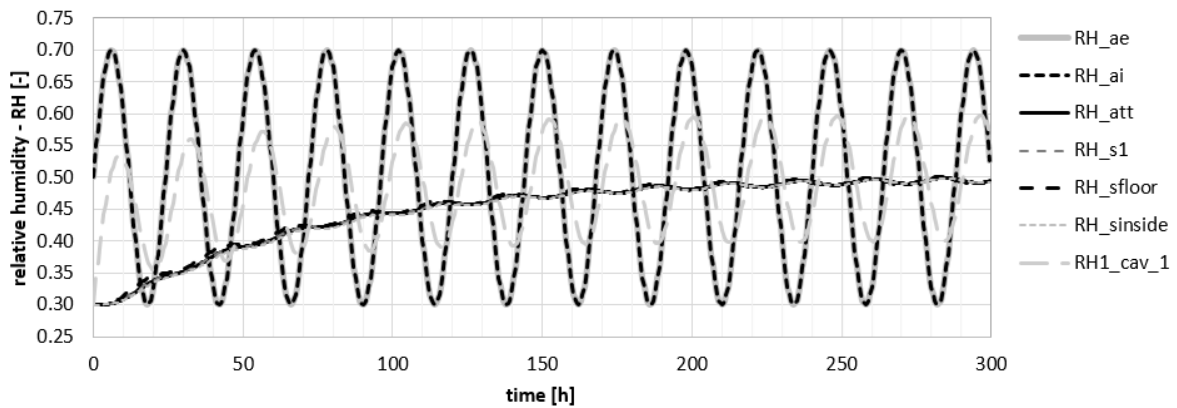


Fig. 90: Ver. Test 28 - Relative humidity courses

29) Constant but different boundary conditions

- Relative humidity was set in exterior equal to 20 % and in interior equal to 70 %.

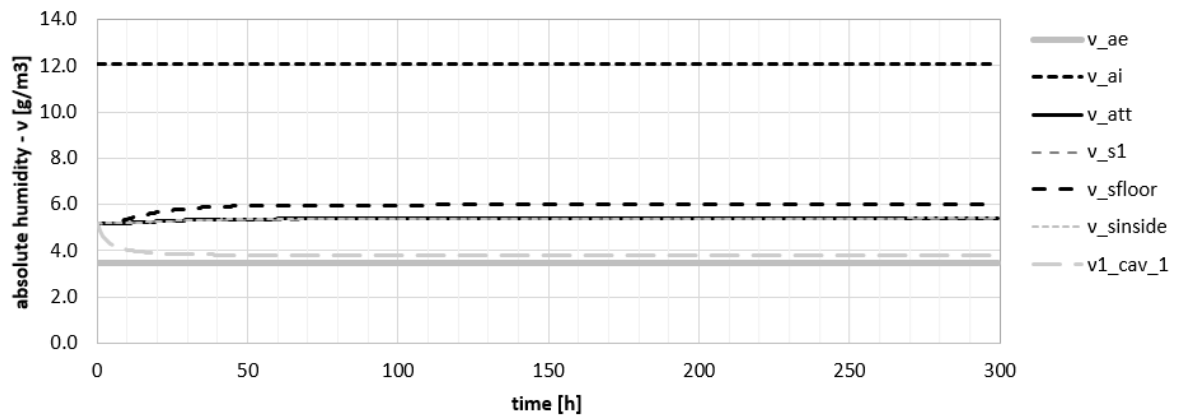


Fig. 91: Ver. Test 29- Absolute humidity courses

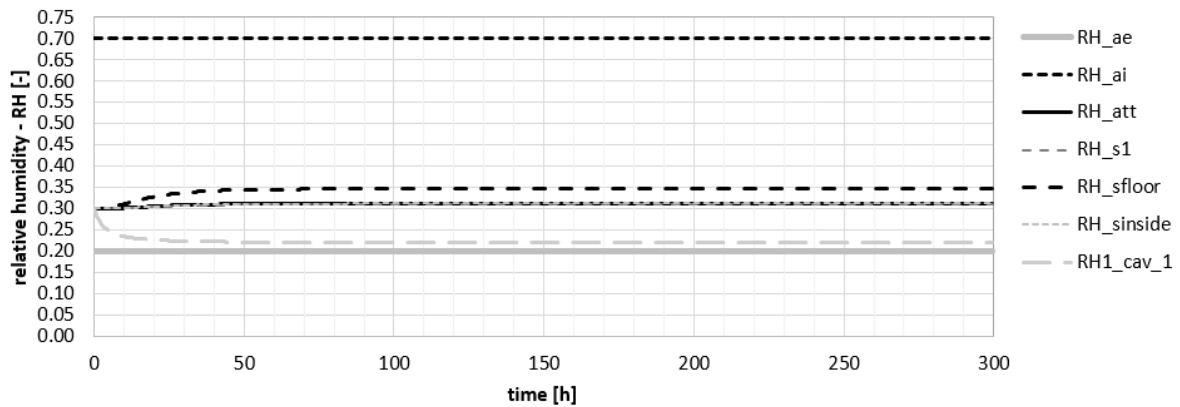


Fig. 92: Ver. Test 29- Relative humidity courses